Fall 12-20-2019

Roles of autism gene ARID1B in murine brain development and behavior

Amanda L. Smith
University of Nebraska Medical Center

ROLES OF AUTISM GENE *ARID1B* IN MURINE BRAIN DEVELOPMENT AND BEHAVIOR

by

Amanda Lee Smith

A DISSERTATION

Presented to the Faculty of
the University of Nebraska Graduate College
in Partial Fulfillment of the Requirements
for the Degree of Doctor of Philosophy

Pharmacology and Experimental Neuroscience
Graduate Program

Under the Supervision of Professor Woo-Yang Kim

University of Nebraska Medical Center
Omaha, Nebraska

December 2019

Supervisory Committee:

Anna Dunaevsky, Ph.D.
Keshore Bidasee, Ph.D.
Yunlong Huang, Ph.D.
Daniel Monaghan, Ph.D.
Huangui Xiong, M.D., Ph.D.

ACKNOWLEDGMENTS

I would first like to acknowledge my mentor, Dr. Woo-Yang Kim, for his consistent hands-on role throughout the duration of my Ph.D. training. Thank you for your support and guidance, while also encouraging my independence. You've helped me transition into a critically thinking scientist, which is invaluable as I move on in my career. Additionally, I owe a great thanks to my committee members, Dr. Anna Dunaevsky, Dr. Huangui Xiong, Dr. Yunlong Huang, Dr. Keshore Bidasee, and Dr. Dan Monaghan. Thank you all for graciously agreeing to be a part of my committee, providing me with your time, expertise, and encouragement throughout my training years. I would also like to acknowledge my former colleague, Dr. Jeffrey Moffat. I am grateful for your guidance in the lab, but even more so for your friendship and welcoming me into your family.

I am also thankful for my girlfriend, Shayla. Thank you for constantly challenging and encouraging me, and for staying up way too late with me. You never let me stop believing in myself, and you truly are the best part of my day. I love you.

I am truly grateful for my family during this journey. To my mom, dad, and sister: thank you for your unwavering support. I could not be where I am today without you all. You've each taught me to always be myself, to work hard, and to be kind. Thank you for traveling to visit me and loving me through all the challenges I've faced. I would finally like to thank my grandparents. My grandpa was the first person to encourage me to pursue a career in science, and taught me to work hard and never give up. To my grandma: Tete, there are not enough words in the world to tell you how much you mean to me. I am incredibly indebted to you for all your support and love throughout my life. I truly would not be the person I am or have accomplished the things I have without you. I wish you could be with me today, and I hope I've made you proud. I love you bigger.

ROLES OF AUTISM GENE *ARID1B* IN MURINE BRAIN DEVELOPMENT AND BEHAVIOR

Amanda L. Smith, Ph.D.

University of Nebraska, 2019

Supervisor: Woo-Yang Kim, Ph.D.

Autism spectrum disorder (ASD) and intellectual disability (ID) are highly prevalent neurodevelopmental disorders characterized by social and communication deficits, stereotyped behaviors, cognitive dysfunction, and deficits in adaptive behaviors. The pathogenesis underlying these disorders remains unknown, and thus no pharmacologic or genetic therapies are currently available. Recent progress in the field has shown that haploinsufficiency of the *AT-rich interactive domain-containing 1B* (*ARID1B*) gene is a genetic cause of ASD and ID. Our lab recently developed an *Arid1b* knockout mouse model to better study its role in the pathogenesis of these disorders. One theory regarding the cause of neurodevelopmental disorders is disruption of the excitatory/inhibitory balance in the brain. We previously showed that interneuron deficits lead to an excitatory/inhibitory imbalance in *Arid1b* knockout mice, playing a significant role in the observed behavioral phenotypes. Interneurons are highly heterogenous cell types in the brain; however, little is known regarding how the different subtypes modulate various behaviors. In chapter 2, we dissect the individual roles of the two most populous interneurons in the cerebral cortex, parvalbumin and somatostatin subtypes, in ASD/ID behaviors seen with *ARID1B* haploinsufficiency. We show that parvalbumin interneurons affect social and emotional behaviors, while somatostatin interneurons primarily affect stereotyped behaviors and cognitive function.

In addition to interneuron deficits, several studies have also implicated altered neurite outgrowth of cortical projection neurons in ASD and ID. Furthermore, deficits in

neurotrophic signaling, a master regulator of neurite outgrowth, is also frequently observed. In chapter 3, we examine a potential role of ARID1B in regulating neurite development of excitatory neurons during corticogenesis. We show that loss of the *Arid1b* gene leads to disrupted neurite outgrowth and altered development of the corpus callosum. Additionally, we suggest a likely role of ARID1B in the BDNF neurotrophic signaling pathway. Together, these studies provide insight into possible roles of ARID1B during neurogenesis, shedding further insight into the pathogenesis of ASD and ID.

TABLE OF CONTENTS

TITLE PAGE i

ACKNOWLEDGMENTS ii

ABSTRACT PAGE iii

TABLE OF CONTENTS v

LIST OF TABLES AND FIGURES ix

LIST OF ABBREVIATIONS xi

CHAPTER1: INTRODUCTION 1

1.1 Cortical neuron development in rodents 1

1.1.1 Development of inhibitory interneurons 1

1.1.2 Interneuron diversity and heterogeneity 4

1.1.3 Development of excitatory projection neurons 10

1.2 Chromatin remodeling in neural development 15

1.2.1 BAF chromatin remodeling complex 16

1.2.2 Role of Arid1b subunit 20

1.2.3 Chromatin remodeling deficits in neurodevelopmental disorders 21

1.3 Haploinsufficiency of *ARID1B* 22

1.3.1 Human ARID1B mutations 22

1.3.2 Knockdown of Arid1b and neuronal development 23

1.3.3 Neural and behavioral deficits in Arid1b haploinsufficient mice 24

1.3.4 Downstream gene expression changes 26

1.4 Autism spectrum disorder and intellectual disability 32

1.4.1 Genetic mouse models 32

1.4.2 Current and prospective therapies 33

1.5 Role of interneurons in neurodevelopmental disorders 35

1.5.1 Excitatory/Inhibitory balance 35

1.5.2 Interneuron deficits in neurodevelopmental disorders 36

1.6 Role of excitatory neurons in neurodevelopmental disorders 38
1.6.1 Regulation of neurite outgrowth 38
1.6.2 Neuron maturation deficits in neurodevelopmental disorders 44
CHAPTER 2: ARID1B MODULATES DISTINCT ASD/ID-LIKE BEHAVIORS THROUGH DIFFERENT INTERNEURON SUBTYPES 47
2.1 Abstract 48
2.2 Introduction 49
2.3 Materials and methods 51
2.3.1 Arid1b conditional knockout mice 51
2.3.2 Immunostaining 51
2.3.3 Behavioral assays 51
2.3.4 Three-chamber test 52
2.3.5 Grooming assessment 52
2.3.6 Open field test 53
2.3.7 Elevated plus maze test 53
2.3.8 Tail suspension test 53
2.3.9 Forced swim test 53
2.3.10 Novel object recognition test 54
2.3.11 Rotarod test 54
2.3.12 Morris water maze test 54
2.3.13 Statistical analysis 55
2.4 Results 56
2.4.1 Arid1b haploinsufficiency in PV and SST interneurons have distinct effects on social and stereotyped behaviors 56
2.4.2 Arid1b haploinsufficiency in PV interneurons, but not SST interneurons, results in heightened anxiety and depression 61
2.4.3 Cognitive deficits are caused by Arid1b haploinsufficiency in SST interneurons 65

2.5 Discussion 69
2.5.1 Interneurons play a significant role in the pathology of Arid1b haploinsufficiency-induced ASD and ID 69
2.5.2 Excitatory/Inhibitory imbalance in neurodevelopmental disorders 71
2.5.3 Arid1b haploinsufficiency in PV and SST interneurons have distinct effects on social, emotional, and cognitive behaviors....72
2.5.4 Conclusion and future prospective....74
CHAPTER 3: A ROLE OF ARID1B IN MEDIATING NEURITE OUTGROWTH OF EXCITATORY CORTICAL NEURONS 76
3.1 Abstract....77
3.2 Introduction 78
3.3 Materials and methods 80
3.3.1 Mice....80
3.3.2 Plasmids....80
3.3.3 Primary neuron cultures and growth factor treatment....80
3.3.4 In utero electroporation 81
3.3.5 Immunostaining 81
3.3.6 Morphometry 81
3.3.7 Western blot analysis....82
3.3.8 Statistical analysis 83
3.4 Results....84
3.4.1 Loss of Arid1b disrupts neurite outgrowth in developing cortical neurons 84
3.4.2 Impaired corpus callosum development with Arid1b deletion 87
3.4.3 Arid1b deletion alters neurite development via BDNF signaling activity 89
3.5 Discussion 93
3.5.1 Proposed pathology underlying neurite deficits in ARID1B haploinsufficiency93
3.5.2 Neurite development and neurotrophic signaling deficits in various neurodevelopmental disorders 95

3.5.3 Conclusion and future prospective.....95
CHAPTER 4: DISCUSSION AND CONCLUSIONS.....97
REFERENCES.....102

LIST OF TABLES AND FIGURES

Tables

Table 1.1 Interneuron diversity 7

Table 1.2 Select downregulated genes with Arid1b haploinsufficiency 31

Table 2.1 Summary of behavioral deficits 70

Figures

Figure 1.1 Spatiotemporal origins of interneurons 9

Figure 1.2 Excitatory neuron development in the rodent cortex 14

Figure 1.3 Altered gene expression and neuronal effects of Arid1b haploinsufficiency ..28

Figure 1.4 Intracellular signaling pathways regulating neurite outgrowth 43

Figure 2.1 ARID1B expression in PV and SST interneurons of Arid1b mutant mice 57

Figure 2.2 Body and brain weight with Arid1b haploinsufficiency in SST neurons.....58

Figure 2.3 Body and brain weight with Arid1b haploinsufficiency in PV neurons.....58

Figure 2.4 Social and stereotyped behaviors in F/+; PV-Cre and F/+; SST-Cre mice 60

Figure 2.5 Heightened anxiety in F/+; PV-Cre mice 62

Figure 2.6 Increased depression behavior in F/+; PV-Cre mice 64

Figure 2.7 Recognition memory and motor learning deficits in F/+; SST-Cre mice 66

Figure 2.8 Dysfunctional spatial learning and memory in F/+; SST-Cre mice.....68

Figure 3.1 Impaired axon growth in neurons with Arid1b deletion 85

Figure 3.2 Impaired dendrite growth in neurons with Arid1b deletion 86

Figure 3.3 Abnormal corpus callosum development in with loss of Arid1b 88

Figure 3.4 Arid1b heterozygous mice exhibit reduced BDNF neurotrophic signaling activity 90

Figure 3.5 Normalizing BDNF signaling levels rescued neurite outgrowth deficits in Arid1b heterozygotes.....92

Figure 3.6 A potential role of ARID1B in the BDNF neurotrophic pathway regulating neurite outgrowth.....94

LIST OF ABBREVIATIONS

Abbreviation	Description
4EBP	Eukaryotic translation initiation factor 4E-binding protein
5HT3aR	5-Hydroxytryptamine receptor 3A
AAV	Adeno-associated virus
AKT	Protein kinase B
Ankrd11	Ankyrin repeat domain 11 gene
ANOVA	Analysis of variance
APC	Adenomatous polyposis coli
ARID1A/B	AT-rich interaction domain 1A/B
ASD	Autism spectrum disorder
ATP	Adenosine triphosphate
BAF	BRG1/BRM-associated factor
BDNF	Brain derived neurotrophic factor
BRG1	Brahma-related gene 1
BRM	Brahma gene
CBP	Creb-binding protein
Ccnd1	Cyclin D1 gene
CDC42	Cell division control protein 42 homolog
CGE	Caudal ganglionic eminence
CHD8	Chromodomain helicase DNA binding protein 8
ChIP	Chromatin immunoprecipitation
CNS	Central nervous system
Cntnap2	Contactin-associated protein-like 2 gene

CP	Cortical plate
CR	Calretinin
Creb	cAMP response element binding gene
CREST	Calcium-responsive transactivator
CRISPR	Clustered Regularly Interspaced Short Palindromic Repeats
CRMP2	Collapsin response mediator protein 2
CSS	Coffin-Siris syndrome
Ctnnb1	β-catenin gene
CXCL12	C-X-C motif chemokine ligand 12
DAPI	4’,6-diamidino-2-phenylindole
Dbx1	Developing brain homeobox protein 1
Dyrk1a	Dual specificity tyrosine phosphorylation regulated kinase 1A gene
E/I	Excitatory/Inhibitory
Egr2	Early growth response 2 gene
Epha6	Ephrin type A receptor 6 gene
ERBB4	Receptor tyrosine kinase Erbb4 gene
ESC	Embryonic stem cell
Etv1	ETS variant 1
EZH2	Enhancer of zeste homolog 2
FGF	Fibroblast growth factor
FMR1	Fragile X mental retardation 1 gene
FXS	Fragile X syndrome
GABA	Gamma-aminobutyric acid
Gad1	Glutamate decarboxylase 1
Gad2	Glutamate decarboxylase 2

Gap43	Growth associated protein 43 gene
GAPDH	Glyceraldehyde 3-phosphate dehydrogenase
GE	Ganglionic eminence
GFP	Green fluorescent protein
GH	Growth hormone
GHRH	Growth hormone-releasing hormone
Gprin1	G protein regulated inducer of neurite outgrowth 1 gene
Grin2b	Glutamate receptor subunit epsilon-2 gene
GSK3	Glycogen synthase kinase 3
GSK3-i	Glycogen synthase kinase 3 inhibitor
HAT	Histone acetyltransferase
HDAC	Histone deacetylase
HDAC4	Histone deacetylase 4
Hmx3	H6 family homeobox 3
Homer1	Homer protein homolog 1 gene
ID	Intellectual disability
IGF1	Insulin-like growth factor 1
IP	Intermediate progenitor cell
Itga4	Integrin alpha 4 gene
KCC2	Potassium chloride cotransporter 2
kDa	Kilodalton
Lama1	Laminin subunit alpha-1 gene
Lef1	Lymphoid enhancer-binding factor 1 gene
Lhx6/8	LIM homeobox 6/8
MACF1	Microtubule actin crosslinking factor 1

MAP	Microtubule-associated protein
MAP2	Microtubule associated protein 2
MECP2	Methyl-CpG binding protein 2 gene
MFI	Mean fluorescence intensity
MGE	Medial ganglionic eminence
mIPSC	Miniature inhibitory postsynaptic current
miRNA	Micro RNA
Mkl2	Myocardin-like protein 2 gene
MT	Microtubule
mTOR	Mammalian target of rapamycin
MZ	Marginal zone
Nbea	Neurobeachin gene
NE	Neuroepithelial cell
Nlgn3	Neuroligin 3 gene
Nlgn4	Neuroligin 4 gene
NMDA	N-Methyl-D-aspartic acid
NOS	Nitric oxide synthase
NP	Neural progenitor cell
NPY	Neuropeptide Y
Nr2f2	Nuclear receptor subfamily 2 group F member 2
NRG1	Neuregulin 1 gene
Nting1	Netrin G1 gene
OCT4	Octamer-binding transcription factor 4
Otx2	Orthodenticle homeobox 2
PAR3/6	Partitioning defective protein 3/6

PAX6	Paired box 6
PCAF	P300/CBP-associated factor
PI3K	Phosphoinositide 3 kinase
PKC	Protein kinase C
pNF-H	Phosphorylated neurofilament heavy subunit
POA	Preoptic area
Prickle 1/2	Prickle planar cell polarity 1/2 gene
Prox1	Prospero homeobox protein 1
Pten	Phosphatase and tensin homolog gene
PV	Parvalbumin
Pvalb	Parvalbumin gene
RAC1	Ras-related C3 botulinum toxin substrate 1
Rbfox1	Fox-1 homolog A gene
REST	RE1-silencing transcription factor
RFP	Red fluorescent protein
RG	Radial glial cell
RHOA	Ras homolog family member A
Robo1	Roundabout homolog 1 gene
S6K	Ribosomal protein S6 kinase beta-1
SEM	Standard error of the mean
SFARI	Simons Foundation Autism Research Initiative
Shank1	SH3 and multiple ankyrin repeat domains 1 gene
Shank3	SH3 and multiple ankyrin repeat domains 3 gene
SHH	Sonic hedgehog
shRNA	Short hairpin RNA

Slc32a1	Vesicular inhibitory amino acid transporter gene
SMAD1	Mothers against decapentaplegic homolog 1
SOX2	SRY-box 2
Sox5/6	SRY-Box 5/6 gene
Sp8	SP family transcription factor 8
Sspo	SCO-spondin gene
SST	Somatostatin
Sst	Somatostatin gene
Sstr2	Type 2 somatostatin receptor gene
Sstr3	Type 3 somatostatin receptor gene
STAT3	Signal transducer and activator of transcription 3
Stmn2	Stathmin-2 gene
SVZ	Subventricular zone
Tac1	Tachykinin 1 peptide
Taok2	Thousand and one amino acid kinase 2 gene
TF	Transcription factor
Thy1	Thymus cell antigen 1 promoter
TrkB	Tropomyosin receptor kinase B
TSC2	Tuberous sclerosis complex 2
UBE3A	Ubiquitin protein ligase E3A gene
VGAT	Vesicular inhibitory amino acid transporter
VIP	Vasoactive intestinal peptide
VZ	Ventricular zone
YFP	Yellow fluorescent protein
Zbtb20	Zinc finger and BTB domain-containing 20 gene

CHAPTER1: INTRODUCTION

1.1 Cortical neuron development in rodents

1.1.1 Development of inhibitory interneurons

Interneurons, which release the inhibitory neurotransmitter gamma-aminobutyric acid (GABA), make up approximately 10-15% of all cortical neurons in rodents (Tremblay et al., 2016). The development of inhibitory interneurons begins with differentiation of interneuron progenitors into immature interneurons (occurs from ~E9.5-E18.5), followed by migration of interneurons to their destination within the cortex (~E13-P6), and finally maturation and integration into the local cortical circuitry (~P4-3rd postnatal week) (Lim et al., 2018). Interneuron progenitor cells reside in the embryonic ganglionic eminence (GE) within the telencephalon, where they give rise to postmitotic interneurons. Newly differentiated postmitotic interneurons undergo two phases of migration: a long tangential migration to reach the cortical plate (~E13-P2), followed by radial migration as they disperse throughout the developing cortex (~E17-P6) (Lim et al., 2018). The majority of cortical interneurons originate from the medial ganglionic eminence (MGE), caudal ganglionic eminence (CGE), and preoptic area (POA), and interneurons from these regions use essentially the same cellular mechanisms as they migrate to the cortex (Cossart, 2011; Wonders and Anderson, 2006). Tangential migration toward the cortex involves an interplay between chemorepulsive factors in the GE, such as semaphorins 3A and 3F, and chemoattractive cues at the cortical plate, such as neuroligin 1 (Lim et al., 2018). Additionally, actin and microtubule dynamics appear to play a mechanistic role in the migration process of interneurons. Ka et al. show that microtubule actin crosslinking factor 1 (MACF1) regulates GABAergic interneuron migration and positioning during mouse cortical development (Ka et al., 2017). Conditional deletion of Macf1 in interneuron progenitors led to fewer cortical

interneurons, abnormal positioning, and altered speed and mode of migration due to decreased microtubule stability (Ka et al., 2017). During tangential migration, interneurons gradually begin to acquire their biochemical markers that contribute to the diversity of subtypes. However, other differentiating characteristics, such as morphology, connections, and physiological properties, do not appear until much later postnatal developmental stages (Cossart, 2011; Lim et al., 2018). Upon reaching the cortical plate, interneurons switch from the tangential mode to the radial mode of migration. Studies indicate that this switch is linked to the interneuron's loss of responsiveness to the chemokine Cxcl12 (Lim et al., 2018). Additionally, pyramidal cells in the cortex express neuregulin 3, facilitating the attraction of interneurons into the laminar dimension of the cortex (Miyoshi and Fishell, 2011). Other studies recapitulate the suggestion that the laminar distribution of interneurons is highly dependent on the activity of pyramidal cells. For example, interneurons do not begin to acquire their position within their cortical layer until after corresponding pyramidal cells have occupied the same layer (Hevner et al., 2004; Pla et al., 2006). Further, disrupting the proper positioning of pyramidal cells results in altered laminar distribution of interneurons (Lodato et al., 2011; Pla et al., 2006). Eventually, upregulation of the potassium/chloride exchanger KCC2 in interneurons reduces the frequency of intracellular calcium transients and inhibits the motility of interneurons (Bortone and Polleux, 2009). This leads to the termination of radial interneuron migration.

Following migration to their final destination in the cortex, interneurons begin to integrate into the functional cortical circuitry. Similar to other neurons in the nervous system, a surplus of GABAergic interneurons is generated during development. About 30% of interneurons are eliminated through apoptosis before the second postnatal week (Lim et al., 2018). Xu et al. show that integration into cortical circuits influences their

probability of survival, and interneurons that do not receive excitatory inputs during the first week of postnatal development are likely to undergo apoptosis (Xu et al., 2004). Interneurons that do survive function in three main circuit motifs in the cortex, including feedforward inhibition, feedback inhibition, and disinhibition (Kepecs and Fishell, 2014; Qu et al., 2016; Tremblay et al., 2016). While all interneuron types likely contribute to these circuit motifs to some extent, it appears that specific subtypes exhibit more prominent roles in one motif over another. For example, optogenetic techniques show that VIP interneurons in the cortex have a primary role in disinhibition of SST interneurons, ultimately inhibiting SST input to pyramidal cells (Pi et al., 2013). Within these various circuit motifs, GABAergic interneurons play important roles in controlling the timing of pyramidal cell firing, synchronizing network activity, and generating cortical rhythms by modulating the level of excitation (Rudy et al., 2011). While the majority of interneurons target nearby cells and control local network activity, some cortical GABAergic neurons also project to other brain regions. Long-range cortical interneurons have been found to connect to other cortical areas, the hippocampus, amygdala, and basal ganglia (Caputi et al., 2013; Lee et al., 2014). In addition to providing inhibitory input, another major function of GABAergic interneurons is to establish transient microcircuits during early postnatal development that modulate the maturation of network oscillations associated with behavioral and cognitive functions (Cossart, 2011; Le Magueresse and Monyer, 2013). Furthermore, in addition to releasing GABA, interneurons are also a source of neuropeptides such as somatostatin, vasoactive intestinal peptide, and neuropeptide Y, which have significant neuromodulatory effects (Rudy et al., 2011; Tremblay et al., 2016). These many facets of interneuron involvement are indicative of their importance in overall brain development and function.

1.1.2 Interneuron diversity and heterogeneity

Cortical interneurons are a highly heterogenous group of cells that exhibit diverse morphologies, molecular markers, connectivity patterns, and physiological properties (Lim et al., 2018; Xu et al., 2004). This level of heterogeneity is obtained throughout development as a result of the combinatorial selection of different transcription modules (Harris et al., 2018; Paul et al., 2017). RNA sequencing studies have revealed a high level of diversity in transcription factor (TF) expression among interneuron progenitors (Mayer et al., 2018). This TF heterogeneity is conserved throughout the maturation trajectory as progenitors differentiate into diverse subtypes of interneurons. Furthermore, mutations in various TFs at different developmental time points leads to several deficits in interneuron fate, including abnormal migration, positioning, marker expression, and synaptic activity, indicating functional importance of the diverse TF expression (Wonders and Anderson, 2006).

Cortical interneurons are organized into several major classes based on their transcriptional similarities and specific marker expression, which are even further broken down based on other factors such as morphology, intrinsic physical properties, and cortical distribution. Previous studies indicate that interneurons expressing the calcium-binding protein parvalbumin (PV), the neuropeptide somatostatin (SST), and the ionotropic serotonin receptor 5HT3a (5HT3aR) account for almost all of the interneurons in the rodent cortex (Rudy et al., 2011). The largest class of interneurons is characterized by PV expression and exhibit fast-spiking firing properties (Kepecs and Fishell, 2014; Lim et al., 2018; Rudy et al., 2011; Tremblay et al., 2016). Three major subclasses of PV interneurons, each exhibiting distinct morphologies, are chandelier cells, basket cells, and translaminar interneurons. Chandelier cells synapse onto pyramidal cells at the initial segment of the axon, and they are primarily located between

cortical layers 1 and 6 and in layer 6 (Somogyi et al., 1982; Taniguchi et al., 2013). Basket cells, the most abundant interneuron type in the cortex, synapse onto the soma and proximal dendrites of pyramidal cells and other interneurons, and they are distributed throughout cortical layers 2 to 6 (Hu et al., 2014; Klausberger and Somogyi, 2008). Translaminar interneurons are a rare category of neurons, primarily in layers 5 and 6, that target pyramidal cells throughout most cortical layers (Bortone et al., 2014). The second largest class of cortical interneurons are characterized by SST expression (Kepecs and Fishell, 2014; Lim et al., 2018; Rudy et al., 2011; Tremblay et al., 2016). Two major types of SST interneurons, Martinotti and non-Martinotti cells, preferentially synapse onto dendrites of other interneurons and pyramidal cells (Klausberger and Somogyi, 2008). Most Martinotti cells reside in layer 5 of the cortex, and they exhibit fairly diverse firing patterns (Hilscher et al., 2017; Silberberg and Markram, 2007), while non-Martinotti cells are distributed throughout layers 2 to 6 and exhibit a higher firing frequency than Martinotti cells (Nigro et al., 2018). The cortex also contains GABAergic interneurons expressing SST that exhibit long-range projections. These cells are primarily found in deep cortical layers, project to other regions in the cortex, and frequently co-express nitric oxide synthase (NOS) and neuropeptide Y (NPY) (He et al., 2016). The third class of cortical interneurons expressing 5HT3aR is highly heterogenous, and the most abundant of these types are those expressing vasoactive intestinal peptide (VIP) (Kepecs and Fishell, 2014; Lim et al., 2018; Rudy et al., 2011; Tremblay et al., 2016). Bipolar VIP interneurons in layers 2 and 3 of the cortex exhibit continuous adapting firing properties and co-express the calcium-binding protein calretinin (CR) (Pronneke et al., 2015). Less is known about multipolar VIP interneurons. 5HT3aR interneurons that do not express VIP are abundant in cortical layer 1, have late spiking firing properties, and frequently co-express reelin and NPY (Lee et al., 2010; Tasic et al., 2016). Table 1.1 summarizes the heterogeneity of interneuron subtypes.

The highly heterogenous nature of interneurons suggest that there is marked functional diversity among them. Current and future studies will further elucidate the various functional differences between subtypes.

Main markers	Parvalbumin (PV)		Somatostatin (SST)		5HT3aR	
					VIP	Non-VIP
Morphological types	Basket	Chandelier	Martinotti	non-Martinotti	Bipolar and multipolar	Single bouquet and neurogliaform
Targeting bias	Soma and proximal dendrites	Axon initial segment	Dendrites	Dendrites	Interneurons	Interneurons
Anatomical properties	• Most common type • Present in L2-L6 • Most prominent in L4 & L5 • Multipolar dendritic arbor • Mostly targets pyramidal cells and other PV cells • Axonal arbor largely dispersed	• Mainly found in L2 & L6 • Multipolar dendritic arbor • Only targets pyramidal cells • Local axonal arbor	• Found in L2-L6 • Abundant in L5 • Multipolar & bitufted dendritic arbor • Local axon arbor • Little connection with other SST cells	• Found in L4 & L5 • Multipolar or bitufted dendritic arbor • Axon arbors in L4 & L5 • Preferentially targets PV cells	• Enriched in L2/3 • Mostly bipolar • Intracolumnar dendritic and axonal arbors	• Found in L1-L6 • Abundant in L1 • Multipolar dendritic arbor • Translaminar axon
Biophysical properties	• Fast spiking firing • Low input resistance • Brief action potential • Little or no spike frequency adaptation	Fast spiking firing, slightly slower than typical FS basket cells	• Low threshold spiking • High input resistance • Spike frequency adaptation • Low max frequency	• Quasi fast spiking firing • Low input resistance • Fast action potential • Spike frequency adaptation • High max frequency	• Irregular spiking and bursting firing patterns • High input resistance • Mostly adapting	• Low spiking firing pattern • High input resistance • Electrically coupled with other interneuron types
Synaptic properties	Fast, strong, and depressing excitatory inputs and inhibitory outputs	Depolarizing postsynaptic effect	Facilitating excitatory inputs		Preferentially contact SST interneurons	Activate $GABA_B$ receptor, synaptic fatigue
Other markers	Tac1	None	CR, NOS, Reelin, NPY		CR	Reelin, NOS, NPY

Table 1.1 Interneuron diversity
Nearly all the interneurons in neocortex express one of the main three non-overlapping markers: parvalbumin (PV, blue), somatostatin (SST, yellow), and the ionotropic serotonin receptor 5HT3a (5HT3aR, green). Further subdivisions within each molecular group are revealed by morphological features, cellular and subcellular targeting biases, and expression of other markers, as well as some known anatomical, electrophysiological, and synaptic properties.

Both spatial and temporal factors, regulated by a network of transcription factors, contribute to the origin of interneuron diversity. The major classes of interneurons are derived from distinct regions. The MGE and POA give rise to both PV and SST interneuron types, and the CGE gives rise to the class of 5HT3aR interneurons (Butt et al., 2017; Lim et al., 2018). Further, PV interneurons are born throughout the majority of the embryonic time window for neurogenesis (E9.5~E18.5), SST interneurons are born during the first half of the neurogenic period (E9.5~E14.5), and 5HT3aR subtypes are born at the latter half of the neurogenic period (E12.5~E18.5) (Butt et al., 2017; Kepecs and Fishell, 2014; Wonders and Anderson, 2006). Figure 1.1 illustrates the spatiotemporal origins of interneuron diversity and the underlying transcription factors involved.

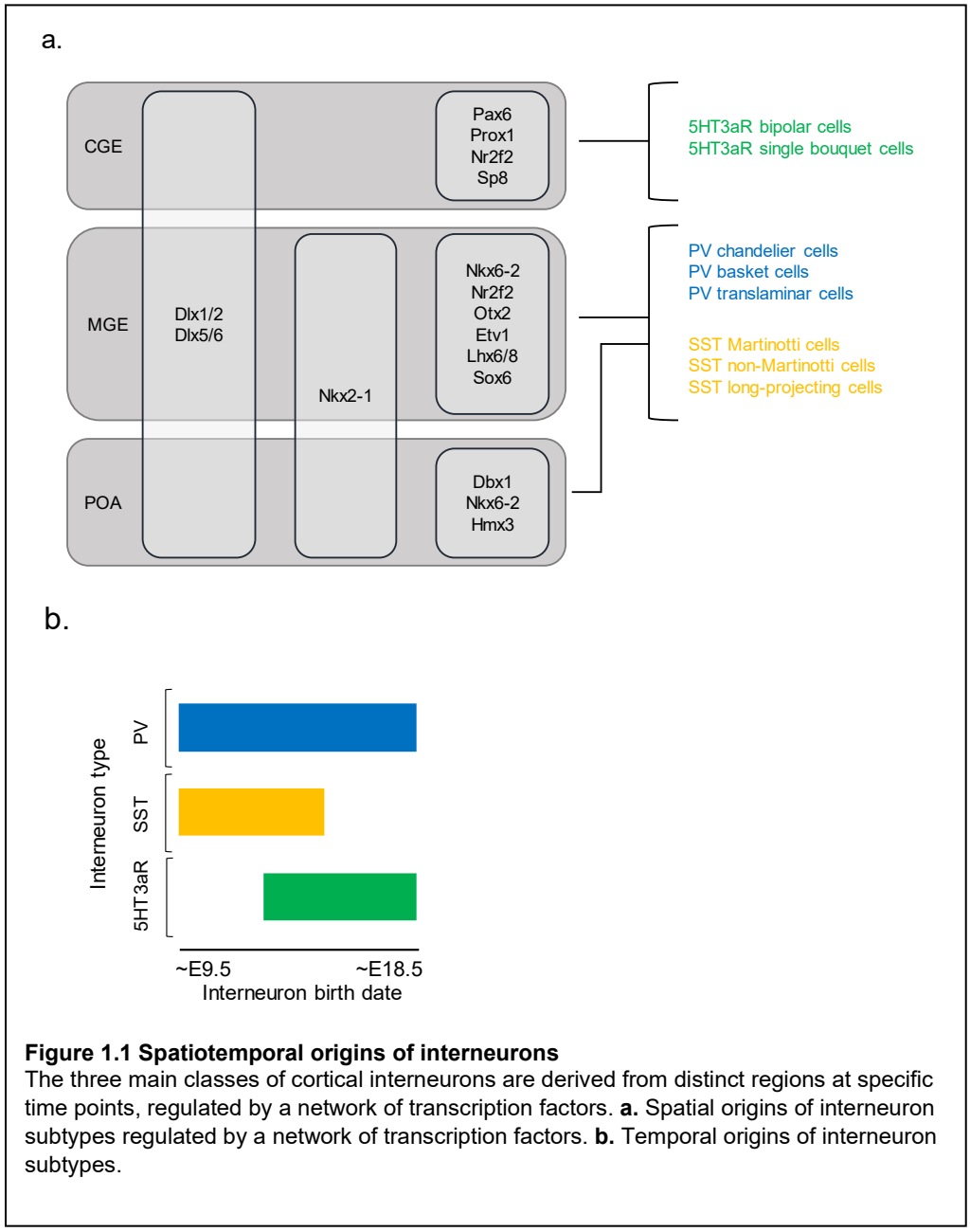

Figure 1.1 Spatiotemporal origins of interneurons
The three main classes of cortical interneurons are derived from distinct regions at specific time points, regulated by a network of transcription factors. **a.** Spatial origins of interneuron subtypes regulated by a network of transcription factors. **b.** Temporal origins of interneuron subtypes.

1.1.3 Development of excitatory projection neurons

Excitatory projection neurons, which release the neurotransmitter glutamate, make up approximately 85-90% of neurons in the rodent cortex (Tremblay et al., 2016). These glutamatergic neurons may project to other cortical areas as well as subcortical targets, and are crucial for transmitting information across brain regions. Cortical development begins at approximately E10, after closure of the neural tube, and continues until around postnatal week three (Azzarelli et al., 2014; Barnes and Polleux, 2009). The first stage of development involves maintaining a pool of embryonic stem cells (ESCs) and neural progenitor cells (NPs), followed by differentiation of NPs into immature neurons. One type of progenitor cell, neuroepithelial cells (NEs), line the lateral ventricles and self-renew to expand the progenitor pool (Azzarelli et al., 2014; Kast and Levitt, 2019). These cells then convert into another type of progenitor cell, radial glial cells (RGs), which are bipolar cells whose cell body resides in the ventricular zone (VZ). These neural precursors can divide symmetrically to self-renew, or asymmetrically to differentiate into immature cortical projection neurons. Initially, RGs generate neurons directly (direct neurogenesis), but begin to produce a second population of neural precursors called intermediate progenitors (IPs) around E13.5. These IPs exhibit a multipolar morphology and migrate along the glial process of RGs to the subventricular zone (SVZ), where they undergo additional rounds of self-renewal to increase the yield of cortical neurons derived from a single RG, followed by asymmetric division to generate immature neurons (indirect neurogenesis) (Barnes and Polleux, 2009). Neural progenitors continue to actively proliferate and generate neurons between E10 and E17 (Azzarelli et al., 2014). The balance between proliferation and differentiation of the different neural progenitors is tightly controlled by cytoskeletal remodeling. Multiple signaling networks regulate these cytoskeletal dynamics. Activity of several small Rho GTPases, including RhoA, Rac1, and Cdc42, initiate downstream

signaling to regulate actin and microtubule (MT) components of the cytoskeleton during proliferation and differentiation (Azzarelli et al., 2014; Namba et al., 2015). Additionally, mammalian target of rapamycin (mTOR) signaling regulates the cell cycle progression of neural progenitors and disrupts progenitor self-renewal by altering cytoskeletal dynamics (Ka et al., 2014a). Mice with loss of mTOR in neural progenitors present with reduced brain size and cortical thickness as well as suppressed differentiation. Ka et al. also showed that glycogen synthase kinase 3 (GSK3), a master regulator of the switch from self-renewal to neurogenesis in neural progenitor cells, controls the activity of mTOR in progenitors (Ka et al., 2014a). GSK3 exhibits a baseline level of activity in resting cells, and inactivation promotes progenitor proliferation while further activation promotes neuronal differentiation (Hur and Zhou, 2010; Jung et al., 2015). Downstream signaling of GSK3 controls neurogenesis by altering MT organization and modulating pathways regulating progenitor proliferation, such as Wnt, Shh, Fgf, and Notch signaling (Hur and Zhou, 2010; Kim et al., 2009). MACF1, a MT plus-end binding protein, also regulates the dynamics of MTs during neurogenesis (Moffat et al., 2017). Loss of MACF1 and abnormal stabilization of MTs can suppress cell division.

Following differentiation, an immature neuron then enters the next stage of development, which is migration to its final destination within the cortex. During migration, which occurs from approximately E11 to E18, newborn neurons detach from the ventricular surface and migrate radially toward the pial surface of the cortex while using RG fibers as a scaffold (Azzarelli et al., 2014). The cortex is generated in an inside-out manner, meaning that neurons born earlier will occupy the deepest layers of the future six-layered neocortex, whereas later born neurons by-pass the early neurons and settle in more superficial layers (Azzarelli et al., 2014; Kast and Levitt, 2019). Immature neurons first acquire a multipolar shape at early stages of migration, and then

transition to a bipolar morphology with a leading and a trailing process (Lewis et al., 2013). The leading process directed toward the pial surface will eventually become the apical dendrite, and the trailing process will become the nascent axon (Azzarelli et al., 2014; Barnes and Polleux, 2009). Cytoskeletal dynamics play an essential role in the multipolar-to-bipolar transition and migration processes. Dynamic organization of actin and microtubules controls the interaction between the migrating neuron and the glial process, and disruption results in deficits in migration (Azzarelli et al., 2014; Barnes and Polleux, 2009). Deletion of mTOR alters downstream cytoskeletal dynamics and results in abnormal migration and neuron positioning (Ka et al., 2014a). Additionally, loss of MACF1 disrupts the leading process morphogenesis and MT dynamics during radial migration, leading to similar deficits in migration and positioning (Ka et al., 2014b; Moffat et al., 2017). Upon reaching their location in the cortex, neurons continue to mature as they develop complex axon and dendrite networks, ultimately constructing the intricate circuitry of the brain. The trailing process becomes the nascent axon as it extends rapidly and is guided to its target area within the brain, which lasts until around postnatal day 7 (P7) (Lewis et al., 2013). During the second and third postnatal week (P8-P21), further axonal branching and dendritic spine formation occurs during the formation of presynaptic contacts with postsynaptic targets (Lewis et al., 2013). Apoptosis is an essential step during the stages of axon growth, branching, and synaptogenesis. Neuronal apoptosis in the cortex occurs during the first 30 postnatal days in order to refine neuronal innervation and network formation (Azzarelli et al., 2014). This accounts for approximately a 30% loss of neurons in the cortex from birth to adulthood. Cortical projection neurons can be divided into three broad classes (Kast and Levitt, 2019). The first is corticothalamic neurons, which are located primarily in layer 6 and project to the thalamus. The second is the pyramidal tract neurons that are exclusively located in layer 5 and have axons that extend toward the brain stem and spinal cord. The third class is

the intratelencephalic neurons within layers 2-6 that extend axons toward targets in the contralateral and ipsilateral cortex, striatum, nucleus accumbens, amygdala, and other structures. Fate decisions of which class projection neurons will belong to occurs shortly after cell division, during the early stages of migration (Kast and Levitt, 2019). Local microcircuitry connections within the cortex are established around the first week, while long-range projections develop over the first two-three postnatal weeks (Kast and Levitt, 2019). The stages of excitatory projection neuron development in the cortex are illustrated in Figure 1.2.

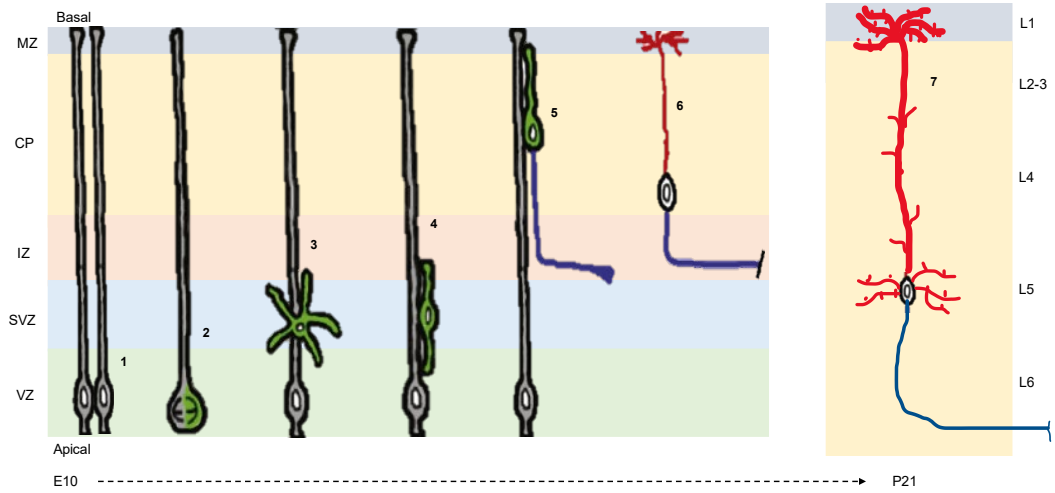

Figure 1.2 Excitatory neuron development in the rodent cortex
The following are the steps of excitatory neuron development in vivo: 1) Radial glial neural progenitor cells undergo symmetric cell division to self-renew. 2) Asymmetric division of a radial glial cell generates an immature projection neuron. 3) The immature neuron detaches from the ventricular surface and begins to migrate radially, acquiring a multipolar morphology. 4) The nascent neuron becomes bipolar, extending a leading process toward the pial surface and trailing process in the opposite direction as it continues migrating along the glial process. 5) During migration, the trailing process becomes the axon and begins to extend and the neuron detaches from the glial process as the leading process reaches the marginal zone. 6) The leading process gives rise to the apical dendrite and initiates branching in the marginal zone as the nascent axon continues to extend. 7) The neuron matures as the axon continues to extend to its final location, basal dendrites develop at the soma, and dendritic spines begin to form.

1.2 Chromatin remodeling in neural development

Proper brain development is regulated by highly orchestrated processes. Master transcription factors must activate or repress specific downstream genes at the right place and right time in a highly coordinated fashion. Genetic material is highly compacted and packaged around histones within the nucleus, so only certain genes are accessible to transcription factors at a given time (Kornberg, 1974). The role of chromatin modifiers is to create dynamic changes in the structure of chromatin, which allows TF access to regulate various genes both spatially and temporally. There are two main epigenetic mechanisms utilized by chromatin modifiers to regulate the state of chromatin. The first is covalent modification of histone tails, such as acetylation, which regulates the accessibility of DNA to regulatory mechanisms (Mehler, 2008; Ronan et al., 2013). The second is ATP-dependent remodeling of DNA-nucleosome topology, which physically alters the state of chromatin by moving nucleosomes in relation to DNA or exchanging nucleosomes into and out of DNA (Ronan et al., 2013; Sim et al., 2015). Both histone modifiers and physical chromatin remodelers work in concert to regulate chromatin structure and gene expression. Several chromatin modifiers and remodelers play important roles in the major events during neural development. BRG1/BRM associated factor (BAF) and chromodomain helicase DNA binding protein 8 (CHD8), which are two ATP-dependent chromatin remodelers, histone deacetylase 4 (HDAC4), and enhancer of zeste homolog 2 (EZH2), which is a histone methyltransferase, all have common pathways in regulating neural development, from proliferation and differentiation to synaptogenesis (Day and Sweatt, 2011; Mehler, 2008; Ronan et al., 2013).

1.2.1 BAF chromatin remodeling complex

One chromatin remodeler, the BAF chromatin remodeling complex, is highly expressed throughout all stages of mammalian brain development (Ho and Crabtree, 2010; Wang et al., 1996). Since its original discovery in yeast, the evolution of the mammalian BAF complex has involved the addition of new subunits and the use of combinatorial subunit assembly to develop different forms of the complex for tissue-specific expression. The primary roles of the additional subunits gained in mammalian complexes appear to be in cell cycle control and regulation of neurodevelopment (Son and Crabtree, 2014). Specific BAF complexes are expressed in embryonic stem cells, neural progenitor cells, and mature neurons, and are referred to as esBAF, npBAF, and nBAF, respectively. All BAF complexes are composed of 12-15 subunits, including a core ATPase subunit (BRG1 or BRM). The ATPase subunits also contain a bromodomain, which binds to acetylated lysine residues in histone N-terminal tails. It is suggested that this helps with stabilizing the association between the complex and chromatin (Ronan et al., 2013). The complex also contains a subunit with a DNA-binding domain, Arid1a or Arid1b, that targets the complex to DNA (Wang et al., 2004). Other subunits in the complex have been shown to interact with DNA regulatory proteins. These subunits bind to transcription activators or repressors, which help target the complex to promoters. Studies have shown that the roles of these subunits have redundant functions to Arid1a/b, and their primary role is to support the function of Arid1a/b (Martens and Winston, 2003). Without these other subunits present, the BAF complex is still successfully targeted to promoter sites. Image reconstruction techniques show that the subunits come together and form a groove within the center of the complex where nucleosome binding and remodeling occurs (Tang et al., 2010).

The BAF complex uses energy from ATP hydrolysis to remodel chromosome structure by altering DNA-histone contacts within a nucleosome (Celen et al., 2017; Martens and Winston, 2003). There are two proposed models regarding the mechanism of chromatin remodeling by the BAF complex: nucleosome sliding and nucleosome ejection and insertion (Peterson and Workman, 2000; Tang et al., 2010; Wilson and Roberts, 2011). The nucleosome sliding mechanism includes binding of the complex to nucleosomal DNA, disruption of the histone-DNA contacts by ATP hydrolysis, translocation of DNA though the ATPase subunit, and finally the formation of a DNA loop that then gets propagated around the nucleosome to generate sites accessible to DNA binding factors. The complex then resets its original position to prepare for a new cycle of remodeling. The mechanism of how nucleosome ejection and insertion occurs is not as well known. It has been suggested that after positioning of the bound nucleosome, histone ejection, with assistance of histone chaperones, may occur at adjacent nucleosomes rather than the nucleosome directly bound to the complex (Peterson and Workman, 2000). The BAF complex acts as both an activator and repressor of gene transcription, either by positioning the nucleosomes away from DNA binding sites to facilitate interaction of TFs, or by moving nucleosomes over binding sites to prevent TF interaction (Lopez and Wood, 2015). The activity of the chromatin remodeler is not directly instructive, but it instead establishes either permissive or restrictive environments for gene expression. This dynamic interplay between gene activation and repression is crucial during the intricate stages of neural development. For example, as proliferating stem cells begin to differentiate into neural progenitors, proliferation-associated genes must become more suppressed while cell lineage specific genes must begin to be activated (Wilson and Roberts, 2011).

As cells mature in the developing brain from embryonic stem cells, to neural progenitor cells, to mature neurons, they undergo global chromatin changes regulated by the expression of tissue-specific BAF complexes: esBAF, npBAF, and nBAF, respectively. This change in BAF subtype requires essential switches in subunit composition in order to perform the functions necessary for different cell types. Several studies have illustrated roles of specific BAF subunits in various stages in neural development. The esBAF complex has an important role in maintaining the self-renewal and pluripotency of mouse embryonic stem cells (Ho and Crabtree, 2010). The BRG1, BAF155, and BAF170 subunits are essential in regulating these processes. Loss of function in any of these components leads to loss of proliferative activity and pluripotency (Son and Crabtree, 2014). To differentiate into cells of different lineages, pluripotent ESCs must suppress genes that potentiate a state of self-renewal. BAF155 and BAF57 subunits are essential to exit from this state (Ho and Crabtree, 2010; Ho et al., 2009). As ESCs differentiate into NPs, esBAFs exclude the BAF60B subunit in exchange for BAF60C to become npBAFs (Lessard et al., 2007). NPs are a focal point for intricate regulation of brain development. They must downregulate the pluripotency gene network while still retaining proliferative properties, and they must simultaneously suppress the neuronal differentiation gene network. BRG1 and BAF155 subunits both participate in progenitor self-renewal in addition to npBAF-specific subunits BAF53A, BAF45A, and BAF60C (Son and Crabtree, 2014). Additionally, BAF170 interacts with Pax6 to regulate the specification of layer identity, which contributes to the regulation of cortex size and composition (Tuoc et al., 2013). Downstream target genes of Pax6 regulate the generation of intermediate progenitors and late cortical progenitors during early stages of development. Loss of BAF170 promotes indirect neurogenesis by increasing the pool of IPs, resulting in increased cortical size and thickness (Tuoc et al., 2013). As NPs leave their stem-cell niche and exit mitosis, the npBAF complex

exchanges BAF45A and BAF53A subunits for BAF45B and BAF53B to become the nBAF complex (Lessard et al., 2007). The nBAF complex interacts with the Ca^{2+}-responsive protein CREST to regulate downstream genes associated with activity-dependent dendrite and axon outgrowth, contributing to proper circuitry formation during late stage development (Lopez and Wood, 2015; Wu et al., 2007). nBAF subunit BAF53B also regulates transcription and cytoskeletal dynamics downstream of activity-triggered Ca^{2+} signaling, affecting the formation of long-term memory (Lopez and Wood, 2015; Son and Crabtree, 2014). Mice with mutations in BAF53B have deficits in spine morphology, synaptic plasticity, cytoskeletal dynamics, and long-term memory (Vogel-Ciernia et al., 2013). A triple negative circuit underlies the mechanism of the switch between BAF complex types (Lessard et al., 2007; Son and Crabtree, 2014). In one cell type, miRNAs bind to the gene transcript of the subunit to be suppressed, resulting in inhibition of translation and subsequent mRNA degradation. The transcriptional repressor REST will repress these miRNAs in the other cell type to maintain expression of the subunit. This mechanism is present in each cell type containing BAFs, so precise control of subunit expression is maintained throughout the stages of neural development (Lessard et al., 2007).

Chromatin remodeling by BAF complexes work in cooperation with covalent chromatin modifiers. The complex has a global effect on epigenetic events, influencing acetylation (active marks) and methylation (repressive marks). Loss of function in the various BAF complexes results in reduced acetylation events and increased methylation events, accompanied by decreased downstream expression of neurodevelopment-associated genes (Narayanan et al., 2015). Therefore, the presence of the BAF complexes provides a crucial balance between active and repressive activity of chromatin during development. In addition, the BAF complexes work with master

transcription factors to maintain proper transcription activity during neurodevelopment. For example, the esBAF complex regulates expression of genes also targeted by TFs known to control stem cell renewal, including OCT4, SOX2, STAT3, and SMAD1 (Ho and Crabtree, 2010). Further, the npBAF complex converges on the same genes of TFs that target pathways involved in neurogenesis, including NOTCH and SHH. The above studies all underscore the important and diverse roles of the BAF complexes during several stages of neurodevelopment.

1.2.2 Role of Arid1b subunit

AT-rich interacting domain-containing protein 1B (ARID1B), one subunit of BAF chromatin remodeling complexes, is a 240 kDa protein that facilitates targeting of the complex to chromatin (Celen et al., 2017). There are three known domains of the *Arid1b* gene. A DNA-binding domain interacts with AT-rich DNA of its target genes and a protein-binding domain interacts with other proteins, including BRG1 and BRM subunits (Sim et al., 2015). A third domain contains a BC box domain, which associates with three additional proteins, Elongin C, Cullin 2, and Roc1, to assemble an E3 ubiquitin ligase (Li et al., 2010; Zheng and Shabek, 2017). This functions to target histone H2B at lysine 120 for monoubiquitination, suggesting a role of Arid1b in the cross talk of histone modifications. Arid1b is expressed throughout the cortical layers and hippocampus of the rodent brain during embryonic and postnatal development and into adulthood (Celen et al., 2017; Ka et al., 2016a). Its expression has also been verified throughout other regions of the brain, including the dorsal and ventral telencephalon and cerebellum. Arid1b is localized within the nucleus and is specific to ESCs and cells in the neuronal lineage, as expression is absent in glial cells (Ka et al., 2016a). The Arid1b subunit of the BAF complex is crucial for cell cycle regulation and differentiation during mammalian brain development. Deficiency of Arid1b reduces the self-renewal capacity of ESCs (Sim

et al., 2015; Yan et al., 2008). In addition, Arid1b is essential for ESCs to maintain pluripotency properties. Inactivation of Arid1b results in ESCs that exhibit characteristics of differentiated cells, such as reduced expression of pluripotency-associated genes and elevated expression of differentiation-associated genes (Yan et al., 2008).

1.2.3 Chromatin remodeling deficits in neurodevelopmental disorders

Deficits in epigenetic modifications have been implicated in neurodevelopmental disorders. Considerable study has been done on the roles of histone acetylation and DNA methylation in disease progression. Mutations in the histone deacetylase HDAC4 and methyltransferase EZH2 have both been associated with ASD and ID (Gibson et al., 2012; Williams et al., 2010). More recently, the role of nucleosome remodelers in these disorders has received considerable attention. Mice with loss of function mutations in the ATPase chromatin remodeler CHD8 exhibit autism-related phenotypes and cognitive dysfunction (O'Roak et al., 2012a). In addition, mutations in a single allele of multiple BAF complex subunits have been discovered in several human patients with ASD and ID. Missense mutations in Arid1a, BRM, BRG1, BAF47, BAF155, BAF170, and BAF180 have all been identified (Neale et al., 2012; O'Roak et al., 2012b; Santen et al., 2012b; Van Houdt et al., 2012). Loss of function mutations in the Arid1b subunit are the most frequently occurring ASD/ID-associated mutations of the BAF complex (Halgren et al., 2012; Hoyer et al., 2012; Santen et al., 2012a; Tsurusaki et al., 2012). The following section discussions these various Arid1b mutations and their role in neurodevelopmental disorders.

1.3 Haploinsufficiency of *ARID1B*

1.3.1 Human ARID1B mutations

Recent studies have shown that *ARID1B* mutations are prevalent in neurodevelopmental disorders, including ASD, ID, and Coffin-Siris syndrome (CSS). ASD, which is characterized by severe social and communication deficits as well as stereotyped behaviors, affects approximately 1 in 68 individuals (Walsh et al., 2011). ID is seen in about 75% of ASD patients, and affects approximately 1-3% of the overall population. Individuals with ID experience significant limitations in cognitive function and adaptive behavior (Ellison et al., 2013). Next generation sequencing from eight ID patients all show *de novo* translocations or deletions that result in a truncated copy of the *ARID1B* gene (Halgren et al., 2012). Of these, five patients exhibit phenotypes consistent with ASD and four patients also have abnormalities of the corpus callosum. Mutational analysis in another 887 patients with unexplained ID showed nine patients with *de novo* nonsense or frameshift mutations resulting in truncated *ARID1B* (Hoyer et al., 2012). CSS is a severe form of intellectual disability, characterized by developmental delay, severe speech impairment, coarse facial features, hypoplastic or absent fifth fingernail or toenail, and agenesis of the corpus callosum (Tsurusaki et al., 2012). Exome sequencing of 23 individuals diagnosed with CSS revealed 6 patients with *de novo* mutations in one copy of *ARID1B* (Tsurusaki et al., 2012). Whole-exome sequencing done by Santen et al. on three patients with CSS also revealed *de novo* truncating mutations of *ARID1B* in all individuals (Santen et al., 2012a). Additionally, copy-number variation analysis in 2,000 individuals affected with ID showed that three subjects with *ARID1B* gene deletions also exhibited phenotypes overlapping with CSS (Santen et al., 2012a).

Most of the discussed mutations are genetically dominant, and they occur in the DNA-binding domain of the gene, affecting the ability of the protein to target the BAF complex to chromatin (Sim et al., 2015). Together, these studies reveal a number of *de novo* mutations resulting in loss of function of one copy of the *ARID1B* gene. These results strongly suggest that haploinsufficiency of *ARID1B* is a genetic cause of ASD and ID, contributing to the evidence that chromatin remodelers play crucial roles during neurodevelopment. Interestingly, Santen et al. discuss that several mutations in *ARID1B* and other BAF subunits are also identified in a wide variety of tumors (Santen et al., 2012b). Because the BAF complexes regulate many different cellular pathways involved in cell proliferation, differentiation, and migration, it makes sense that inactivating mutations may affect cancer development. Santen et al. suggest that there could be an increased risk of malignancies in ASD/ID patients that carry mutations in these genes.

1.3.2 Knockdown of Arid1b and neuronal development

Maturation of neurons during the late stages of development involves intricately regulated neurite outgrowth (Barnes and Polleux, 2009; Tsaneva-Atanasova et al., 2009). The use of shRNA delivery into rodent brains via *in utero* electroporation revealed that Arid1b plays a role in regulating the maturation of neurons during development. Knockdown of Arid1b led to a reduction in dendritic outgrowth and arborization of pyramidal neurons in the cortex and hippocampus (Ka et al., 2016a). This was accompanied by a reduction in various neurite growth-associated genes, such as *Stmn2, Gprin1,* and *Gap43.* In addition, Arid1b knockdown resulted in fewer dendritic innervations into layer 1 of the cortex (Ka et al., 2016a). This is likely to alter synaptic connectivity in the cortex, disrupting the balance between excitation and inhibition. Following neurite development, mature neurons undergo synaptogenesis to form connections and generate proper circuitry (Barnes and Polleux, 2009). After shRNA

delivery, Arid1b-deficient neurons exhibit fewer dendritic spines, and of the spines present, many of them exhibited immature, filopodia-like morphology (Ka et al., 2016a). Abnormal spine development leads to impaired synaptic connectivity, likely contributing to the pathology underlying ASD and ID.

1.3.3 Neural and behavioral deficits in Arid1b haploinsufficient mice

Three groups, including our own, have generated mouse models of *Arid1b* haploinsufficiency that exhibit significant abnormalities in neural composition and behavior (Celen et al., 2017; Jung et al., 2017; Shibutani et al., 2017). Both Jung et al. and Celen et al. generated heterozygous mice by removing exon 5 in one copy of the gene, while Shibutani et al. removed exon 3. All methods resulted in frameshift mutations and loss of function of the gene. Jung et al. observe abnormal cellular composition in the cortex of *Arid1b* heterozygous mice. While there are no differences in excitatory pyramidal neurons, oligodendrocytes, or astrocytes, GABAergic interneurons are markedly reduced and abnormally positioned within the cortex (Jung et al., 2017). Interneurons containing parvalbumin, somatostatin, calbindin, and calretinin are all prominent in the makeup of cortical circuitry (Tremblay et al., 2016); however, only a reduction in the PV subtype is observed (Jung et al., 2017). This is consistent with previous studies linking a reduction in PV interneurons to ASD and related disorders (Fukuda et al., 2005; Gogolla et al., 2009; Selby et al., 2007; Zikopoulos and Barbas, 2013). Previous studies have also indicated a disruption in inhibitory synaptic activity in ASD (Fatemi et al., 2009; Jamain et al., 2008; Piton et al., 2013; Tabuchi et al., 2007). Consistent with this, *Arid1b* heterozygous mice had fewer inhibitory synaptic puncta, particularly vesicular inhibitory amino acid transporter- (VGAT) and glutamic acid decarboxylase 2- (GAD2) positive puncta, as well as decreased miniature inhibitory postsynaptic currents (mIPSCs) in the cortex, suggesting impaired inhibitory

transmission (Jung et al., 2017). Deficits in interneuron number and activity together lead to an excitatory/inhibitory imbalance in these *Arid1b* heterozygous mice. Celen et al. also report various neuroanatomical abnormalities in *Arid1b* haploinsufficient mice, including reduced corpus callosum volume, smaller dentate gyrus, and reduced cortical thickness, likely resulting from decreased NP proliferation (Celen et al., 2017). These mice also exhibit body growth impairments due to deficiencies in the growth hormone-releasing hormone – growth hormone – insulin-like growth factor 1 (GHRH-GH-IGF1) axis. Shibutani et al. report similar reduced body weight and hydrocephalus in *Arid1b* heterozygous mice (Shibutani et al., 2017).

Heterozygous mice from all three groups also exhibit behavioral deficits consistent with other ASD/ID mouse models and human patients. The findings between the groups are primarily consistent, with a few exceptions. Social and communication deficits and stereotyped behaviors are two hallmark features of ASD (Walsh et al., 2011). All three groups report deficits in social behavior in the three-chamber test and/or open field sociability test (Celen et al., 2017; Jung et al., 2017; Shibutani et al., 2017). Celen et al. and Jung et al. also report stereotyped behaviors indicated by excessive self-grooming, and Celen et al. report altered ultrasonic vocalizations, suggesting communication deficits (Celen et al., 2017; Jung et al., 2017). Anxiety and depression are common comorbidities seen with ASD (Fakhoury, 2015; Reid et al., 2011). The elevated plus maze and open field test indicated increased anxiety in *Arid1b* heterozygotes in all three groups (Celen et al., 2017; Jung et al., 2017; Shibutani et al., 2017). Jung et al. also show increased depression-like behavior via the tail suspension and forced swim tests (Jung et al., 2017). Interestingly, Shibutani et al. show contradicting results in the forced swim test, suggesting reduced depression behavior (Shibutani et al., 2017). Various factors, including animal handling and environmental

stimuli, may affect contradictory results. ID is primarily characterized by deficits in cognition (Daily et al., 2000; Ellison et al., 2013). *Arid1b* heterozygous mice present with significant cognitive dysfunction. Jung et al. report deficits in learning and memory in the novel object recognition test and Morris water maze (Jung et al., 2017). These mice also present with motor learning deficits, indicated by the rotarod test. Shibutani et al. show deficits in long-term fear memory, but novel object recognition and Morris water maze assays were not performed (Shibutani et al., 2017). Celen at al. performed the Morris water maze, but surprisingly, results indicated no dysfunction in spatial reference memory (Celen et al., 2017). This is unusual given the prevalence of *ARID1B* mutations identified in human ID patients (Halgren et al., 2012; Hoyer et al., 2012; Santen et al., 2012a). Together, these results all suggest that *Arid1b* heterozygous mice recapitulate the majority of behavioral phenotypes seen in ASD and ID, therefore providing a useful tool moving forward to better understand the pathology underlying these disorders.

1.3.4 Downstream gene expression changes

As a chromatin remodeler, the primary function of the BAF complex is to regulate gene expression in the brain (Son and Crabtree, 2014; Tang et al., 2010). Loss of the Arid1b subunit, whose main role is to target the complex to its target genes, leads to altered gene expression and contributes to the downstream neuronal effects of *Arid1b* haploinsufficiency (Figure 1.3). Celen et al. report significant downregulation of 56 genes and up-regulation of 79 genes in *Arid1b* heterozygous mice (Celen et al., 2017). The majority of altered genes were associated with nervous system development and psychological, behavioral, and developmental disorders. Approximately 10% of the differentially regulated genes were among the highest-ranking autism risk genes identified in the SFARI gene database (Basu et al., 2009; Celen et al., 2017). Additionally, about 65% of these genes showed direct binding to the BAF complex

(Celen et al., 2017). Using genome-wide RNA-Sequencing, Shibutani et al. showed that the gene expression pattern of *Arid1b* heterozygote brains is similar to that in the brains of autistic patients (Shibutani et al., 2017).

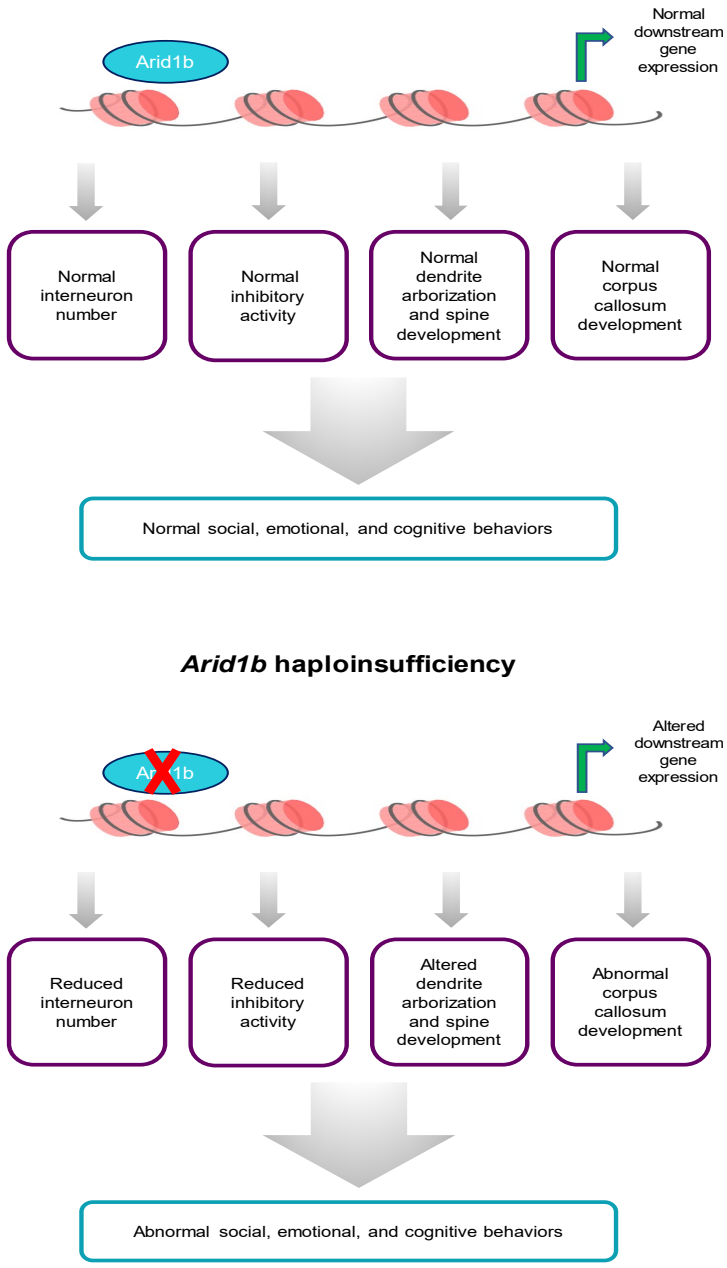

Figure 1.3 Altered gene expression and neuronal effects of *Arid1b* haploinsufficiency
Arid1b haploinsufficient mice exhibit altered expression of downstream genes, leading to functional, anatomical, and behavioral deficits.

Covalent modifications of histones, including acetylation and methylation, are essential regulators of transcription (Day and Sweatt, 2011; Mehler, 2008). Jung et al. report that *Arid1b* heterozygotes present with reduced acetylation of histone H3 at lysine 9 (H3K9ac) and tri-methylation of histone H3 at lysine 4 (H3K4me3), markers of transcriptional activation, and increased tri-methylation of histone H3 at lysine 27 (H3K27me3), a marker of transcriptional repression (Jung et al., 2017). While this would suggest that *Arid1b* haploinsufficiency suppresses activity of histone acetyltransferases (HATs) or enhances activity of histone deacetylases (HDACs), no global differences in HAT or HDAC activity were observed (Jung et al., 2017). However, levels of two HATs, acetyl-CREB-binding protein (CBP) and P300/CBP-associated factor (PCAF), bound to histone H3 were decreased in heterozygotes (Jung et al., 2017). These results indicate that Arid1b may bridge the interaction between histone H3 and various HATs, supporting evidence that chromatin remodelers and covalent modifiers work in cooperation with one another to regulate gene expression.

Jung et al. also report a reduction in the *parvalbumin* (*Pvalb*) gene with *Arid1b* haploinsufficiency, which is consistent with the observed decrease in PV positive interneurons in the cortices of these mice (Jung et al., 2017). A reduction in the amount of Arid1b bound to the *Pvalb* promoter and a decrease in H3K9ac at the promoter site is also reported, likely resulting in decreased initiation of transcription of the gene (Jung et al., 2017). Two additional genes associated with interneuron development, *Gad1* and *Slc32a1*, shared similar results: reduced gene expression and decreased binding of Arid1b at the promoter sites (Jung et al., 2017). These results implicate the importance of Arid1b in regulating interneuron-associated genes by interacting with gene promoters, recruiting HATs, and facilitating chromatin remodeling for initiating transcription. Furthermore, *Arid1b* haploinsufficiency was shown to reduce the expression of β-catenin

and its localization to the nucleus, consequently reducing expression of several target genes, including *Cyclin D1, c-Myc, n-Myc, Creb, Lef1,* and *Ctnnb1* (Jung et al., 2017). Wnt-β-catenin signaling plays a crucial role in regulating ventral progenitor proliferation during neurodevelopment (Hur and Zhou, 2010; Vasileiou et al., 2015). Future studies may reveal a role of Arid1b in the regulation of Wnt-β-catenin signaling and ventral progenitor proliferation. A summary of ASD-associated genes with altered expression levels in *Arid1b* heterozygotes can be found in Table 1.2.

Gene	Description/Function	Gene	Description/Function
Grin2b	NMDA receptor subunit	*Zbtb20*	Transcription factor
Prickle1	Nuclear receptor	*Nting1*	Neurite outgrowth-promoting protein
Prickle2	Nuclear receptor	*Robo1*	Membrane protein involved in axon guidance and cell migration
Homer1	Postsynaptic density scaffolding	*Sspo*	Neuronal aggregation modulator
Sox5	Transcription factor	*Pvalb*	Calcium-binding protein
Egr2	Transcription factor	*Gad1*	Enzyme for producing GABA neurotransmitter
Epha6	Receptor tyrosine kinase	*Slc32a1*	Vesicular inhibitory amine acid transporter
Lama1	Laminin alpha 1 subunit	*Ctnnb1*	Transduction of Wnt signaling
Rbfox1	Alternative splicing regulator	*Ccnd1*	Cell cycle regulation
Mkl2	Transcriptional coactivator	*c-Myc/n-Myc*	Transcription factors
Itga4	Integrin subunit	*Creb*	Transcription factor
Nbea	A-kinase anchor protein	*Lef1*	Activates T-cell receptor-alpha

Table 1.2 Select downregulated genes with *Arid1b* haploinsufficiency
Haploinsufficiency of *Arid1b* leads to reduced expression of several categories of genes, including transcription factors, receptors and receptor subunits, regulators of cell cycle, and components contributing to synaptic function.

1.4 Autism spectrum disorder and intellectual disability

1.4.1 Genetic mouse models

To better elucidate the mechanisms underlying ASD, ID, and related developmental disorders, several animal models have been developed. Rodents are an ideal model for the study of neurodevelopmental and psychiatric disorders, as the majority of these disorders have at least some component of genetic origins (Ayhan and Konopka, 2019; Ellison et al., 2013; Krumm et al., 2014; Ropers and Wienker, 2015; Srivastava and Schwartz, 2014) and there is significant homology between the human and mouse genome (Eppig et al., 2015; Pennacchio, 2003). Additionally, rodents exhibit an array of complex behaviors, which is helpful for studying disorders with significant behavioral phenotypes. With the rise of novel tools for studying and manipulating genetics, researches can better study the behavioral effects of genetic manipulation in rodents (Heidenreich and Zhang, 2016).

ASD is characterized primarily by stereotyped behaviors and deficits in sociability and communication (Fakhoury, 2015; Walsh et al., 2011). ID, characterized by significant cognitive dysfunction and adaptive behavior deficits, is seen in approximately 75% of individuals with ASD (Ellison et al., 2013). Several mouse models for ASD/ID have been generated in addition to *Arid1b* knockout mice. One of the most frequent genetic causes of ASD is fragile X syndrome (FXS), caused by expanded CGG repeats in the 5’ untranslated region of the *fragile X mental retardation 1 gene* (*FMR1*), leading to loss of the FMR1 protein (Harris et al., 2008; Kogan et al., 2009). *Fmr1* knockout mouse models exhibit several behavioral abnormalities recapitulated in human ASD patients, including social and cognitive deficits, anxiety-like behaviors, and epilepsy (Gibson et al., 2008; McNaughton et al., 2008; Selby et al., 2007; Yabe et al., 2004). Other mouse models of ASD that have been generated and extensively studied are

knockouts of *neuroligin 3* (*Nlgn3*), *neuroligin 4* (*Nlgn4*), *contactin-associated protein-like 2* (*Cntnap2*), and *SH3 and multiple ankyrin repeat domains 3* (*Shank3*) genes. These mice exhibit behavioral abnormalities consistent with human patients with mutations in these genes, including social deficits, stereotyped behaviors, and increased seizure susceptibility (Jamain et al., 2008; Peca et al., 2011; Penagarikano et al., 2011). Rett syndrome, which is characterized by ASD-like behavior, learning impairments, motor deficits, and epilepsy, is caused mutations in the gene encoding *methyl-CpG binding protein 2* (*MECP2*), leading to loss of MECP2 protein expression (Chahrour and Zoghbi, 2007). *Mecp2* knockout mice have similar behavioral phenotypes to human patients (Calfa et al., 2011; Chen et al., 2001; Guy et al., 2001). Additionally, Angelman syndrome, caused by loss of the maternal *ubiquitin protein ligase E3A* (*UBE3A*) allele, has a frequent co-morbidity with autism (Steffenburg et al., 1996; Trillingsgaard and JR, 2004). Mouse models exhibit phenotypes similar to human patients, including high susceptibility to seizures due to dysfunction in inhibitory activity (Wallace et al., 2012). While the genetic causes of ASD and related disorders are highly heterogenous, comparisons of neural and behavioral deficits across these diverse models can hopefully provide insight on converging mechanisms underlying the pathogenesis.

1.4.2 Current and prospective therapies

There is no treatment tool available for the core symptoms of ASD and ID. Current pharmacologic strategies focus on GABAergic modulation to normalize the deficits in inhibitory activity. GABA agonists to enhance inhibition, such as benzodiazepines and anticonvulsants, have been useful in treating some behaviors associated with ASD in humans, including aggressive and hyperactive behaviors (Belsito et al., 2001; Di Martino and Tuchman, 2001). Use of clonazepam, a positive modulator of the $GABA_A$ receptor, to enhance inhibitory activity in mouse models has also been

successful in rescuing both behavioral phenotypes and inhibitory activity deficits (Han et al., 2012; Jung et al., 2017). In some cases, excessive inhibitory activity has been observed in ASD/ID and related disorders (Fernandez et al., 2007). Treatment with a GABA antagonist in mouse models with elevated inhibition successfully rescued neural and behavioral deficits both in adolescents and into adulthood (Cui et al., 2008). Several studies have also implicated the contribution of brain-derived neurotrophic factor (BDNF) signaling deficits to the pathology of ASD and ID (Hur and Zhou, 2010; Jiang et al., 2005; Ka et al., 2014a; Witte and Bradke, 2008), and as such, ongoing research also focuses developing pharmacologic treatments targeting this pathway.

In addition to pharmacologic treatments, a major focus in the field has shifted to genetic treatment strategies. Gene therapy relies on virus-mediated delivery of the affected gene to normalize its expression in the brain. A handful of studies have demonstrated that normalizing expression and function of an affected gene during postnatal development and adulthood can rescue the neurological deficits associated with ASD and ID (Daily et al., 2011; Guy et al., 2007; Mei et al., 2016). Use of adeno-associated viruses (AAVs) for gene therapy is currently being used in clinical or pre-clinical trials for various CNS disorders, including Alzheimer's, Parkinson's, epilepsy, and pain disorders (Hocquemiller et al., 2016). The success of AAVs for gene delivery in CNS disorders together with the ability to rescue ASD/ID phenotypes after early developmental stages provides a promising outlook on the future of genetic therapy. A prominent shortcoming of these strategies is that they are currently non-specific and aim to target the brain as a whole. As we continue to gain a better understanding of the cellular and molecular events that lead to these neurodevelopmental disorders, we can develop more targeted therapeutic strategies, such as targeting specific cell types and circuits.

1.5 Role of interneurons in neurodevelopmental disorders

1.5.1 Excitatory/Inhibitory balance

While the pathology underlying ASD and ID is still largely unknown, it has been hypothesized that individuals affected exhibit disproportionately weak levels of inhibition or high levels of excitation in brain circuits regulating social, communication, and cognitive functions (Gogolla et al., 2009; Nelson and Valakh, 2015; Rubenstein and Merzenich, 2003). High levels of circuit plasticity during critical periods of early development allow neurons to form these functional connections through an experience-dependent phase of maturation (Gogolla et al., 2009). A controlled balance between excitation and inhibition (E/I balance) is formed during this period, and maintaining this balance is essential for proper circuit function (Lee et al., 2017). Several factors contribute to the regulation of normal neuronal E/I balance, including excitatory/inhibitory synapse development, synaptic transmission and plasticity, and proper signaling pathways that mediate these functions (Gatto and Broadie, 2010; Lee et al., 2017). Dysfunction in these processes, due to various genetic mutations or environmental factors, leads to a disrupted E/I balance and is implicated in several neurodevelopmental disorders (Gatto and Broadie, 2010; Rubenstein and Merzenich, 2003; Zikopoulos and Barbas, 2013). Converging evidence from several animal and human studies suggest that cellular anatomical features of neurons, such as axon and spine development, also contribute to changes in circuit connectivity that leads to E/I imbalances (Zikopoulos and Barbas, 2013). While the E/I imbalance theory is a convincing model of the pathogenesis of neurodevelopmental disorders, it is important to acknowledge that it is an overly simplistic model. Individual microcircuits throughout brain regions exhibit different combinations of excitation and inhibition levels and sources of input, which may affect neuronal functions differently (Rubenstein and Merzenich, 2003). However, despite these complexities, many signaling pathways and activity-dependent processes that

affect excitatory and inhibitory transmission are conserved in circuits across multiple brain regions (Nelson and Valakh, 2015). It is not unreasonable to assume that neurodevelopmental disorders may similarly affect excitatory or inhibitory synaptic function throughout distributed areas of the brain.

It is also important to note a recent study that presents an alternate perspective to the E/I theory of autism. Antoine et al. examine the hypothesis that in increased E/I ratio causes hyperexcitability and excess spiking in four different mouse models of autism (Antoine et al., 2019). While they verified an increase in the E/I ratio, this did not cause an excess of synaptic depolarization or spiking of pyramidal cells, suggesting that the common assumption that an increase in the E/I synaptic conductance ratio necessarily predicts increased spiking excitability is incorrect (Antoine et al., 2019). Given these results, an alternative explanation suggests that various ASD mutations alter cortical spiking activity, which secondarily engages an E/I homeostasis mechanism to restore normal cortical firing rate, thus altering the E/I balance. ASD symptoms may still arise as a result of imperfect or insufficient homeostasis.

1.5.2 Interneuron deficits in neurodevelopmental disorders

Perturbation of the well-balanced excitatory and inhibitory components can lead to life-long cognitive, social, and emotional disabilities. Impairments in GABAergic interneuron development has been implicated in several neurodevelopmental disease states. Many studies have shown that mutations in ASD/ID-associated genes frequently alter GABAergic function. Mouse models with gain of function mutations in *Nlgn3* exhibit elevated levels of inhibitory activity (Tabuchi et al., 2007), and mice with loss of function mutations in the *Nlgn4* gene show a reduction of inhibitory activity (Jamain et al., 2008; Zhang et al., 2009). Truncating mutations in several genes affecting GABA receptors have also been shown in human ASD/ID patients (Piton et al., 2013), and post-mortem

brains of these patients exhibit a reduction in GABA receptors (Fatemi et al., 2009; Oblak et al., 2011). Mouse models of Rett syndrome have consistently exhibited a reduction in expression of Gad1, Gad2, and GABA, leading to decreased inhibitory activity (Chen et al., 2001; Guy et al., 2001). FXS mouse models show decreased inhibitory neuron output as well as fewer GABAergic neurons (Curia et al., 2009; Gibson et al., 2008; Selby et al., 2007). Angelman syndrome has also been shown to have reduced inhibition onto pyramidal neurons, resulting in decreased excitatory outputs in both mouse models and humans (Wallace et al., 2012). Human patients with schizophrenia, another neurodevelopmental disorder caused by loss of function mutations in genes encoding *neuregulin 1* (*NRG1*) and its receptor tyrosine kinase *ERBB4*, also show a reduction in Gad1, Gad2, and GABA expression leading to inhibitory activity deficits (Chen et al., 2010; Wen et al., 2010). Additionally, ample evidence suggests a relationship between PV/SST interneuron abnormalities and the behavioral deficits seen in ASD and ID. *Fmrp, Mecp2,* and *Nlgn4* knockout mouse models all exhibit a reduction in PV interneurons within the cortex (Fukuda et al., 2005; Gogolla et al., 2009; Selby et al., 2007), and post-mortem brains of autistic patients show a similar decrease in PV subtypes (Hashemi et al., 2017; Zikopoulos and Barbas, 2013). Mice with loss of the *phosphatase and tensin homolog* (*Pten*) gene, another ASD-associated gene, have fewer SST interneurons in the cortex (Vogt et al., 2015). *Shank1* and *Cntnap4* knockout mice both show reduced levels of PV interneuron output (Karayannis et al., 2014; Mao et al., 2015). Heterozygous and homozygous deletion of the *parvalbumin* (*Pvalb*) gene leads to ASD-associated developmental anatomical changes and disruption in both excitatory and inhibitory transmission (Wohr et al., 2015). The high incidence of interneuron abnormalities in these disorders strongly supports the theory that disruption of the E/I balance contributes to the pathology of neurodevelopmental disorders.

1.6 Role of excitatory neurons in neurodevelopmental disorders

1.6.1 Regulation of neurite outgrowth

Neurite development can be divided into three main steps: axon and dendrite specification during neuronal polarization, neurite growth and guidance, and neurite branching and synaptogenesis (Barnes and Polleux, 2009; Lewis et al., 2013). The basis of mediating these steps is dynamic organization of the cytoskeleton. Actin and microtubule dynamics play a crucial role during neuronal polarization. The primary way for the axon to differentiate from other neurites that become dendrites is to exhibit different cytoskeleton dynamics (Barnes and Polleux, 2009; Lewis et al., 2013; Shi et al., 2003). The tip of the neurite that becomes the axon contains unstable actin filaments that are more dynamic and flexible than those in other neurites (Witte and Bradke, 2008). This polarized destabilization of actin allows invasion of distally polymerizing MTs into the growth cone, promoting preferential elongation of the axon (Lalli, 2014; Witte and Bradke, 2008). Several microtubule-associated proteins (MAPs) play a critical role in the stabilization and polymerization of MTs. Different MAPs are distinctly localized to neurites that become dendrites and the neurite to become the axon via selective motor protein transport, contributing to the establishment of polarity (Lewis et al., 2013; Namba et al., 2015). Dendrite-specific MAP1B and axon-specific Tau and collapsing response mediator protein 2 (CRMP2) prevent interactions between microtubule-severing proteins and MTs, thus stabilizing them and promoting extension at the distal plus end. Another microtubule associated protein, adenomatous polyposis coli (APC), is expressed in both axons and dendrites (Lalli, 2014; Lewis et al., 2013). Rather that nonstop outgrowth, neurites grow in a noncontinuous fashion, undergoing frequent pauses and retractions, followed by resumed forward growth (Lewis et al., 2013). This process facilitates the complex branching observed in mature neurons. Neurite branching allows for a single neuron to connect to a broad range of postsynaptic targets and receive several inputs.

Branching occurs through two different mechanisms. The first is through splitting of the growth cone, and is the primary mechanism utilized by axons (Luo and O'Leary, 2005). The second, known as interstitial branching, occurs through the formation of collateral branches directly along the neurite shaft (Gomez et al., 2001; Gomez and Spitzer, 1999; Luo and O'Leary, 2005). F-actin filaments accumulate along the neurite shaft and serve as nucleators to give rise to a protrusion. MTs along the main shaft get fragmented, followed by invasion and elongation within the protrusion (Lewis et al., 2013). Most dendritic branching occurs through interstitial branching. Time lapse imaging has shown that this type of branching occurs after the pausing phase of neurite extension, shortly before continuing the forward growth (Catalano and Shatz, 1998). Interestingly, the plasticity of cytoskeletal dynamics in neuronal polarity and outgrowth does not end during early neuronal development. After the severing of an axon, a dendrite still has the capacity to become a new axon with relocalization of polarity molecules (Barnes and Polleux, 2009; Witte and Bradke, 2008).

Several factors influence the regulation of cytoskeletal dynamics. Intracellular signaling pathways are the primary regulators of cytoskeletal dynamics that mediate neurite development. BDNF neurotrophic signaling is a master regulator of neurite development (Hur and Zhou, 2010; Yoshimura et al., 2005). Tropomyosin receptor kinase B (TrkB) activation by BDNF leads to a downstream intracellular signaling cascade. Phosphoinositide 3-kinase (PI3K) becomes activated by phosphorylation, which subsequently phosphorylates and activates protein kinase B (AKT), which then phosphorylates GSK3β rendering it inactive (Hur and Zhou, 2010; Jiang et al., 2005). This intracellular signaling pathway controls MT stabilization and elongation by acting on proteins involved in MT dynamics, including CRMP2, Tau, MAP1B, and APC (Skene, 1989; Yoshimura et al., 2005). During establishment of polarity, phosphorylated GSK3β

(p-GSK3β), the inactive form of the protein, accumulates specifically at the tip of the neurite that becomes the nascent axon, while non-phosphorylated GSK3β is expressed throughout other neurites (Jiang et al., 2005; Skene, 1989). Activation of GSK3β in dendrites above basal levels leads to activation of the ubiquitin/proteasome protein degradation system, which causes local degradation of CRMP2, Tau, and other axon-specific proteins within the dendritic compartment (Barnes and Polleux, 2009; Hur and Zhou, 2010). When CRMP2, APC, and Tau are phosphorylated by GSK3β, their ability to bind to tubulin dimers is abolished, which inhibits neurite elongation (Skene, 1989; Yoshimura et al., 2005). Inactivation of GSK3β in the nascent axon thus promotes association between CRMP2/APC/Tau and microtubule plus ends, stabilizing the growing ends of MTs to promote axon elongation. Phosphorylation of MAP1B by active GSK3β renders MAP1B more stable, maintaining MTs in a dynamic state and promoting extension of dendrites (Hur and Zhou, 2010; Yoshimura et al., 2005). During genesis of cortical projection neurons, axon outgrowth begins during migration, and rapid extension and branching of the axon continues after migration ends. In contrast, dendrite growth and branching does not begin until after cells have reached their location in the cortex, and dendritic growth occurs 5-10 times slower than axon growth (Azzarelli et al., 2014; Lalli, 2014). Once the neuron reaches the target location, dendrites gradually begin to express the phosphorylated form of GSK3β, though at much lower concentrations than in axons (Hur and Zhou, 2010). The combination of active and inactive forms results in stabilization of APC in addition to MAP1B, contributing to increased dendrite growth. Studies have shown that overexpression of p-CRMP2 and p-Tau leads to reduced axon growth and branching (Jung et al., 2015; Kim et al., 2009; Yoshimura et al., 2005). Additionally, expression of a constitutively active form of GSK3β results in inhibition of axon formation. In contrast, inhibition of GSK3β activity results in formation of multiple axons (Jiang et al., 2005; Kim et al., 2006). These manipulations further underscore the

importance of molecular polarization during the specification of axons and dendrites. Interestingly, GSK3β knockout mouse models do not exhibit deficits in neurite development, but mice lacking both GSK3α and GSK3β isoforms do, suggesting a compensatory mechanism of GSK3α when GSK3β is lost (Kim et al., 2006).

In addition to BDNF signaling, multiple other intracellular pathways converge onto GSK3β and affect neurite development. mTOR is another downstream component of the BDNF signaling pathway. Activation of PI3K and AKT leads to inhibition of the tuberous sclerosis complex 2 (TSC2), a negative regulator of mTOR, thus activating mTOR and its downstream targets eukaryotic translation initiation factor 4E-binding protein (4EBP) and ribosomal protein S6 kinase beta-1 (S6K) (Barnes and Polleux, 2009; Hur and Zhou, 2010). Evidence suggests that mTOR activation is localized specifically within the neurite to become the axon and initiates translation of axon-specific microtubule-associated proteins CRMP2 and Tau (Hur and Zhou, 2010; Morita and Sobue, 2009). When GSK3β is in its active form, it activates TSC2, thus inhibiting activity of mTOR. Upon phosphorylation and inactivation of GSK3β, activity of mTOR is increased (Ka et al., 2014a). This suggests a direct interplay between mTOR and GSK3β that enhances downstream signaling to maintain proper cytoskeletal dynamics in neurites. Additionally, signaling involving the partitioning defective protein 3/6/protein kinase C (PAR3/PAR6/PKC) complex is essential for establishing proper specification of axons and dendrites (Barnes and Polleux, 2009; Hur and Zhou, 2010). PAR3 and PAR6 are localized at the tips of all neurites prior to polarization, and later become enriched in the axon growth cone to aid in axon elongation (Lewis et al., 2013; Shi et al., 2003). Inactivation of GSK3β is required to mediate targeting of these components to the axon and to initiate formation of the complex (Shi et al., 2003). GSK3β-mediated phosphorylation of MACF1 in neurites to become dendrites also modulates actin and MT

dynamics and regulates dendritic arborization (Moffat et al., 2017). Mice with loss of MACF1 exhibited altered cytoskeleton arrangements in neurites and showed decreased dendritic arborization in cortical and hippocampal neurons (Ka and Kim, 2016). GSK3β also plays a role in regulating Wnt/β-catenin signaling, a master regulator of neurodevelopment. GSK3β forms a destruction complex with other proteins and targets β-catenin for degradation. In the presence of Wnt, the complex is then recruited to the frizzled receptor, inhibiting GSK3β and allowing accumulation of β-catenin and subsequent targeting to the nucleus to initiate transcription of cytoskeletal-associated genes (Hur and Zhou, 2010; Namba et al., 2015). The complex intracellular signaling network regulating cytoskeleton dynamics and neurite outgrowth is illustrated in Figure 1.4.

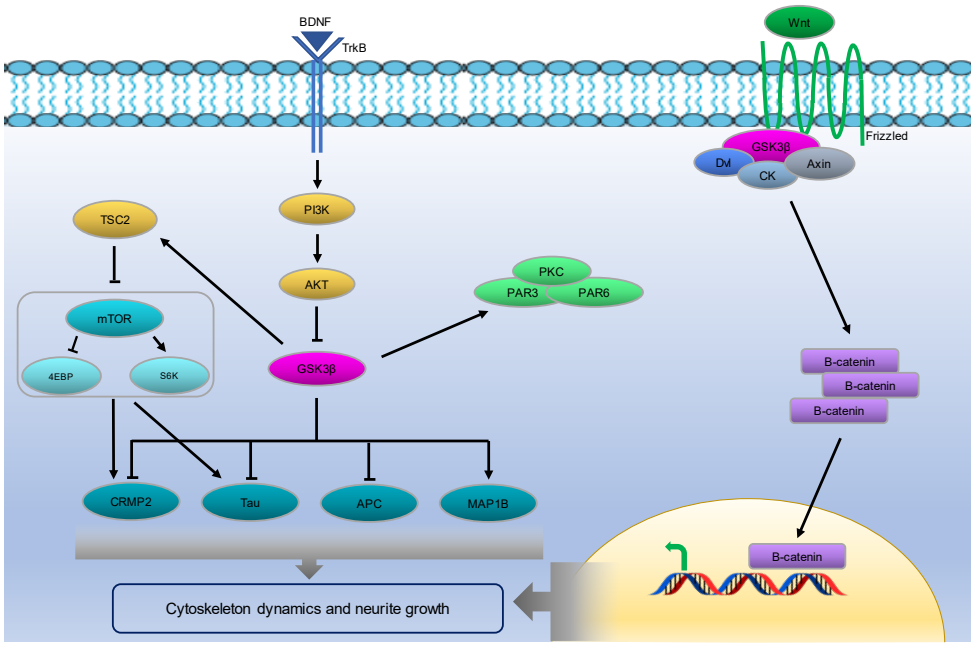

Figure 1.4 Intracellular signaling pathways regulating neurite outgrowth
BDNF neurotrophic signaling is a master regulator of cytoskeleton dynamics and neurite outgrowth. GSK3β, a downstream component of BDNF signaling,acts as a hub while also playing a role in multiple other intracellular pathways regulating these processes, including mTOR, PAR complex, and Wnt/β-catenin signaling.

Interestingly, once neurite outgrowth is complete, the machinery responsible remains at the proximal end of the axon/dendrite near the soma (Namba et al., 2015). This allows for a neuron to regenerate a neurite if it gets severed. In culture, if an axon is severed very near the soma at the proximal end, it is unable to regenerate (Sengottuvel et al., 2011). Instead, one of the dendrites becomes the new axon. When severed more distally, the axon regrows back to its original length (Sengottuvel et al., 2011). Additionally, *in vivo* studies of nerve injury show that after crushing or severing the nerve, MT stabilization is able to induce complete axon regeneration (Hellal et al., 2011). Furthermore, with loss of BDNF signaling downstream of PI3K, axon regeneration is unable to occur after nerve injury (Park et al., 2008). These studies indicate that although adult neurons lose much of their plasticity after fully maturing, neurite deficits may still be salvageable beyond the critical developmental period by normalizing neurotrophic signaling and cytoskeletal dynamics.

1.6.2 Neuron maturation deficits in neurodevelopmental disorders

Deficits in neuron maturation have been implicated in the pathology of many neurodevelopmental and psychiatric disorders (Chapleau et al., 2009; Fiala et al., 2002; Kaufmann and Moser, 2000; Machado-Salas, 1984; Penzes et al., 2011). In addition to neurite outgrowth, dendritic spine development is an essential step in neuron maturation, as spines are the main site of excitatory input and form the basis of synaptic circuitry (Bourne and Harris, 2008; Harris and Kater, 1994). Post-mortem brains of human ASD and ID patients frequently exhibit altered axon fibers of the corpus callosum, abnormal dendritic arborization, and increased spine density in cortical pyramidal neurons (Aoki et al., 2017; Gilbert and Man, 2017; Hutsler and Zhang, 2010; Huttenlocher, 1974; Kucharsky Hiess et al., 2015; Martínez-Cerdeño, 2017; Penzes et al., 2011). Rett syndrome patients also have reduced dendritic arborization and abnormal spine

development in the cortex (Armstrong, 2005; Belichenko et al., 1994; Kaufmann and Moser, 2000). Abnormal spine development is a primary characteristic of cortical neurons in patients with Down syndrome, which is the most common cause of ID (Kaufmann and Moser, 2000). Individuals affected generally have reduced spine density, spine size, and abnormal spine morphology, such as short stubby spines or long filopodia-like spines (Marin-Padilla, 1976; Roberts et al., 1996). Post-mortem brains from patients with tuberous sclerosis, a condition frequently co-occurring with ASD, have a similar atypical morphology and reduction in spine number and size (Machado-Salas, 1984). Additionally, FXS is characterized by an increase in spine density (Fiala et al., 2002; Kaufmann and Moser, 2000).

Mouse models of various neurodevelopmental disorders recapitulate several of these deficits seen in human patients. Downregulation of *thousand and one amino acid kinase 2* (*Taok2*), an ASD susceptibility gene, disrupts the formation of basal dendrites and axonal projections in cortical pyramidal neurons (de Anda et al., 2012). In a mouse model of Rett syndrome, *Mecp2* deficient neurons have deficits in neurite outgrowth due to altered MT dynamics (Nectoux et al., 2012). *Mecp2* deficient mice also exhibit reduced cortical thickness, reduced spine density, abnormal dendritic development, and delayed neuronal maturation within the cortex (Fukuda et al., 2005; Irwin et al., 2002; Jentarra et al., 2010). Mecp2 duplication syndrome, a neurodevelopmental disorder characterized by ID, autism, motor abnormalities, and epilepsy, results in increased spine density and dendritic overgrowth (Jiang et al., 2013). Overexpression of the Down syndrome-associated gene *dual specificity tyrosine phosphorylation regulated kinase 1a* (*Dyrk1a*) leads to reduced spine density and abnormal spine morphology caused by changes in the dynamic reorganization of the cytoskeleton (Martinez de Lagran et al., 2012; McKinney et al., 2005). Multiple mouse models of FXS also exhibit increased

dendritic spine density and atypical spine dynamics and morphology (Han et al., 2015; Nagaoka et al., 2016).

Additional studies have suggested that BDNF signaling is involved in the pathology of various neurodevelopmental disorders. Haploinsufficiency of the chromatin regulator gene *ankyrin repeat domain 11* (*Ankrd11*) has been associated with ASD and ID (Isrie et al., 2012; Lo-Castro et al., 2013; Sirmaci et al., 2011). Knockdown of the gene results in deficits in dendritic arborization and spine development as well as reduced BDNF signaling and decreased expression of downstream targets (Ka and Kim, 2018). Altered BDNF signaling has also been implicated in several other established mouse models of FXS, Rett syndrome, and Angelman syndrome (Cao et al., 2013; Chang et al., 2006; Lauterborn et al., 2007). Changes in GSK3 signaling activity has been associated with altered neurite development and ASD/ID-related behaviors (Jiang et al., 2005; Jung et al., 2015; Kim et al., 2006; Lalli, 2014), and thus GSK3 has been a common therapeutic target for various psychiatric drugs (Hur and Zhou, 2010). Together, these studies indicate that deficits in neurite growth and synaptogenesis, mediated by altered BDNF signaling, is a likely component of the underlying pathology of ASD/ID and related disorders.

CHAPTER 2: ARID1B MODULATES DISTINCT ASD/ID-LIKE BEHAVIORS THROUGH DIFFERENT INTERNEURON SUBTYPES

Amanda L Smith[1], Eui-Man Jung[2], Byeong-Tak Jeon[3], and Woo-Yang Kim[3*]

[1]Department of Pharmacology and Experimental Neuroscience, University of Nebraska Medical Center, Omaha, NE 68198, USA

[2]Laboratory of Veterinary Biochemistry and Molecular Biology, Chungbuk National University, Cheongju, Chungbuk 28644, Republic of Korea

[3]Department of Biological Sciences, Kent State University, Kent, OH 44242, USA

2.1 Abstract

Inhibitory interneurons are essential for proper brain development and function. Dysfunction of interneurons is implicated in several neurodevelopmental disorders, including autism spectrum disorder (ASD) and intellectual disability (ID). We have previously shown that *Arid1b* haploinsufficiency interferes with interneuron development and leads to social, cognitive, and emotional impairments consistent with ASD and ID. It is unclear, however, whether interneurons play a major role for the behavioral deficits in *Arid1b* haploinsufficiency. Furthermore, it is critical to determine which interneuron subtypes contribute to distinct behavioral phenotypes. In the present study, we generated *Arid1b* haploinsufficient mice in which a copy of the *Arid1b* gene is deleted in either parvalbumin (PV) or somatostatin (SST) interneurons, and examined their ASD- and ID-like behaviors. We found that *Arid1b* haploinsufficiency in PV or SST interneurons resulted in distinct features that do not overlap with one another. *Arid1b* haploinsufficiency in PV neurons contributed to social and emotional impairments, while the gene deletion in the SST population caused stereotypies and cognitive dysfunction. These findings demonstrate a critical role of interneurons in *Arid1b* haploinsufficient pathology and suggest that PV and SST interneurons may have distinct roles in modulating neurological phenotypes in *Arid1b* haploinsufficiency-induced ASD and ID.

2.2 Introduction

Autism spectrum disorder (ASD) and intellectual disability (ID) are highly prevalent neurodevelopmental disorders, characterized by social communication impairments and cognitive dysfunction, respectively (Ellison et al., 2013; Fakhoury, 2015). Emotional disturbance such as aggressive behavior, depression, and anxiety is another significant aspect of ASD and ID (Benson and Brooks, 2008; DeFilippis, 2018; Fitzpatrick et al., 2016; Matson and Nebel-Schwalm, 2007; van Steensel et al., 2013; White et al., 2009). While behaviors of ASD and ID are relatively well characterized, the neuropathogenesis of these conditions is poorly understood. Accordingly, no pharmacologic or genetic interventions are available for ASD or ID. Haploinsufficiency of the *AT-rich interactive domain 1B* (*ARID1B*) gene has been shown to cause ASD and ID in humans (Halgren et al., 2012; Hoyer et al., 2012; Santen et al., 2012a). ARID1B is a component of the Brg/Brm associated factor (BAF) chromatin remodeling complex in the brain (Tang et al., 2010; Wang et al., 2004). It binds to DNA through its AT-rich DNA-binding domain and alters chromatin structure, facilitating transcription factor access and regulating gene expression.

Many neurodevelopmental disorders exhibit improper inhibitory interneuron development, resulting in excitatory/inhibitory (E/I) imbalance (Marin, 2012; Nelson and Valakh, 2015; Ramamoorthi and Lin, 2011). We have previously generated an *Arid1b* mouse model and showed that *Arid1b* haploinsufficient (*Arid1b*$^{+/-}$) mice recapitulate ASD and ID behavior (Jung et al., 2017). Importantly, *Arid1b* haploinsufficient mice exhibit a reduction and abnormal distribution of interneurons as well as abnormal inhibitory synaptic activity in the cerebral cortex (Jung et al., 2017). No clear anatomical or physiological phenotype has been found in excitatory neurons, suggesting a more

prominent effect on interneuron abnormalities in potentially creating a range of social, intellectual, and emotional deficits in *Arid1b* haploinsufficient mice.

Thus, we hypothesized that *Arid1b* haploinsufficiency-induced neurological behavior is mediated by interneurons. To test this idea, we conditionally knocked out the *Arid1b* gene in parvalbumin (PV) and somatostatin (SST) interneurons using specific Cre-drivers and examined neurological behaviors in interneuron-specific *Arid1b* haploinsufficient mice. PV and SST neurons are the most populous interneuron subtype in the cortex, each constituting 30%-40% of the inhibitory interneuron population (Rudy et al., 2011). These subtypes exhibit a range of different morphological, electrophysiological, and molecular properties, and appear to play roles in distinct circuit functions (Kepecs and Fishell, 2014; Klausberger and Somogyi, 2008). Little is known regarding how these individual interneuron subtypes differentially modulate various behaviors. Here, we show that *Arid1b* haploinsufficiency in PV and SST neurons has distinct, non-overlapping behavioral phenotypes that recapitulate behavioral deficits seen in *Arid1b* haploinsufficient mice. PV interneurons with *Arid1b* haploinsufficiency alter social and emotional behaviors, while SST interneurons of the gene mutation affect cognitive and stereotyped behaviors. Our findings demonstrate that interneurons mediate *Arid1b* haploinsufficiency-induced behaviors and suggest distinct individual roles of PV and SST interneurons for ASD and ID behavior.

2.3 Materials and methods

2.3.1 Arid1b conditional knockout mice

The *Arid1b*-floxed allele (Jung et al., 2017) was crossed with either the PV-Cre (B6;129P2-Pvalb$^{tm1(cre)Arbr}$/J; JAX 008069) or SST-Cre (B6N.Cg-Sst$^{tm2.1(cre)Zjh}$/J; JAX 018973) allele. After weaning, all mice were group housed (no more than 5 mice per cage) as a mix of genotypes on a 12-hour light/dark cycle. All mice used as “stranger mice” in behavioral assays were housed separately from experimental mice. All husbandry and experimental procedures were reviewed and approved by the Institutional Animal Care and Use Committee (IACUC) of Kent State University and the University of Nebraska Medical Center.

2.3.2 Immunostaining

Immunostaining of brain sections was performed as described previously (Ka and Kim, 2018; Ka et al., 2016b) . The following primary antibodies were used: anti-Parvalbumin (Millipore, Rabbit, AB1572), anti-Arid1b (Abcam, Mouse, ab57461), and anti-Somatostatin (Millipore, Rat, AB1572). 4′,6-diamidino-2-phenylindole (DAPI; Sigma) was used for counterstaining. Appropriate secondary antibodies conjugated with Alexa Fluor dyes (Invitrogen) were used to detect primary antibodies. All slides were visualized and imaged under FV3000 (Olympus) fluorescent confocal microscope system. The levels of protein expression were quantified by measuring fluorescence intensities using NIH ImageJ.

2.3.3 Behavioral assays

All behavior assays were performed during the light cycle. Health conditions, including weight, activity, and feeding were checked before assays. Male and female mice at ages 2-4 months were used for all behavior assays, and all assays were done in the same chronological order and timeframe. For social behavior assays, only male-

male or female-female social interactions were examined to avoid interference of male-female sexual interactions and estrous cycle timing. All behavioral assays were done blind to genotypes, with age-matched littermates.

2.3.4 Three-chamber test

A rectangular, transparent Plexiglas box (60 x 40 cm, Ugobasile) divided by walls with openings into three equal-sized compartments was used. Before starting any behavior testing, test mice were habituated to the empty apparatus for 5 minutes. For sociability testing, the test mouse was placed in the center chamber (chamber 2), an empty wire enclosure was placed in chamber 1, and an unfamiliar stimulus mouse designated as “stranger 1” was placed in a wire enclosure in chamber 3. The test mouse was allowed to explore the entire apparatus for 10 minutes. For the social novelty test, the stranger 1 mouse in its wire enclosure was randomly placed in either chamber 1 or 3, and a novel mouse designated as “stranger 2” was taken from a different home cage and placed in the empty wire enclosure within the other flanking chamber. The test mouse was placed back into chamber 2 and allowed to explore the original stranger 1 or the novel stranger 2 for 10 minutes. Video recordings were taken of the test mouse during both sociability and social novelty tests. Time spent interacting with each wire enclosure was analyzed using video tracking EthoVision XT 7 software (Noldus). Both stranger mice were age- and sex-matched wild type mice.

2.3.5 Grooming assessment

A test mouse was placed in a clear plastic cage (17 x 32 x 14 cm) with normal housing bedding. Food and water were removed. The mouse was habituated to the cage for 10 minutes, followed by a 10-minute testing period in which the mouse was allowed to explore the cage freely. The movement of the mouse was recorded by a camera during the testing period, and the total time spent grooming was analyzed. Head

washing, body grooming, genital/tail grooming, and paw and leg licking were all considered grooming behavior.

2.3.6 Open field test

A test mouse was placed near the wall of a 35 x 42 cm open field arena and allowed to explore freely for 5 minutes. The movement of the mouse during the 5-minute testing period was recorded by a camera. The number of entries into and the overall time spent in the center of the arena (15 x 15 cm imaginary square) were analyzed using EthoVision XT 7 software (Noldus). The open field arena was cleaned with ethanol and dried between each trial. The mice were not habituated to the arena before testing.

2.3.7 Elevated plus maze test

The elevated plus maze was performed as previously described (Jung et al., 2017) (Jung et al., 2016). The apparatus (EB Instrument) was elevated 45 cm above the floor, and the test mouse was placed on the central platform (5 x 5 cm). The mouse was allowed to freely explore either the two open arms (35 x 5 cm) or two enclosed arms (35 x 5 x 15 cm) for 5 minutes. The number of entries into and total time spent in open and closed arms were recorded.

2.3.8 Tail suspension test

A test mouse was suspended from 60 cm above the surface of a table using adhesive tape at the tip of the tail. The mouse was acclimatized for 1 minute, followed by a 5-minute testing period in which the total duration of immobility was measured. Passive, completely motionless hanging was considered immobile behavior.

2.3.9 Forced swim test

A test mouse was placed into a plastic cylinder (20 cm height, 17 cm diameter) filled with room temperature water to a depth of 10 cm. The mouse was acclimatized for

1 minute, followed by a testing period of 5 minutes in which the duration of immobility was measured. A mouse floating motionlessly was considered immobile.

2.3.10 Novel object recognition test

A test mouse was placed into an empty open field arena (35 x 42 cm) and allowed to explore freely during a 5-minute habituation period. The mouse was then removed and two objects of similar size (10.5 x 4.5 x 2.5 cm), but different shape and color, were placed in opposite corners of the arena, 7 cm from the side walls. The mouse was placed back into the arena and allowed to explore the two objects for 10 minutes. The mouse was returned to its home cage, and after 6 hours, one object was replaced with a novel object of a similar size but different shape and color than the previous object. The same test mouse was placed back in the arena to explore the familiar and novel objects for another 10 minutes while being recorded by a camera. The amount of time the mouse spent interacting with the two objects was analyzed using EthoVision XT software (Noldus).

2.3.11 Rotarod test

Mice were placed on rotating drums (3 cm diameter) of an accelerating rotarod (Rotamex 4/8, Columbus Instruments International). Three 5-minute trials per day (at constant speeds of 4, 8, and 12 rpm) were performed for three days of training. The following nine testing days consisted of one test trial per day, with the speed of the rotarod accelerating from 4 to 40 rpm over a 5-minute period. The time taken for the mouse to fall off the rotating rod was measured for each trial and recorded as its latency to fall.

2.3.12 Morris water maze test

A circular tank 110 cm in diameter and 91 cm in height (San Diego Instruments) was filled with water and divided into four equal quadrants (Q1-4) by lines drawn on the

floor. Visual cues of different color and shape were present on the wall of each quadrant as a spatial reference. A 10 cm circular plexiglass platform was submerged 1 cm deep in Q2, hidden from the mice. For each trial, test mice were placed at the perimeter of the tank in one of four quadrants. Four trials were performed per mouse per day during a ten-day training phase. Each trial ended when the mouse climbed onto and remained on the hidden platform for ten seconds. The mouse was given 20 seconds to rest on the platform between trials. The time taken by the mouse to reach the platform was recorded as its latency. The time for four trials was averaged and recorded as a result for each mouse on each day. To test memory retention, the mice were subjected to a single 60-second probe trial on day 11. The hidden platform was removed and each mouse started the trial from Q4. The swim path was video recorded, and the number of annulus crossings, velocity, and swim distance were analyzed using EthoVision XT 7 tracking software (Noldus).

2.3.13 Statistical analysis

Normal distribution was tested using the Kolmogorov-Smirnov test and variance was compared between populations. Statistical significance was determined using two-tailed unpaired Student’s t-tests for two population comparisons or repeated measures ANOVA. Data were analyzed using GraphPad Prism and presented as means ± SEM.

2.4 Results

2.4.1 Arid1b haploinsufficiency in PV and SST interneurons have distinct effects on social and stereotyped behaviors

Our previous study has shown that *Arid1b* haploinsufficient (*Arid1b*$^{+/-}$) mice exhibit social, emotional, and cognitive deficits as seen in ASD and ID (Jung et al., 2017). To determine the contributions of PV and SST interneurons to the ASD- and ID-like behaviors observed in *Arid1b*$^{+/-}$ mice, we generated two lines of conditional knockout mice lacking one copy of *Arid1b* in either PV (F/+; PV-Cre) or SST (F/+; SST-Cre) neurons by crossing floxed *Arid1b* mice with PV-Cre or SST-Cre mice, respectively. We then characterized these mice with multiple behavioral assays. *Arid1b* wild-type littermates with a Cre driver (+/+; PV-Cre or +/+; SST-Cre) were used as controls. To verify successful generation of conditional knockout mice, we examined ARID1B expression by co-labeling cortical sections with antibodies to ARID1B and PV or ARID1B and SST (Fig. 2.1). The level of ARID1B was decreased in the F/+; PV-Cre cortex by 42% compared to the protein level in control samples (Fig. 2.1a, b). A reduction in the ARID1B level by 48% was also observed in F/+; SST-Cre tissues (Fig. 2.1c, d). F/+; PV-Cre and F/+; SST-Cre mice show no changes in overall body or brain weight compared to littermate controls (Fig. 2.2-2.3).

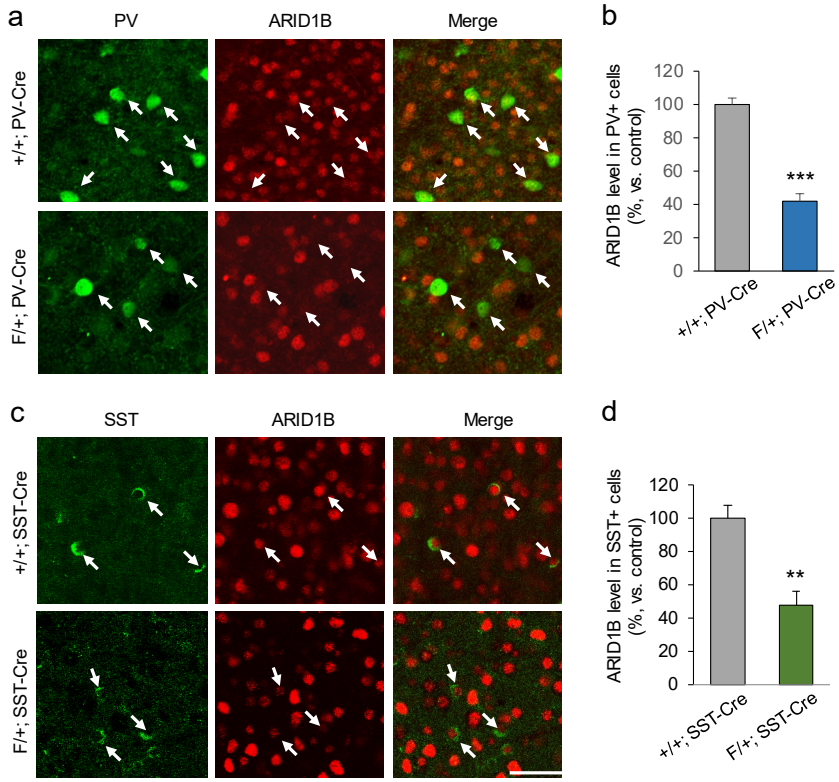

Figure 2.1 ARID1B expression in PV and SST interneurons of *Arid1b* mutant mice

a. Cortical sections from P60 +/+; PV-Cre and F/+; PV-Cre mice were co-immunolabeled with antibodies to ARID1B and PV. **b.** Quantification of ARID1B levels in PV interneurons of +/+; PV-Cre and F/+; PV-Cre mice (***p<0.0001; n=4 for +/+; PV-Cre mice and n=5 for F/+; PV-Cre mice; two-tailed Student's t test). **c.** Cortical sections from P60 +/+; SST-Cre and F/+; SST-Cre mice were co-immunolabeled with ARID1B and SST. **d.** Quantification of ARID1B levels in SST interneurons of +/+; SST-Cre and F/+; SST-Cre mice (**p=0.0017; n=3 for +/+; SST-Cre mice and n=4 for F/+; SST-Cre mice; two-tailed Student's t test). Data shown are mean ± SEM.

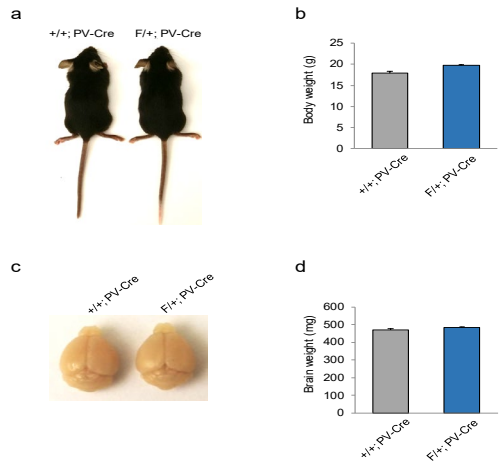

Figure 2.3 Body and brain weight with *Arid1b* haploinsufficiency in PV neurons

a. Representative images of +/+; PV-Cre and F/+; PV-Cre mice. **b.** No change was found in overall body weight between +/+; PV-Cre and F/+; PV-Cre mice (p=0.435; n=4 mice for +/+; PV-Cre and n=5 mice for F/+; PV-Cre; two-tailed Student's t test). **c.** Representative images of isolated brains from +/+; PV-Cre and F/+; PV-Cre mice. **d.** There was no change in brain weight between +/+; PV-Cre and F/+; PV-Cre mice (p=0.909; n=4 mice for +/+; PV-Cre and n=5 mice for F/+; PV-Cre; two-tailed Student's t test). Data shown are mean ± SEM.

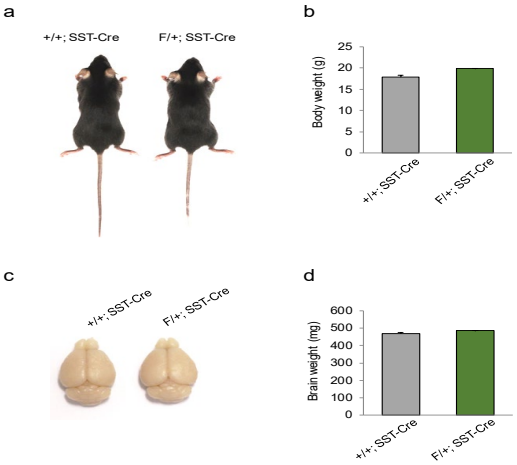

Figure 2.2 Body and brain weight with *Arid1b* haploinsufficiency in SST neurons

a. Representative images of +/+; SST-Cre and F/+; SST-Cre mice. **b.** Compared to +/+; SST-Cre mice, F/+; SST-Cre mice showed no difference in overall body weight (p=0.054; n=3 mice for +/+; SST-Cre and n=4 mice for F/+; SST-Cre; two-tailed Student's t test). **c.** Representative images of isolated brains from +/+; SST-Cre and F/+; SST-Cre mice. **d.** There was no change in brain weight between +/+; SST-Cre and F/+; SST-Cre mice (p=0.8075; n=3 mice for +/+; SST-Cre and n=4 mice for F/+; SST-Cre; two-tailed Student's t test). Data shown are mean ± SEM.

We first examined social and stereotyped behaviors. Social impairments and repetitive behaviors are two core features of ASD. We assessed sociability and social novelty using the three-chamber test. In the sociability test, +/+; PV-Cre control mice spent more time in the chamber containing the stranger 1 mouse than in the empty chamber, whereas F/+; PV-Cre mice showed no preference for either chamber. In the social novelty test, control mice showed preference for the novel stranger 2 mouse, whereas F/+; PV-Cre mice spent more time in the chamber containing the more familiar stranger 1 mouse (Fig. 2.4a). In contrast, F/+; SST-Cre mice showed a preference for the chamber with the unfamiliar stranger mouse in both the sociability and social novelty tests, similar to their control counterparts (Fig. 2.4b). We then examined the incidence of repetitive, stereotyped behaviors by looking at spontaneous grooming. F/+; PV-Cre mice showed no change in the amount of time spent self-grooming compared to +/+; PV-Cre controls (Fig. 2.4c). On the other hand, F/+; SST-Cre mice exhibited an increase in self-grooming time in comparison to control mice (Fig. 2.4c). Together, these results show that *Arid1b* haploinsufficiency in PV neurons produces deficits in social behaviors, while the haploinsufficiency in SST neurons leads to excessive repetitive behaviors.

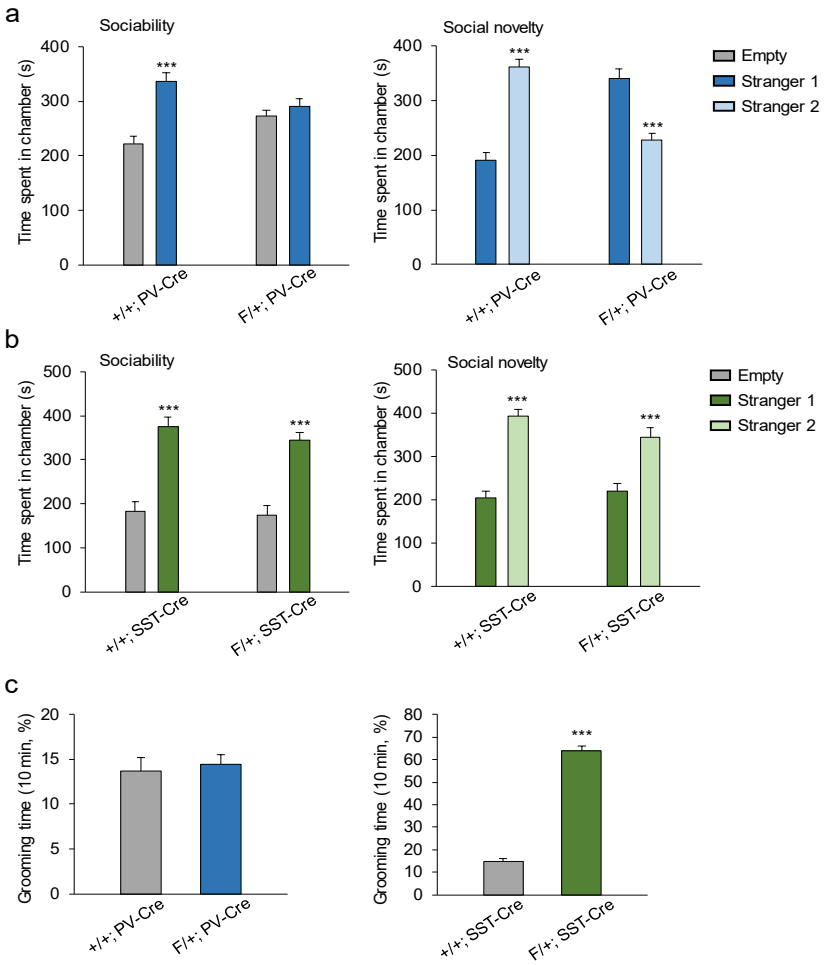

Figure 2.4 Social and stereotyped behaviors in F/+; PV-Cre and F/+; SST-Cre mice
a. In the three-chamber test for sociability, F/+; PV-Cre mice spent a similar amount of time with the empty cage as with the stranger mouse (stranger 1), whereas control counterparts stayed more time with stranger 1 (+/+; PV-Cre: ***p=0.0002; F/+; PV-Cre: p=0.3701; n=8 mice for +/+; PV-Cre and n=9 mice for F/+; PV-Cre; two-tailed Student's t test). In the three-chamber test for social novelty, F/+; PV-Cre mice spent less time with the novel stranger (stranger 2) than with the familiar mouse (stranger 1), in contrast to controls (+/+; PV-Cre: ***p<0.0001; F/+; PV-Cre: ***p=0.0002; n=8 mice for +/+; PV-Cre and n=9 mice for F/+; PV-Cre; two-tailed Student's t test). **b.** F/+; SST-Cre mice showed increased time spent with stranger 1 compared with the empty cage in the sociability test, similar to their control counterparts (+/+; SST-Cre: ***p<0.0001; F/+; SST-Cre: ***p<0.0001; n=12 mice for +/+; SST-Cre and n=8 mice for F/+; SST-Cre; two-tailed Student's t test). F/+; SST-Cre also spent more time with the novel stranger compared to stranger 1 during the social novelty test, which is comparable to control mice (+/+; SST-Cre: ***p<0.0001; F/+; SST-Cre: ***p=0.0012; n=12 mice for +/+; SST-Cre and n=8 mice for F/+; SST-Cre; two-tailed Student's t test). **c.** F/+; PV-Cre mice exhibited a similar level of grooming time compared to +/+; PV-Cre mice (p=0.7022; n=8 mice for +/+; PV-Cre and n=9 mice for F/+; PV-Cre; two-tailed Student's t test). F/+; SST-Cre mice, however, showed increased grooming time compared to +/+; SST-Cre mice (***p<0.0001; n=12 mice for +/+; SST-Cre and n=8 mice for F/+; SST-Cre; two-tailed Student's t test). Data shown are mean ± SEM.

2.4.2 Arid1b haploinsufficiency in PV interneurons, but not SST interneurons, results in heightened anxiety and depression

Because heightened levels of anxiety and depression are among the most common comorbid disorders in those with ASD, we next investigated the contribution of interneurons subtypes in these psychiatric conditions in *Arid1b* conditional knockout mice. The open field test was performed to gauge the levels of anxiety in F/+; PV-Cre and F/+; SST-Cre mice. We found that F/+; PV-Cre mice made fewer entries and spent less time in the center of the open field compared to +/+; PV-Cre controls, preferring to stay on the edges and in corners of the arena (Fig. 2.5a, b). However, F/+; SST-Cre mice showed no differences in anxiety behavior compared to control mice, spending similar amounts of time in the center of the open field (Fig. 2.5c, d). We crosschecked the increased anxiety in F/+; PV-Cre mice with the elevated plus maze test. F/+; PV-Cre mice exhibited greater levels of anxiety compared to controls, making fewer entries and spending less time in the open arms (Fig. 2.5e). There were no differences in the amount of time and the number of entries to the open arms between controls and F/+; SST-Cre mice (Fig. 2.5f). Again, these results suggest PV interneuron dysfunction as a mediator of *Arid1b* haploinsufficiency-induced anxiety.

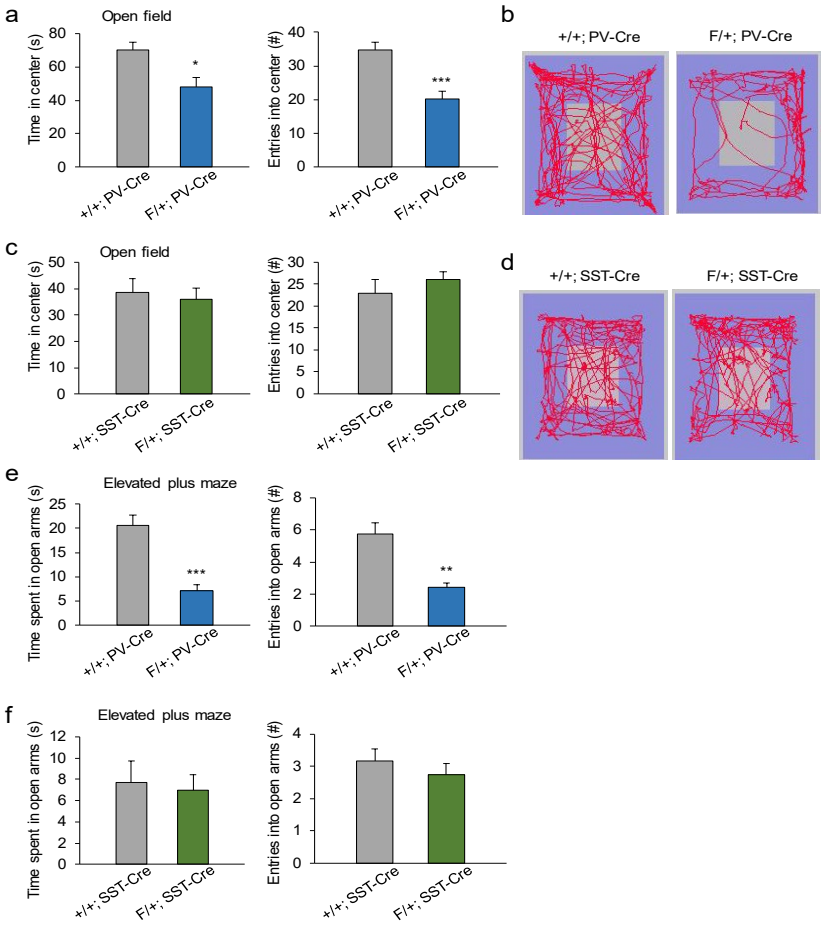

Figure 2.5 Heightened anxiety in F/+; PV-Cre mice
a. In the open field test, time spent in the center and number of entries into the center were both decreased in F/+; PV-Cre mice compared to +/+; PV-Cre mice (time in center: *p=0.0100; center entries: ***p=0.0004; n=11 mice for +/+; PV-Cre and n=12 mice for F/+; PV-Cre; two-tailed Student's t test). **b.** Representative tracings of the open field activity in +/+; PV-Cre and F/+; PV-Cre mice. **c.** F/+; SST-Cre mice showed a similar amount of time spent in the center and similar number of entries into the center compared to +/+; SST-Cre mice in the open field test (time in center: p=0.7632; center entries: p=0.4300; n=12 mice for +/+; SST-Cre and n=8 mice for F/+; SST-Cre; two-tailed Student's t test). **d.** Representative tracings of the open field activity in +/+; SST-Cre and F/+; SST-Cre mice. **e.** In the elevated plus maze, F/+; PV-Cre mice exhibited less time in open arms and fewer entries into open arms compared to control counterparts (time in open arms: ***p=0.0001; open arm entries: **p=0.0019; n=8 mice for +/+; PV-Cre and n=9 mice for F/+; PV-Cre; two-tailed Student's t test). **f.** F/+; SST-Cre mice showed no change in time spent in open arms or total entries into open arms compared to +/+; SST-Cre mice (time in open arms: p=0.8053; open arm entries: p=0.4670; n=12 mice for +/+; SST-Cre and n=8 mice for F/+; SST-Cre; two-tailed Student's t test). Data shown are mean ± SEM.

The level of depression was also measured by the tail suspension and forced swim tests. F/+; PV-Cre mice displayed heightened levels of depression-like behavior, indicated by an increase in total immobility time in the tail suspension test compared to control mice (Fig. 2.6a). However, there was no significant difference in immobility time between F/+; SST-Cre and control mice, suggesting little change in depression behavior. The forced swim test of F/+; PV-Cre and F/+; SST-Cre mice resulted in a similar pattern to the tail suspension test. F/+; PV-Cre mice revealed an increased time of immobility compared to control mice while F/+; SST-Cre mice showed no significant change (Fig. 2.6b). These results demonstrate that PV-specific *Arid1b* haploinsufficiency leads to a similar increase in anxiety and depression that is seen in global *Arid1b* haploinsufficiency. In contrast, SST-specific *Arid1b* haploinsufficiency appears to have no contribution to emotional behaviors.

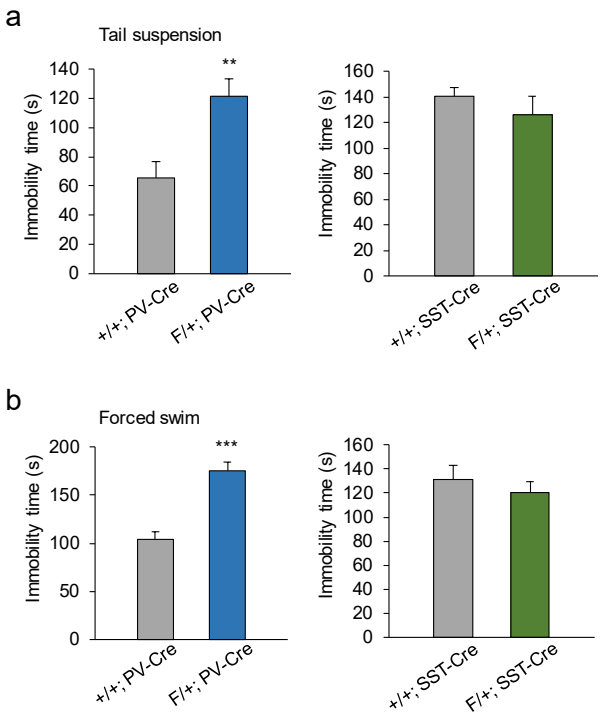

Figure 2.6 Increased depression behavior in F/+; PV-Cre mice
a. In the tail suspension test, F/+; PV-Cre mice showed increased immobility time compared to control mice (**p=0.0055; n=8 mice for +/+; PV-Cre and n=9 mice for F/+; PV-Cre; two-tailed Student's t test). F/+; SST-Cre mice showed no change in immobility time compared to controls in the tail suspension test (p=0.4381; n=12 mice for +/+; SST-Cre and n=8 mice for F/+; SST-Cre; two-tailed Student's t test). **b.** In the forced swim test, F/+; PV-Cre mice showed increased immobility time compared to controls (***p<0.0001; n=8 mice for +/+; PV-Cre and n=9 mice for F/+; PV-Cre; two-tailed Student's t test). F/+; SST-Cre mice showed no change in immobility time in the forced swim test compared to their controls (p=0.5225; n=12 mice for +/+; SST-Cre and n=8 mice for F/+; SST-Cre; two-tailed Student's t test). Data shown are mean ± SEM.

2.4.3 Cognitive deficits are caused by Arid1b haploinsufficiency in SST interneurons

Severe cognitive impairments, the primary feature of ID, are found in *Arid1b*$^{+/-}$ mice (Jung et al., 2017). To examine cognitive functions in F/+; PV-Cre and F/+; SST-Cre mice, we used several behavior assays of testing different types of learning and memory. We first performed the novel object recognition test to assess recognition memory. Control mice spent more time with a novel object than with a familiar object. F/+; PV-Cre mice behaved similar to controls, approaching and interacting more with the novel object (Fig. 2.7a). In contrast, F/+; SST-Cre mice showed no preference for exploring either the familiar or novel object, suggesting impairments in recognition memory. In the rotarod test for motor learning, both F/+; PV-Cre mice and controls showed a strong increase in the latency to fall during the three-day training phase (Fig. 2.7b). Throughout the testing phase (days 4 to 12), both control and F/+; PV-Cre mice revealed a consistent latency to fall. However, F/+; SST-Cre mice did not show the same increase in the latency to fall compared to controls during the training phase (Fig. 2.7c). In addition, they showed decreased latencies to fall throughout the testing phase compared to control mice, suggesting deficits in motor learning ability.

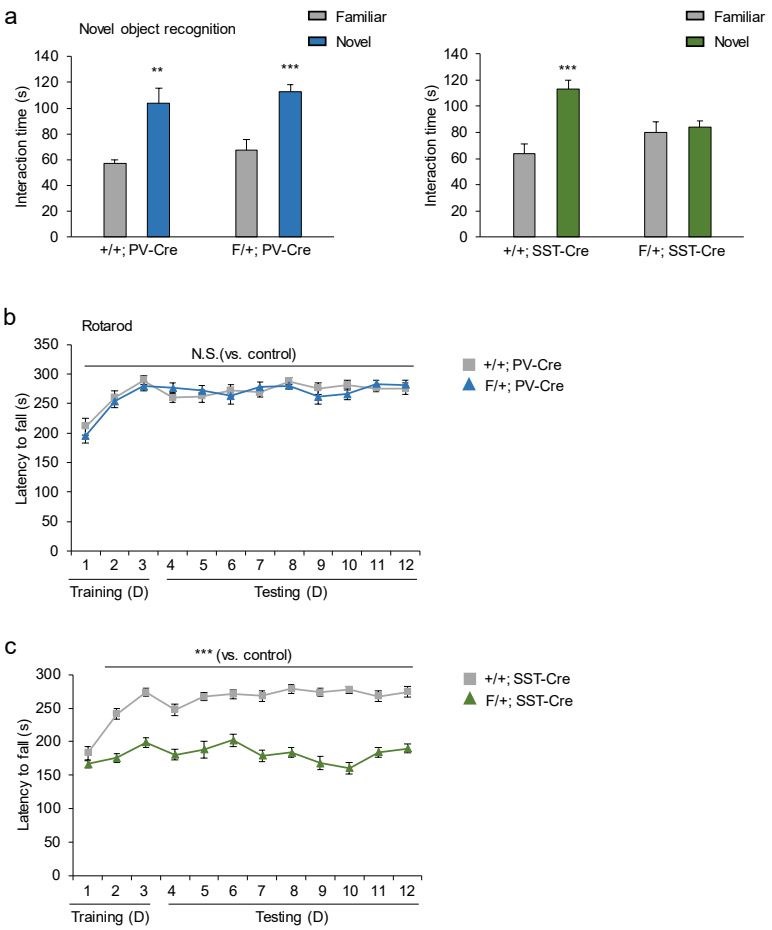

Figure 2.7 Recognition memory and motor learning deficits in F/+; SST-Cre mice

a. In the novel object recognition test, both +/+; PV-Cre and F/+; PV-Cre mice showed greater interaction time with the novel object compared to the familiar object (+/+; PV-Cre: **p=0.0032; F/+; PV-Cre: ***p=0.0001; n=11 mice for +/+; PV-Cre and n=12 mice for F/+; PV-Cre; two-tailed Student's t test). F/+; SST-Cre mice showed no change in the amount of time spent with the novel object versus the familiar object, whereas +/+; SST-Cre mice interacted more with the novel object (+/+; SST-Cre: ***p<0.0001; F/+; SST-Cre: p=0.7009; n=12 mice for +/+; SST-Cre and n=8 mice for F/+; SST-Cre; two-tailed Student's t test). **b.** +/+; PV-Cre and F/+; PV-Cre mice exhibited similar latencies to fall during both the training and testing phases of the rotarod test (d1: p=0.4500; d2: p=0.6978; d3: p=0.3718; d4: p=0.2056; d5: p=0.5397; d6: p=0.6487; d7: p=0.5175; d8: p=0.4032; d9: p=0.4076; d10: p=0.2905; d11: p=0.4571; d12: p=0.5813; n=8 mice for +/+; PV-Cre and n=8 mice for F/+; PV-Cre; repeated measures ANOVA). **c.** F/+; SST-Cre mice showed a decreased latency to fall during the rotarod test from day 2 to day 12 (d1: p=0.1556; d2: ***p<0.0001; d3: ***p<0.0001; d4: ***p<0.0001; d5: ***p=0.0004; d6: ***p<0.0001; d7: ***p<0.0001; d8: ***p<0.0001; d9: ***p<0.0001; d10: ***p<0.0001; d11: ***p<0.0001; d12: ***p<0.0001; n=8 mice for +/+; SST-Cre and n=8 mice for F/+; SST-Cre; repeated measures ANOVA). Data shown are mean ± SEM.

To test spatial learning and reference memory, we next performed the Morris water maze test. During the 10-day training phase, F/+; PV-Cre mice showed similar latencies to the hidden platform as control mice (Fig. 2.8a). In a probe trial to assess spatial memory following training, F/+; PV-Cre mice crossed the platform location a similar number of times as controls (Fig. 2.8b, c). These mice also showed no difference in the total swimming distance or speed (Fig. 2.8c). F/+; SST-Cre mice showed similar latencies to the platform compared to controls for the first three days of training, but then exhibited higher latency times throughout the remainder of the training phase (Fig. 2.8d). Thus, F/+; SST-Cre mice may have an ability to initiate the learning process, but the capacity of further spatial learning appears to be limited. They crossed the platform location fewer times compared to controls during the probe trial (Fig. 2.8e, f). No difference was observed in the total swimming distance or speed, verifying that these factors did not contribute to the decrease in platform crosses (Fig. 2.8f). Together, these results suggest that SST-specific *Arid1b* haploinsufficiency, but not the PV-specific *Arid1b* loss, leads to several cognitive impairments.

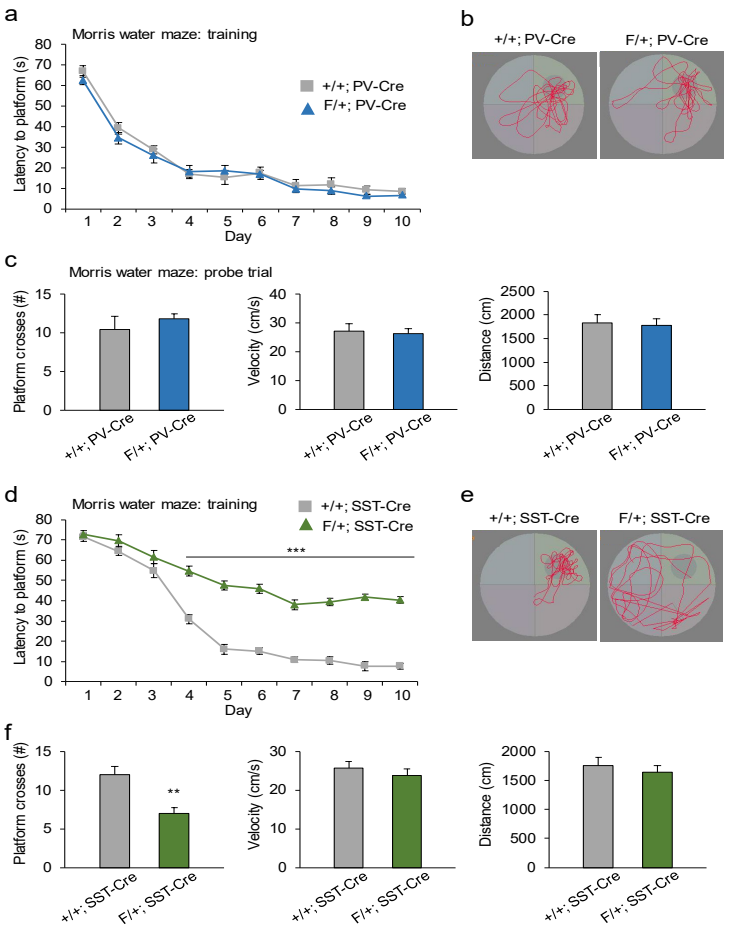

Figure 2.8 Dysfunctional spatial learning and memory in F/+; SST-Cre mice
a. The training phase of the Morris water maze test showed no change in latency to the platform in F/+; PV-Cre mice compared to control mice (d1: p=0.2811; d2: p=0.2898; d3: p=0.4904; d4: p=0.7700; d5: p=0.5078; d6: p=0.8765; d7: p=0.6736; d8: p=0.4795; d9: p=0.2874; d10: p=0.3262; n=8 mice for +/+; PV-Cre and n=8 mice for F/+; PV-Cre; repeated measures ANOVA). **b.** Representative swim paths of +/+; PV-Cre and F/+; PV-Cre mice during a probe trial after training. **c.** During a probe trial, F/+; PV-Cre mice showed no change in the number of platform crosses, average velocity, or total distance traveled compared to controls (platform crosses: p=0.4776; average velocity: p=0.7694; distance traveled: p=0.8522; n=8 mice for +/+; PV-Cre and n=8 mice for F/+; PV-Cre; two-tailed Student's t test). **d.** F/+; SST-Cre mice showed an increased latency to the platform from day 4 to day 10 during the training phase of the Morris water maze test (d1: p=0.6765; d2: p=0.1794; d3: p=0.2084; d4: ***p<0.0001; d5: ***p<0.0001; d6: ***p<0.0001; d7: ***p<0.0001; d8: ***p<0.0001; d9: ***p<0.0001; d10: ***p<0.0001; n=8 mice for +/+; SST-Cre and n=8 mice for F/+; SST-Cre; repeated measures ANOVA). **e.** Representative swim paths of +/+; SST-Cre and F/+; SST-Cre mice during a probe trial after training. **f.** During a probe trial, F/+; SST-Cre mice showed fewer platform crosses compared to control mice, while average velocity and total distance traveled were unchanged (platform crosses: **p=0.0037; average velocity: p=0.5127; distance traveled: p=0.5982; n=8 mice for +/+; SST-Cre and n=8 mice for F/+; SST-Cre; two-tailed Student's t test). Data shown are mean ± SEM.

2.5 Discussion

2.5.1 Interneurons play a significant role in the pathology of Arid1b haploinsufficiency-induced ASD and ID

Arid1b haploinsufficiency causes ASD and ID, leading to a broad range of neurobehavioral phenotypes in humans and rodents (Celen et al., 2017; Halgren et al., 2012; Hoyer et al., 2012; Jung et al., 2017; Santen et al., 2012a; Shibutani et al., 2017). Given the abnormal anatomy and physiology of interneurons as a major hallmark of *Arid1b* haploinsufficiency (Jung et al., 2017), we hypothesized that interneurons play a critical role in mediating *Arid1b* haploinsufficiency-induced cognitive, social, and emotional impairments. The heterogenous nature of the interneuron population led us to investigate the contributions of the two most populous interneuron subtypes, PV and SST, to the behavioral phenotypes associated with *Arid1b* haploinsufficiency. Our results suggest that PV and SST interneurons contribute distinct, complementary aspects of the major ASD- and ID-like phenotypes in *Arid1b*$^{+/-}$ mice. F/+; PV-Cre and F/+; SST-Cre mice recapitulate the major deficits induced by *Arid1b* haploinsufficiency (Table 2.1).

Behavior	*Arid1b*$^{+/-}$	F/+; PV-Cre	F/+; SST-Cre
Social behavior	↓	↓	-
Stereotyped behavior	↑	-	↑
Anxiety	↑	↑	-
Depression	↑	↑	-
Recognition memory	↓	-	↓
Motor learning	↓	-	↓
Spatial reference memory	↓	-	↓

Table 2.1 Summary of behavioral deficits
PV and SST interneurons contribute complementary aspects of the ASD and ID phenotypes seen with *Arid1b* haploinsufficiency.

2.5.2 Excitatory/Inhibitory imbalance in neurodevelopmental disorders

Perturbation of the well-balanced excitatory and inhibitory components can lead to life-long cognitive, social, and emotional disabilities. Impairments in inhibitory interneuron development and function have been implicated in several neurodevelopmental conditions including ASD and ID (Fatemi et al., 2009; Jamain et al., 2008; Oblak et al., 2011; Piton et al., 2013; Tabuchi et al., 2007; Zhang et al., 2009), Rett syndrome (Chen et al., 2001; Guy et al., 2001), Schizophrenia (Chen et al., 2010), Angelman syndrome (Wallace et al., 2012), and fragile X syndrome (Curia et al., 2009; Gibson et al., 2008; Selby et al., 2007). Particularly, it has been increasingly evident that PV or SST interneurons are dysfunctional in ASD and ID. Several studies have shown a reduction of PV interneurons in rodent models of ASD and ASD-related disorders, such as *Fmrp*, *Mecp2*, and *Nlgn3* knockout mice (Fukuda et al., 2005; Gogolla et al., 2009; Selby et al., 2007). Two mouse models of ASD, *Shank1* and *Cntnap4* knockout, also exhibit reduced levels of PV interneuron output (Karayannis et al., 2014; Mao et al., 2015). Furthermore, post-mortem brains of patients with ASD and ID show fewer PV interneurons within the cerebral cortex (Hashemi et al., 2017; Zikopoulos and Barbas, 2013). Altered functional networks within the cortex of human patients has also been shown, indicated by a decrease in baseline gamma-band power in the cortex during developmental stages. As PV interneurons play a pivotal role in the generation of gamma oscillations, it has been implicated that deficits in PV neuron development contributes to the aberrant gamma responses (Kuki et al., 2015; Newson and Thiagarajan, 2018; Takahashi et al., 2017). Fewer SST neurons within the cerebral cortex has also been found in a *Pten* knockout mouse model of ASD (Vogt et al., 2015). It is likely that the anatomical or functional impairments of these interneurons cause the excitatory/inhibitory imbalance, resulting in abnormal neurobehaviors.

2.5.3 Arid1b haploinsufficiency in PV and SST interneurons have distinct effects on social, emotional, and cognitive behaviors

Although inhibitory interneurons are implicated in neurodevelopmental pathology, it has been unclear whether their subtypes play unique roles in distinct neural behavior. In this study using *Arid1b* mouse models, we show that PV interneurons are strongly associated with social behavior deficits, a core feature of ASD. These results are consistent with previous studies showing a prominent role of PV neurons in social behavior. *Pvalb* knockout mice display social behavior deficits and reduced vocalizations (Wohr et al., 2015). Reducing inhibitory output by knocking out an NMDA receptor specifically in PV neurons also results in reduced sociability in mice (Saunders et al., 2013). In addition, we show a prominent role of PV interneurons in emotional behavior. Recent studies support this finding as chemogenetic manipulation of PV interneurons modulates anxiety and depression behavior (Chen et al., 2019; Zou et al., 2016). An autism mouse model by maternal immune activation also shows that PV neuron dysfunction leads to elevated anxiety and depression (Canetta et al., 2016). Our results show no clear association between SST interneurons and emotional behavior. However, previous studies have reported that SST interneurons are involved in anxiety and depression (Engin et al., 2008; Fuchs et al., 2017a; Fuchs et al., 2017b; Lin and Sibille, 2015). In post-mortem examination of humans with major depressive disorder, there is reduced expression of SST in the prefrontal cortex (Seney et al., 2015; Tripp et al., 2011). In addition, *Sst* knockout mice show elevated anxiety and depression (Lin and Sibille, 2015). There are some possibilities for the contradicting results. First, a loss or reduction of SST might have a more dramatic effect on SST neurons, whereas haploinsufficiency of the *Arid1b* gene in SST cells could result in less potency on the interneuron activity. It is likely that *Arid1b* haploinsufficiency elicits a different downstream mechanism than removing the SST peptide. Also, expression of the *Arid1b*

gene could be different in interneuron subtypes and brain regions. In areas strongly associated with emotional behavior, such as the amygdala and pre-frontal cortex, *Arid1b* may be expressed at a lower level compared to other regions.

We further show that cognitive dysfunction in the *Arid1b* haploinsufficient condition is primarily modulated by SST interneurons. Studies have revealed the prominent role of SST interneurons in various cognitive functions. The SST subtype controls disinhibition of principle cells in the hippocampus, regulating sensory processing, learning, and memory (Artinian and Lacaille, 2018). This subtype also inhibits distal dendrites of principal neurons in layer 1 of the motor cortex to regulate changes in excitatory synapses during motor learning (Celen et al., 2017). SST neurons in the prefrontal cortex maintains working memory during a delay phase (Kim et al., 2016). In contrast, PV neurons play no significant role in maintaining working memory, but they have a stronger response in reward processing during the choice phase (Kim et al., 2016). Studies have also shown that signaling downstream of the SST peptide in interneurons affects learning and memory. For example, knockout of the *Type 3 somatostatin receptor* (*Sstr3*) or *Type 2 somatostatin receptor* (*Sstr2*) gene inhibits SST signaling, which results in impaired object recognition memory (Einstein et al., 2010) or spatial learning and reference memory (Dutar et al., 2002), respectively. Additionally, fear conditioning studies support the contribution of SST neurons to cognitive behaviors. Classical fear conditioning of a whisker stimulus results in increased activity of SST neurons in the corresponding area of the barrel cortex (Cybulska-Klosowicz et al., 2013; Gierdalski et al., 2001). Contrary to SST neurons, PV cells show no change in the barrel cortex activity during fear conditioning (Siucinska and Kossut, 2006). These findings suggest distinct contributions of different interneurons to neural behaviors. Indeed, there is a recent study in which the Rett syndrome gene *Mecp2* is engineered to be deleted in

either PV or SST interneurons (Ito-Ishida et al., 2015). Loss of *Mecp2* function in PV or SST interneurons shows non-overlapping effects on motor/sensory coordination, learning and memory, social interaction, and stereotyped behaviors in the mouse models.

Arid1b$^{+/-}$ mice exhibited a reduction in overall body weight (Celen et al., 2017; Jung et al., 2017; Shibutani et al., 2017). It is suggested that *Arid1b* haploinsufficiency causes deficits in the growth hormone-releasing hormone—growth hormone—insulin-like growth factor (GHRH-GH-IGF) axis, ultimately affecting growth control (Celen et al., 2017). Knockout mouse models of other chromatin remodelers such as BAF53B exhibit similar deficits in body growth control (Lopez and Wood, 2015; Ronan et al., 2013). In the current study, we see no major changes in body weight in either F/+; PV-Cre or F/+; SST-Cre mice, suggesting no significant role of PV-specific or SST-specific *Arid1b* haploinsufficiency in growth control.

2.5.4 Conclusion and future prospective

There is no treatment tool available for the core symptoms of ASD and ID. Current pharmacologic strategies focus on GABAergic modulation to normalize inhibitory activity. GABA agonists to enhance inhibition, such as benzodiazepines and anticonvulsants, have been helpful in alleviating aggressive and hyperactive behaviors associated with ASD in humans (Belsito et al., 2001; Di Martino and Tuchman, 2001). Use of clonazepam, a positive modulator of the $GABA_A$ receptor, to enhance inhibitory activity has also successfully rescued behavioral phenotypes in mouse models of ASD and ID (Han et al., 2012; Jung et al., 2017). A prominent shortcoming of these strategies is that they are currently not subtype-specific to inhibitory neurons. As we continue to gain a better understanding of how individual interneuron subtypes modulate distinct

behaviors in ASD and/or ID, therapeutic strategies could become even more targeted, with greater efficacy and fewer side effects as a result.

CHAPTER 3: A ROLE OF ARID1B IN MEDIATING NEURITE OUTGROWTH OF EXCITATORY CORTICAL NEURONS

Amanda L Smith[1], Eui-Man Jung[2], Minhan Ka[3], and Woo-Yang Kim[4*]

[1]Department of Pharmacology and Experimental Neuroscience, University of Nebraska Medical Center, Omaha, NE 68198, USA

[2]Laboratory of Veterinary Biochemistry and Molecular Biology, Chungbuk National University, Cheongju, Chungbuk 28644, Republic of Korea

[3]Research Center for Substance Abuse Pharmacology, Korea Institute of Toxicology, Daejeon 34114, Republic of Korea

[4]Department of Biological Sciences, Kent State University, Kent, OH 44242, USA

3.1 Abstract

Proper neurite outgrowth during development of the cerebral cortex is crucial for establishing proper circuitry and mediating normal behavior. Deficits in neurite development via neurotrophin signaling pathways have been implicated in neurodevelopmental disorders such as autism spectrum disorder (ASD) and intellectual disability (ID). Recent studies have shown that haploinsufficiency of the *AT-rich interactive domain-containing 1B (ARID1B)* gene is a genetic cause of ASD and ID in humans. While behavioral aspects of these neurodevelopmental disorders are well characterized, the underlying neuropathogenesis remains largely unknown. Here we examine the effects that *Arid1b* deletion has on the developing brain using a previously developed *Arid1b* knockout mouse model. We show that cultured cortical neurons exhibit marked reduction in neurite outgrowth with loss of *Arid1b*. Additionally, *Arid1b* knockout mice have improper development of the axon fibers comprising the corpus callosum, a feature frequently observed in patients. Heterozygous brains also showed reduced levels of BDNF neurotrophin signaling activity, and normalization of signaling was able to rescue the observed neurite outgrowth deficits. Our results indicate a critical role of ARID1B in mediating proper neurite outgrowth during brain development and suggest a possible role of ARID1B in the BDNF signaling pathway. This insight into the underlying pathogenesis of these disorders will hopefully pave the way for potential genetic or pharmacologic therapeutic targets.

3.2 Introduction

Autism spectrum disorder (ASD), which affects approximately 1 in 68 individuals worldwide, is characterized primarily by stereotyped behaviors and social and communication deficits (Ellison et al., 2013; Halgren et al., 2012). Nearly 75% of individuals with ASD are also diagnosed with intellectual disability (ID), exhibiting severe limitations in cognitive and adaptive behaviors (Daily et al., 2000; Hoyer et al., 2012). While the behavioral features of these disorders are well characterized, the underlying neuropathogenesis is largely unknown, and thus no pharmacologic or genetic interventions are currently available. Current treatment for ASD and ID are primarily limited to behavioral, occupational, and physical therapies until further research identifies potential causative factors and therapeutic targets.

Deficits in excitatory neuron development have been implicated in neurodevelopmental disorders (Kast and Levitt, 2019). Development of excitatory neurons in the rodent cerebral cortex consists of three primary stages. Initially, neural progenitors differentiate into an immature neuron, followed by migration through the cortex to its final location, and finally neurite outgrowth (Azzarelli et al., 2014; Barnes and Polleux, 2009). These neurites eventually become the axons and dendrites that comprise the complex circuitry of the brain, mediating proper neurotransmission and communication among brain regions (Tsaneva-Atanasova et al., 2009). Several mouse models of ASD/ID and related disorders have deficits in the neurite outgrowth stage of development, exhibiting abnormal dendritic arborization and reduced axon growth and branching (Gilbert and Man, 2017; Irwin et al., 2002; Jiang et al., 2013; Kaufmann and Moser, 2000). Disruptions in brain-derived neurotrophic factor (BDNF) signaling, a key regulator of neurite outgrowth, is also prevalent among these disease states. Altered glycogen synthase kinase 3 (GSK3) and mammalian target of rapamycin (mTOR)

activity, two downstream components in BDNF signaling, frequently accompanies impaired neurite outgrowth and ASD/ID-like behavioral deficits in mouse models (Jiang et al., 2005; Morita and Sobue, 2009; Zhou et al., 2004). Furthermore, several studies indicate that chromatin remodeling is a crucial player in regulating various stages of cortical development. Specifically, mutations in various components of the Brg1/Brm-associated factor (BAF) chromatin remodeling complex lead to altered neurite development in the rodent cortex (Bachmann et al., 2016; Choi et al., 2015; Weinberg et al., 2013).

Recent progress in genetic studies has revealed that haploinsufficiency of the *AT-rich interactive domain-containing 1B (ARID1B)* gene, a component of the BAF chromatin remodeling complex, is a genetic cause of ASD and ID in humans (Halgren et al., 2012; Hoyer et al., 2012; Santen et al., 2012a). Our lab has previously developed an *Arid1b* knockout mouse model and demonstrated that *Arid1b* heterozygotes, which resemble haploinsufficiency seen in human patients, exhibit severe cognitive, social, and emotional impairments that recapitulate other models of ASD and ID (Jung et al., 2017). While loss of Arid1b results in significant behavioral deficits, its effect in the developing brain is still unknown. Based on the prevalence of neurite outgrowth deficits in neurodevelopmental disorders and the key involvement of neurotrophin signaling in regulating this process, we hypothesized that ARID1B affects neurite development via neurotrophin signaling activity. In this study, we indeed demonstrate a key role of ARID1B in mediating proper neurite outgrowth in the developing brain, and we propose a possible role of ARID1B in the BDNF neurotrophin signaling pathway. Our findings suggest that these neurite outgrowth deficits may contribute to the behavioral impairments seen in ASD and ID.

3.3 Materials and methods

3.3.1 Mice

Generation of *Arid1b* knockout mice was described previously (Jung et al., 2017). Thy1-YFP-H mice were purchased from the Jackson Laboratory (B6.Cg-Tg(Thy1-YFP)HJrs/J; JAX 003782) and crossed with *Arid1b* heterozygous mice to generate YFP-expressing knockout mice. After weaning, all mice were group housed (no more than 5 mice per cage) as a mix of genotypes on a 12-hour light/dark cycle. All husbandry and experimental procedures were reviewed and approved by the Institutional Animal Care and Use Committee (IACUC) of the University of Nebraska Medical Center.

3.3.2 Plasmids

We generated two short hairpin (sh) ARID1Bs using two different targeting sequences (5'-GGAACCAGTTATGACCGAAGGC-3' and 5'-GCAAGTCAAAGGACAGCTATG-3') and their complement sequences. The oligomers were cloned into a modified pSuper-Basic vector or pLVX-shRNA2 vector (Clontech), as previously described (Kim et al., 2006). For controls, non-silencing shRNAs were generated using scrambled targeting sequences (5'-GACGACTGCGACGGGATAATA-3' and 5'-GAATACGACCGACACCTACTA-3').

3.3.3 Primary neuron cultures and growth factor treatment

Primary neuron cultures were done as described previously (Jung et al., 2017; Ka et al., 2016a). Cortical neurons were isolated from embryonic day 14-6 (E14-E16) mice. Meninges were removed and cortical cells were dissociated with tituration after trypsin/EDTA treatment. The cells were plated onto poly-D-lysine/laminin-coated coverslips and cultured for 6 DIV in a medium containing Neurobasal medium (Invitrogen), 2 mM glutamine (Invitrogen), 2% (v/v) B27 supplement (Invitrogen), 1% (v/v) N2 supplement (Invitrogen), and 50 U/ml penicillin/streptomycin (Invitrogen). In

cultures that underwent treatment for the rescue experiment, 1 µl of either 50 ng/ml BDNF, 25 nM Gsk3 inhibitor, 50 ng/ml IGF, or 4 µg/ml SC79 were added to wells at day 3 *in vitro*.

3.3.4 In utero electroporation

In utero electroporation was performed as described previously (Ka et al., 2016a). Timed pregnant female mice from E14.5 gestation were deeply anesthetized, and the uterine horns were gently exposed. The lateral ventricles of an embryonic brain were injected with plasmid DNA (2 µg/µl), encoding either shARID1B or control shRNA, using a Picospritzer II (Parker Inc.). Electroporation was achieved by placing two sterile forceps-type electrodes on opposing sides of the uterine sac around the embryonic head and applying a series of short electrical pulses using a BTX ECM 830 electroporator (five pulses with 100 ms length separated by 900 ms intervals were applied at 45 V). The small electrical pulses drive charged DNA constructs into surrounding cells in the embryonic brain. Embryos were then allowed to develop *in utero* and be birthed normally.

3.3.5 Immunostaining

Immunostaining of brain sections or dissociated cells was performed as described previously (Jung et al., 2017; Ka et al., 2016a). Primary antibodies used were chicken anti-MAP2 (PhosphoSolutions), mouse anti-pNF-H (BioLegend), chicken anti-GFP (AVES), and rabbit anti-RFP (Chemicon). Appropriate secondary antibodies conjugated with Alexa Fluor dyes (Invitrogen) were used to detect primary antibodies. DAPI (Sigma-Aldrich) was used to stain nuclei.

3.3.6 Morphometry

Morphometric analysis was performed as described previously (Jung et al., 2017; Ka et al., 2016a). For quantifying numbers and lengths of neurites in cultures, at least 20

cells from different fields of view were selected at random per embryo brain and imaged with a Zeiss LSM710 confocal microscope. Images were analyzed using ImageJ (NIH). Primary, secondary, and tertiary axon and dendrite numbers and lengths were measured. Cells from a single embryo were averaged for a single value for that animal, and the values from all animals of a genotype were averaged to calculate the mean. N numbers for each experiment are described in figure legends. To quantify corpus callosum thickness and mean fluorescent intensity, images of five different brain sections at periodic distances along the rostrocaudal axis were taken with the Zeiss LSM710 confocal microscope and analyzed with ImageJ. Corpus callosum thickness and the mean fluorescent intensity of RFP- or YFP-labeled fibers from the five sections were averaged and reported as values for one mouse, and values from all animals in a genotype were averaged to calculate the mean. N values for each experiment are described in figure legends. Some results were recalculated as relative changes versus control.

3.3.7 Western blot analysis

Western blotting was performed as described previously (Jung et al., 2017; Ka et al., 2016a). Cellular lysates from E14-E16 brain cortices were prepared using RIPA buffer and the protein content was determined by a Bio-Rad Protein Assay system. Proteins were separated on a 4-12% SDS-PAGE gradient gel and transferred onto a nitrocellulose membrane. The membrane was incubated with mouse anti-ARID1B (Abcam), rabbit anti-p-AKT (Cell Signaling), rabbit anti-AKT (Cell Signaling), mouse anti-p-GSK3β (Upstate), mouse anti-GSK3 (BD Transduction Laboratory), rabbit anti-p-mTOR (Cell Signaling), rabbit anti-mTOR (Cell Signaling), or mouse anti-GAPDH (Millipore) at 4°C overnight. Appropriate secondary antibodies conjugated to HRP were used (Cell Signaling Technology) and the ECL reagents (GE Healthcare Bio-Sciences)

were used for immunodetection. For quantification of band intensity, blots from three independent experiments for each molecule of interest were used. Signals were measured using ImageJ software (NIH) and averages from the three blots are reported. GAPDH was used as an internal control to normalize band intensity.

3.3.8 Statistical analysis

Normal distribution was tested using the Kolmogorov-Smirnov test and variance was compared. Unless otherwise stated, statistical significance was determined using two-tailed unpaired Student's *t* tests for two-population comparisons or ANOVA followed by Bonferroni's post hoc test for multiple comparisons. Data were analyzed using GraphPad Prism and were presented as the means ± SEM. *P* values for each comparison are described in the figure legends. To determine and confirm sample sizes (N), we performed a power analysis. The values for statistical power (1-β) and type I error rate (α) were 0.8 and 0.05 (or 0.01), respectively. Each experiment in this study was performed blind and randomized. Animals were assigned randomly to the various experimental groups, and data were collected and processed randomly. The allocation, treatment, and handling of animals were the same across study groups. Control animals were selected from the same liter as the test group. The individuals conducting the experiments were blinded to group allocation and allocation sequence. Exclusion criteria for mice were based on abnormal health conditions, including weights below 20% of the intergroup and intragroup average and noticeably reduced activity or feeding.

3.4 Results

3.4.1 Loss of Arid1b disrupts neurite outgrowth in developing cortical neurons

To determine the effect of *Arid1b* deletion on neurite outgrowth, we first cultured cortical neurons from *Arid1b*$^{+/+}$, *Arid1b*$^{+/-}$, and *Arid1b*$^{-/-}$ embryos and labeled cells with anti-pNF-H and anti-MAP2 antibodies, markers for axons and dendrites, respectively. We then quantified the numbers and lengths of primary, secondary, and tertiary axons and dendrites. Both *Arid1b*$^{+/-}$ and *Arid1b*$^{-/-}$ neurons showed a decrease in secondary and tertiary axon numbers compared to *Arid1b*$^{+/+}$ controls, with no change in primary axon number (Fig. 3.1a,b). Primary, secondary, and tertiary axon lengths were also decreased in *Arid1b*$^{+/-}$ and *Arid1b*$^{-/-}$ neurons compared to controls (Fig. 3.1a,c). Additionally, *Arid1b*$^{+/-}$ and *Arid1b*$^{-/-}$ also showed a reduction in primary, secondary, and tertiary dendrite number compared to controls (Fig. 3.2a,b). No significant changes in dendrite lengths were observed (Fig. 3.2a,c). These results indicate that deletion of the *Arid1b* gene impairs outgrowth and branching of axons and dendrites in developing cortical neurons. It also appears that *Arid1b* deletion may exhibit a more prominent effect on axons compared to dendrites. Future experiments we will focus solely on *Arid1b* heterozygous mice, as they best recapitulate *ARID1B* haploinsufficiency in the human condition. *Arid1b*$^{-/-}$ mice are also lethal after birth, and therefore cannot be used on any postnatal experiments.

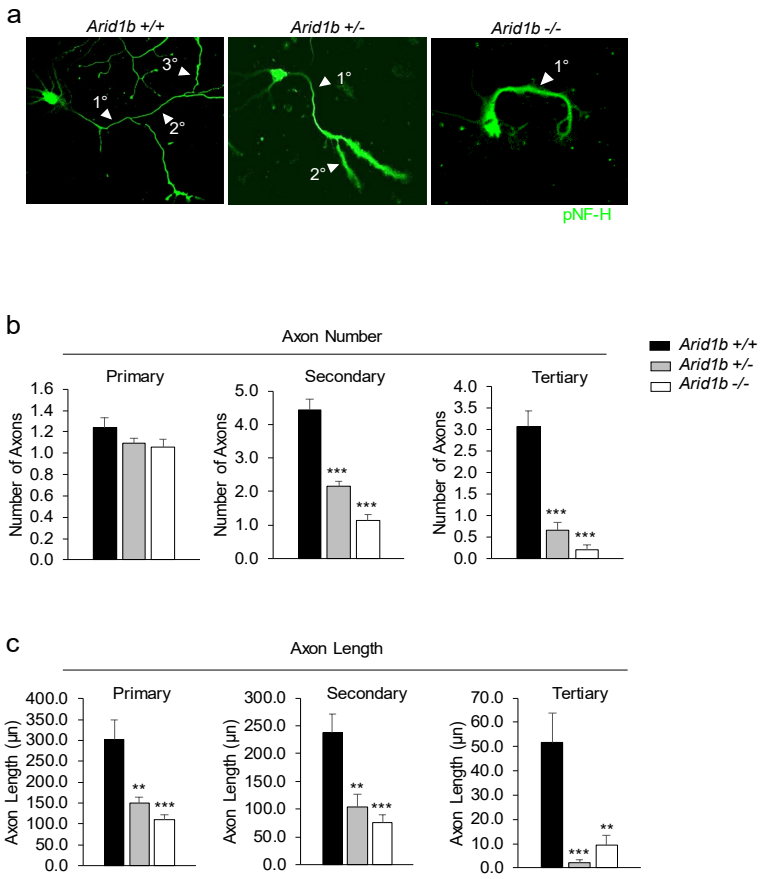

Figure 3.1 Impaired axon growth in neurons with *Arid1b* deletion
a. Representative images of cultured neurons from all three mouse genotypes with axons labeled with pNF-H. White arrow heads indicate primary, secondary, or tertiary axons. **b.** Quantification of the number of primary, secondary, and tertiary axon numbers (secondary: ***P<0.001 for *Arid1b*$^{+/+}$ vs. *Arid1b*$^{+/-}$ and *Arid1b*$^{+/+}$ vs. *Arid1b*$^{-/-}$; tertiary: ***P<0.001 for *Arid1b*$^{+/+}$ vs. *Arid1b*$^{+/-}$ and *Arid1b*$^{+/+}$ vs. *Arid1b*$^{-/-}$). **c.** Quantification of primary, secondary, and tertiary axon lengths (primary: **P<0.01 for *Arid1b*$^{+/+}$ vs. *Arid1b*$^{+/-}$, ***P<0.001 for *Arid1b*$^{+/+}$ vs. *Arid1b*$^{-/-}$; secondary: **P<0.01 for *Arid1b*$^{+/+}$ vs. *Arid1b*$^{+/-}$, ***P<0.001 for *Arid1b*$^{+/+}$ vs. *Arid1b*$^{-/-}$; tertiary: ***P<0.001 for *Arid1b*$^{+/+}$ vs. *Arid1b*$^{+/-}$, **P<0.01 for *Arid1b*$^{+/+}$ vs. *Arid1b*$^{-/-}$). The number of embryos used was N=6 for each genotype. Significance was determined across genotypes using one-way ANOVA with Bonferroni's post-hoc correction. Data shown are mean +/- SEM.

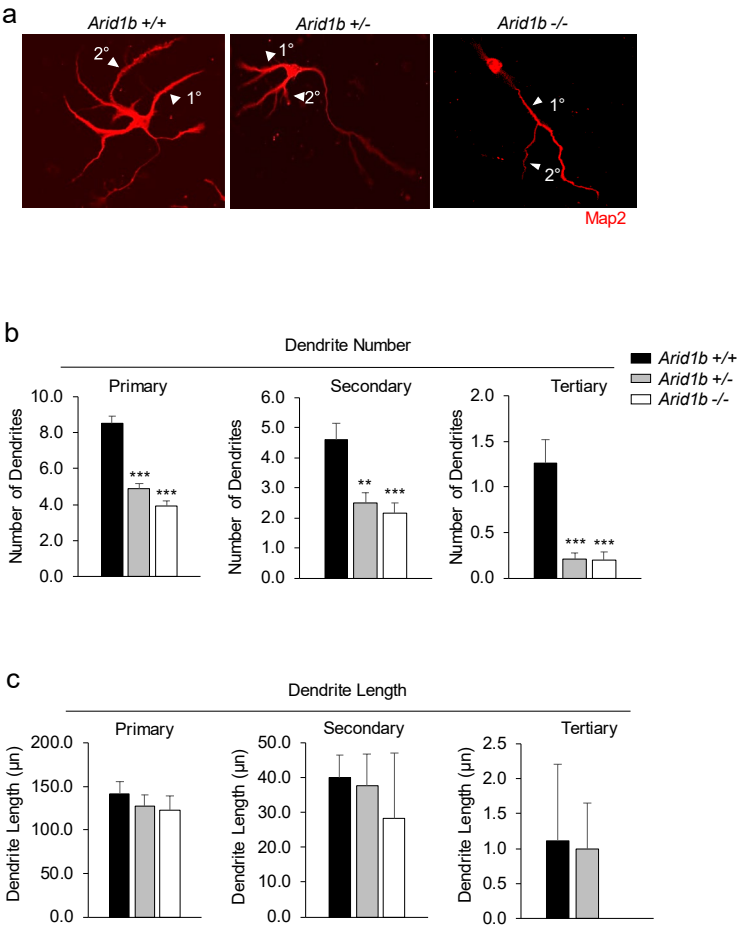

Figure 3.2 Impaired dendrite growth in neurons with *Arid1b* deletion
a. Representative images of cultured neurons from all three mouse genotypes with dendrites labeled with MAP2. White arrow heads indicate primary, secondary, or tertiary dendrites. **b.** Quantification of the number of primary, secondary, and tertiary dendrite numbers (primary: ***P<0.001 for *Arid1b*$^{+/+}$ vs. *Arid1b*$^{+/-}$ and *Arid1b*$^{+/+}$ vs. *Arid1b*$^{-/-}$; secondary: **P<0.01 for *Arid1b*$^{+/+}$ vs. *Arid1b*$^{+/-}$, ***P<0.001 for *Arid1b*$^{+/+}$ vs. *Arid1b*$^{-/-}$; tertiary: ***P<0.001 for *Arid1b*$^{+/+}$ vs. *Arid1b*$^{+/-}$ and *Arid1b*$^{+/+}$ vs. *Arid1b*$^{-/-}$). **c.** Quantification of primary, secondary, and tertiary dendrite lengths. The number of embryos used was N=6 for each genotype. Significance was determined across genotypes using one-way ANOVA with Bonferroni's post hoc correction. Data shown are mean +/- SEM.

3.4.2 Impaired corpus callosum development with Arid1b deletion

To confirm that loss of *Arid1b* has the same effect on neurite development *in vivo*, we examined axons in cortical mouse brain sections. A neural deficit frequently seen in human patients with *ARID1B* haploinsufficiency is agenesis of the corpus callosum (Halgren et al., 2012; Santen et al., 2012a), so we specifically examined axon fibers comprising the corpus callosum. We first performed in utero electroporation to incorporate *Arid1b* shRNA into the brains of mouse embryos. Adult mice injected with *Arid1b* shRNA exhibited a reduction in fluorescent intensity of axon fibers within the midline region of the corpus callosum compared to mice injected with control shRNA, implying fewer axon fibers comprising the corpus callosum (Fig. 3.3a,b). In addition, mice with *Arid1b* shRNA had decreased fluorescent intensity of axon fibers in the lateral regions of the corpus callosum as well as altered fiber direction, indicated by an increase in the number of fiber cross points, compared to control mice (Fig. 3.3c,d). Together, these results indicate that knockdown of *Arid1b* alters the development of white matter axon fibers in the cortex, in particular the corpus callosum. Since shRNA knockdown results in inconsistent gene dosage, we also wanted to examine the corpus callosum effects on *Arid1b* heterozygous knockout mice. *Arid1b*$^{+/-}$ mice were crossed with a Thy1-YFP-H mouse, resulting in *Arid1b*$^{+/-}$ mice with YFP-labeled callosal fibers. *Arid1b*$^{+/-;}$ YFP mice showed a decrease in midline corpus callosum thickness and a reduction in axon fiber fluorescent intensity compared to *Arid1b*$^{+/+}$; YFP control mice (Fig. 3.3e,f), confirming a role of ARID1B in mediating proper corpus callosum development.

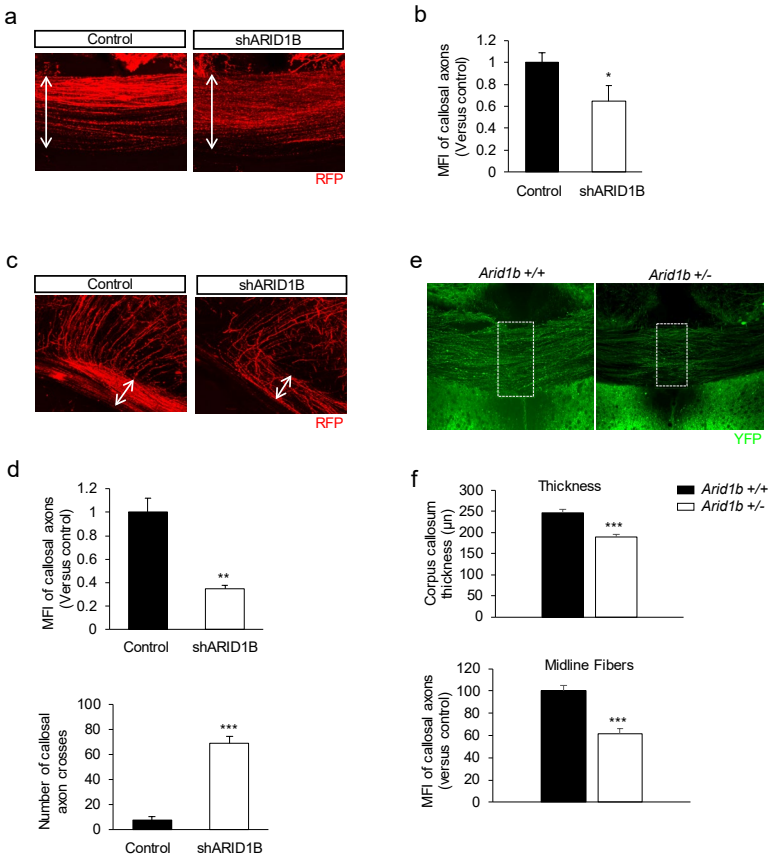

Figure 3.3 Abnormal corpus callosum development in with loss of Arid1b
a. Representative images of medial corpus callosum axon fibers labeled with RFP in adult mice injected with either shARID1B or control shRNA. **b.** Quantification of the mean fluorescence intensity of midline axon fibers comprising the corpus callosum (*P<0.05 for control vs. shARID1B). **c.** Representative images of lateral corpus callosum axon fibers labeled with RFP in adult mice injected with either shARID1B or control shRNA. **d.** Quantification of the mean fluorescence intensity of axon fibers comprising the lateral region of the corpus callosum (**P<0.01 for control vs. shARID1B) and the number of axon crosses within the lateral region of the corpus callosum (***P<0.001 for control vs. shARID1B). The number of animals used was N=5 each for mice injected with control shRNA and mice injected with shARID1B. **e.** Representative images of medial corpus callosum axon fibers labeled with YFP in adult (4 wk) *Arid1b*$^{+/+}$ and *Arid1b*$^{+/-}$ mice. **f.** Quantification of the total corpus callosum thickness at the midline (***P<0.001 for *Arid1b*$^{+/+}$ vs. *Arid1b*$^{+/-}$) and the mean fluorescence intensity of midline axon fibers (***P<0.001 for *Arid1b*$^{+/+}$ vs. *Arid1b*$^{+/-}$). The number of animals used was N=6 for each genotype. Significance for all experiments was determined using two-tailed unpaired Student's t tests. Data shown are mean +/- SEM.

3.4.3 Arid1b deletion alters neurite development via BDNF signaling activity

BDNF neurotrophin signaling is a key regulator in multiple stages of neuron development, including neurite outgrowth (Jiang et al., 2005; Morita and Sobue, 2009; Zhou et al., 2004). To determine whether ARID1B plays a role in this signaling pathway, we first examined protein expression levels of key signaling components. *Arid1b*$^{+/-}$ mouse brain cortices showed a decrease in the level of phosphorylated forms of protein kinase B (Akt) and its downstream targets mTor and Gsk3β compared to wild type controls, with no change in levels of non-phosphorylated forms, indicating altered activity of this pathway (Fig. 3.4a,b). These results suggest a possible role of ARID1B upstream of AKT in the neurotrophin signaling pathway in regulating neurite outgrowth.

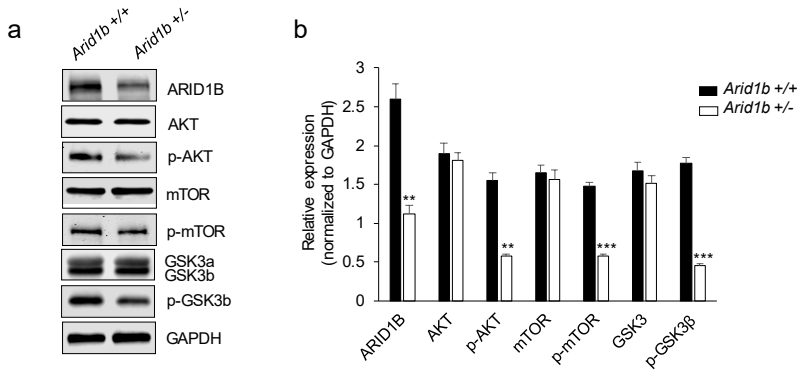

Figure 3.4 *Arid1b* heterozygous mice exhibit reduced BDNF neurotrophic signaling activity
a. Representative images of western blots showing reduced phosphorylation of proteins in the BDNF neurotrophic signaling pathway in *Arid1b*$^{+/-}$ mouse cortices. **b.** Quantification of **a**. The band intensity of each protein was normalized to GAPDH levels (ARID1B: **P<0.01; p-AKT: **P<0.01; p-mTOR: ***P<0.001; p-GSK3β: ***P<0.001). 3 independent experiments were done using 3 mice per genotype, and significance was determined using two-tailed unpaired Student's t tests. Data shown are mean +/- SEM.

We then wanted to determine whether normalizing this pathway activity in *Arid1b*-deficient neurons to wild type levels could rescue the neurite outgrowth deficits seen previously. To do this, we treated cultured neurons with various molecules to normalize BDNF signaling activity. We analyzed the total number and length of axons and dendrites after treatments with each of the following: SC79 (an AKT protein activator), BDNF (a growth factor acting on the TrkB receptor), IGF-1 (a growth factor acting on the TrkB receptor), and GSK3-i (a GSK3 inhibitor). Each treatment showed a rescue of the total axon number and length as well as total dendrite number in *Arid1b*$^{+/-}$ mouse neurons to wild type levels (Fig. 3.5a-d). Together, these results demonstrate that normalization of the BDNF signaling pathway in *Arid1b*-deficient mice rescues the impaired neurite outgrowth seen with loss of *Arid1b*, suggesting a possible mechanistic role of ARID1B in this pathway.

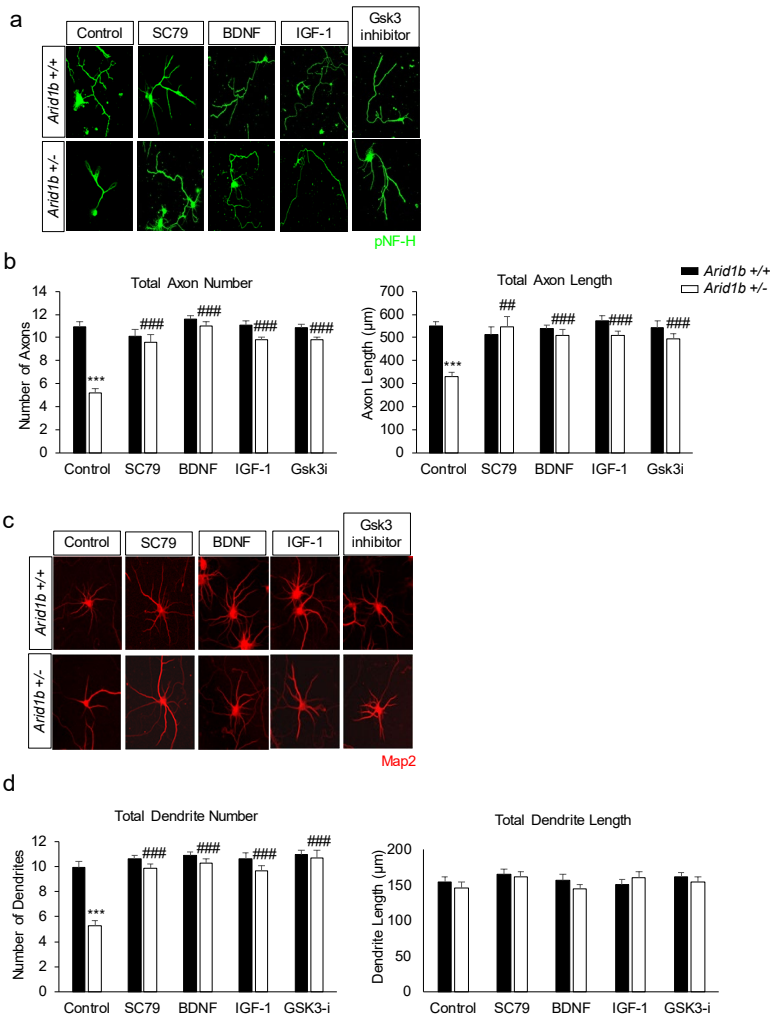

Figure 3.5 Normalizing BDNF signaling levels rescued neurite outgrowth deficits in *Arid1b* heterozygotes

a. Representative images of cultured neurons from *Arid1b*$^{+/+}$ and *Arid1b*$^{+/-}$ embryos treated with SC79, BDNF, IGF-1, GSK3-i, or no treatment. Axons are labeled with pNF-H. **b.** Quantification of the total number of axons (***P<0.001 for *Arid1b*$^{+/+}$ control vs. *Arid1b*$^{+/-}$ control; ###P<0.001 for *Arid1b*$^{+/-}$ control vs. *Arid1b*$^{+/-}$ + SC79; ###P<0.001 for *Arid1b*$^{+/-}$ control vs. *Arid1b*$^{+/-}$ + BDNF; ###P<0.001 for *Arid1b*$^{+/-}$ control vs. *Arid1b*$^{+/-}$ + IGF-1; ###P<0.001 for *Arid1b*$^{+/-}$ control vs. *Arid1b*$^{+/-}$ + GSK3-i) and total axon lengths (***P<0.001 for *Arid1b*$^{+/+}$ control vs. *Arid1b*$^{+/-}$ control; ##P<0.01 for *Arid1b*$^{+/-}$ control vs. *Arid1b*$^{+/-}$ + SC79; ###P<0.001 for *Arid1b*$^{+/-}$ control vs. *Arid1b*$^{+/-}$ + BDNF; ###P<0.001 for *Arid1b*$^{+/-}$ control vs. *Arid1b*$^{+/-}$ + IGF-1; ###P<0.001 for *Arid1b*$^{+/-}$ control vs. *Arid1b*$^{+/-}$ + GSK3-i) following each treatment. **c.** Representative images of cultured neurons from *Arid1b*$^{+/+}$ and *Arid1b*$^{+/-}$ embryos treated with SC79, BDNF, IGF-1, GSK3-i, or no treatment. Dendrites are labeled with MAP2. **d.** Quantification of the total number of dendrites (***P<0.001 for *Arid1b*$^{+/+}$ control vs. *Arid1b*$^{+/-}$ control; ###P<0.001 for *Arid1b*$^{+/-}$ control vs. *Arid1b*$^{+/-}$ + SC79; ###P<0.001 for *Arid1b*$^{+/-}$ control vs. *Arid1b*$^{+/-}$ + BDNF; ###P<0.001 for *Arid1b*$^{+/-}$ control vs. *Arid1b*$^{+/-}$ + IGF-1; ###P<0.001 for *Arid1b*$^{+/-}$ control vs. *Arid1b*$^{+/-}$ + GSK3-i) and total dendrite lengths following each treatment. For both axon and dendrite rescue experiments, 4 embryos per genotype were used for each treatment group. Significance was determined using one-way ANOVA with Bonferroni's post hoc correction. Data shown for all experiments are mean +/- SEM.

3.5 Discussion

3.5.1 Proposed pathology underlying neurite deficits in ARID1B haploinsufficiency

Haploinsufficiency of *ARID1B,* a genetic cause of ASD and ID, causes several behavioral phenotypes and anatomical changes in humans and rodents (Celen et al., 2017; Halgren et al., 2012; Hoyer et al., 2012; Jung et al., 2017; Santen et al., 2012a; Shibutani et al., 2017). Given the prevalence of neurite deficits in these disorders (Chapleau et al., 2009; Fiala et al., 2002; Kaufmann and Moser, 2000; Machado-Salas, 1984; Penzes et al., 2011) and the prominent role of chromatin remodeling during neurodevelopment (Day and Sweatt, 2011; Mehler, 2008; Ronan et al., 2013), we hypothesized that *ARID1B* deletion disrupts neurite growth during excitatory cortical neuron development. In the present study, we indeed show that deletion of *Arid1b* leads to deficits in neurite development of cortical neurons and suggest a potential mechanism of ARID1B in the BDNF signaling pathway. During proper development of the cortex, BDNF signaling mediates downstream phosphorylation of mTOR and GSK3β, which subsequently activate several proteins associated with cytoskeletal dynamics (Barnes and Polleux, 2009; Hur and Zhou, 2010; Yoshimura et al., 2005). Precise organization of actin and microtubules is the basis of the mechanism mediating neurite outgrowth and branching (Barnes and Polleux, 2009; Lewis et al., 2013). Figure 3.6 illustrates the potential pathology underlying altered neurite development in *ARID1B* haploinsufficiency. We suggest that loss of ARID1B, likely acting upstream of AKT, reduces BDNF signaling activity and ultimately disrupts the downstream actin and microtubule dynamics mediating neurite outgrowth.

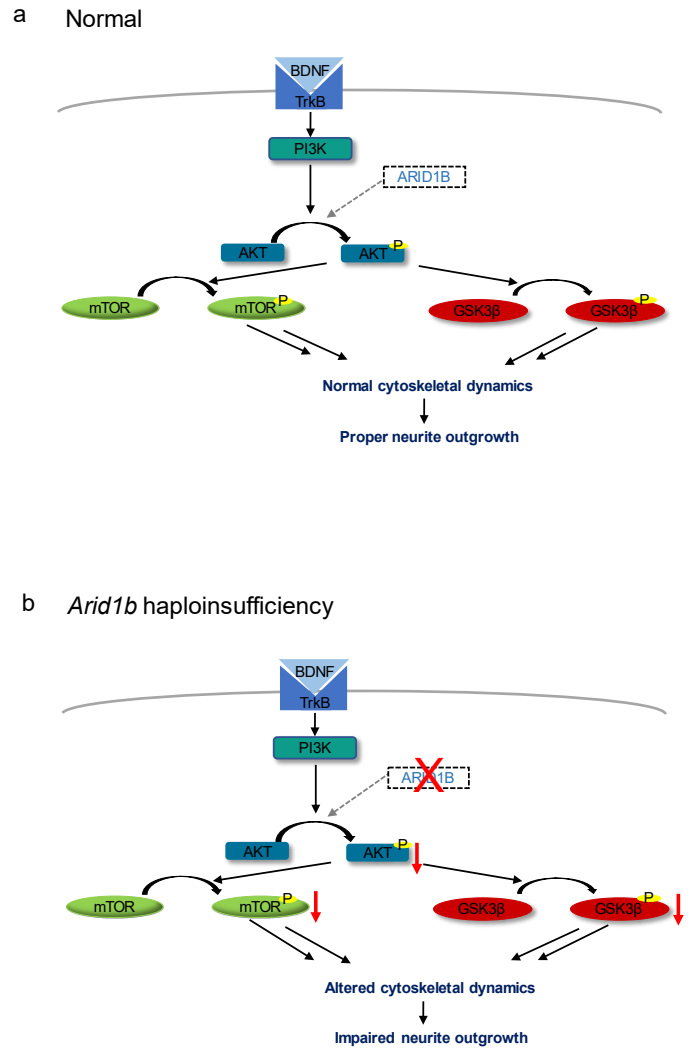

Figure 3.6 A potential role of ARID1B in the BDNF neurotrophic pathway regulating neurite outgrowth
a. A proposed role of ARID1B upstream of AKT in the BDNF signaling pathway, leading to normal cytoskeletal dynamics and proper neurite outgrowth. **b.** Loss of ARID1B in neurons leads to reduced phosphorylation of downstream AKT, mTOR, and GSK3β, resulting in altered cytoskeletal dynamics and impaired neurite outgrowth.

3.5.2 Neurite development and neurotrophic signaling deficits in various neurodevelopmental disorders

Our lab has previously shown that loss of *Arid1b* has a significant effect on inhibitory interneuron development (Jung et al., 2017). Jung et al. observed that *Arid1b* deletion led to fewer interneurons, abnormal interneuron placement, and reduced interneuron synaptic activity. Further, pharmacologic activation of interneuron activity successfully rescued several of the behavioral deficits associated with loss of the gene (Jung et al., 2017). However, in addition to deficits in interneuron development, several human patients and animal models of ASD, ID, and related disorders implicate deficits in neurite growth of excitatory neurons. For example, post-mortem brains of patients with ASD and Rett syndrome, a neurodevelopmental disorder characterized by autism- and ID-like traits, exhibit abnormal dendritic arborization and atypical genesis of the corpus callosum axon tracts (Armstrong, 2005; Belichenko et al., 1994; Halgren et al., 2012; Huttenlocher, 1974; Santen et al., 2012a). Mouse models of ASD, including knockout of *Taok2* and *Ankrd11* genes, have similar deficits in dendrite formation and axonal projections (de Anda et al., 2012; Ka and Kim, 2018). *Mecp2* knockout mice, a model for Rett syndrome, also exhibit abnormal dendritic outgrowth due to altered microtubule dynamics (Nectoux et al., 2012). Additionally, several mouse models of ASD/ID, Rett syndrome, and fragile X syndrome have decreased levels of BDNF signaling and reduced expression of downstream targets accompanying deficits in neuron maturation (Cao et al., 2013; Chang et al., 2006; Jung et al., 2016). Together, these studies contribute to the growing evidence that deficits in neurite development via disrupted neurotrophic signaling have pathogenic roles in neurodevelopmental disorders.

3.5.3 Conclusion and future prospective

Therapeutic tools to treat the core symptoms of ASD and ID are severely lacking. While the behavioral phenotypes of these disorders have been well defined,

pharmacologic treatments are not currently available. By better understanding the various mechanisms that underlie the pathology of neurodevelopmental disorders, we can determine potential pharmacologic therapeutic targets. We expect that the deficits in neurite outgrowth leads to altered connectivity among brain regions and likely contribute to the behavioral phenotypes seen with *ARID1B* haploinsufficiency-associated ASD and ID. Further research to elucidate the precise mechanism of ARID1B may lead to potential therapeutic targets within the BDNF signaling pathway.

CHAPTER 4: DISCUSSION AND CONCLUSIONS

The above chapters have discussed two major roles of ARID1B in the pathology of neurodevelopmental disorders such as autism spectrum disorder and intellectual disability. This section will summarize each chapter and discuss their implications for the field and future research avenues.

Previous work in our lab has shown that *Arid1b* haploinsufficiency leads to deficits in cortical interneuron development, suggesting disruption in the E/I balance. Mice with loss of one copy of *Arid1b* had fewer interneurons, abnormal interneuron distribution, and impaired inhibitory synaptic activity (Jung et al., 2017). Additionally, these mice exhibited several behavioral phenotypes consistent with ASD and ID, including social impairments, stereotyped behaviors, elevated anxiety and depression, and cognitive dysfunction (Jung et al., 2017). In the study presented in Chapter 2, we sought to elucidate the functional diversity among interneuron subtypes that contribute to various behavioral phenotypes seen with *Arid1b* haploinsufficiency. It is well established that interneuron classes are highly diverse and heterogenous (Kepecs and Fishell, 2014; Lim et al., 2018; Rudy et al., 2011), but little is known regarding how each subtype may modulate behaviors. Interestingly, we show that *Arid1b* haploinsufficiency in either PV or SST interneurons led to distinct behavioral phenotypes that did not overlap with one another, but recapitulated the phenotypes seen with global haploinsufficiency. Loss of Arid1b in PV interneurons had prominent effects on social behavior and anxiety- and depression-like behavior, while loss of Arid1b in SST interneurons primarily affected stereotyped behaviors and cognitive function.

Our conclusions from Chapter 2 suggest that the different subtypes of interneurons distinctly modulate behaviors. This insight will be valuable in moving

forward with developing novel therapeutic options for neurodevelopmental disorders. While the focus on normalizing inhibitory interneuron activity is a promising therapeutic technique, this method is currently non-specific and targets all interneurons in the brain. By better defining the specific behavioral roles of interneuron subtypes, pharmacologic and genetic treatments can be more targeted to modulate only certain subsets of cell types. It is important for future studies to continue to elucidate the distinct behavioral roles of interneuron subtypes in other neurodevelopmental disorder mouse models. *ARID1B* haploinsufficiency accounts for less than 1% of individuals with ASD and ID (Halgren et al., 2012; Hoyer et al., 2012; Krumm et al., 2014; Ropers and Wienker, 2015; Santen et al., 2012a; Santen et al., 2012b). While this may seem insignificant in the big picture of diagnosed individuals, it is likely that several causal genes converge on common pathways and exhibit similar underlying pathology. Indeed, most ASD/ID-associated genes are a part of one of three major classes: chromatin remodeling, transcriptional control, and synaptic structure and function (Ayhan and Konopka, 2019; Krumm et al., 2014). Further, several human patients and mouse models exhibit similar deficits in interneuron development and function (Marin, 2012; Ramamoorthi and Lin, 2011; Robertson et al., 2016). It will be interesting to see how our results compare to similar studies done with other models. Similar findings of distinct behavioral roles of interneurons may be promising for future therapies for a range of neurodevelopmental disorders.

In the study from Chapter 3, we examined the potential role of ARID1B in the development of excitatory projection neurons in the cortex. Excitatory neuron development occurs in three primary stages: proliferation/differentiation, migration, and neurite outgrowth (Azzarelli et al., 2014; Barnes and Polleux, 2009; Lalli, 2014). Each of these steps are important for proper brain circuity and synaptic connections. Disruption

of any of these processes may affect how information is transmitted throughout the brain, therefore altering normal behavior. Previous studies in our lab show no changes in number, distribution, or synaptic function of excitatory neurons within the cortex of *Arid1b*-deficient mice, suggesting proliferation/differentiation or migration issues are not causing any significant deficits within these cell types (Jung et al., 2017). While Jung et al. do report minor deficits in proliferation and apoptosis, these do not appear have any lasting affect that alters the excitatory neuron makeup of the mature cortex. It is possible that a compensatory mechanism normalizes these stages so there is still proper number and distribution of these neurons throughout the cortex.

Studies indicate that deficits in neurite outgrowth are frequently observed in mouse models and human patients of ASD and related disorders (Belichenko et al., 1994; Huttenlocher, 1974; Jiang et al., 2013; Kaufmann and Moser, 2000). Additionally, Jung et al. demonstrated that treatment of *Arid1b* heterozygous mice with a GABAergic modulator to normalize inhibitory activity was successful in rescuing ASD- and ID-like behavioral phenotypes (Jung et al., 2017). However, not all behavior deficits were completely rescued to wild type levels, suggesting a potential pathological role of excitatory neurons in addition to inhibitory interneurons. As excitatory neurons are responsible for several long-range projections to various brain regions, it would be reasonable to suggest that deficits in axon and dendrite development will affect communication between cells and alter normal behavior. This led us to examine neurite outgrowth in *Arid1b*-deficient excitatory neurons and the potential role that ARID1B plays in the process. We showed that loss of Arid1b led to deficits in neurite outgrowth and branching as well as altered corpus callosum development. Since BDNF neurotrophic signaling is a known master regulator of neurite growth and is disrupted in various neurodevelopmental disorders (Jiang et al., 2005; Morita and Sobue, 2009; Zhou et al.,

2004), we sought whether ARID1B may be playing a role in this particular pathway. We indeed showed that neurite deficits were accompanied by altered BDNF signaling, and normalization of this pathway was successful in rescuing these deficits. Interestingly, while BDNF signaling regulates axon/dendrite specification as well as neurite outgrowth, our data still show a single axon with multiple dendrites. This suggests that the deficits resulting from loss of BDNF signaling are affecting neurite growth without affecting polarity. It is possible that loss of BDNF signaling activity triggers a compensatory mechanism that normalizes the polarity specification stage during development, or that the level of activity was still sufficient to properly establish polarity. It is also possible that the BDNF signaling pathway was disrupted at a specific developmental time point after polarity has been established. It would be important in the future to determine the precise developmental stage at which BDNF signaling is disrupted.

Our results from Chapter 3 suggest a novel role of ARID1B in the development of projection neurons in the cerebral cortex, indicating a possible avenue for pharmacologic or genetic treatment targets. Further study is necessary to elucidate the precise mechanism of ARID1B. For example, the use of ChIP assays can determine whether ARID1B is directly interacting with and regulating gene expression of any components in BDNF signaling. It may also be beneficial to examine how Arid1b loss affects BDNF signaling at different developmental stages and in different subcellular compartments to determine if there is a spatiotemporal regulatory component. Given that cytoskeleton dynamics are the basis of the mechanism mediating neurite outgrowth, it would be interesting to examine how loss of Arid1b affects the cytoskeleton during neurite growth via time lapse imaging. Previous studies have been successful in rescuing neurotrophic signaling deficits by microinfusion of BDNF into the ventricles of adult mice, which led to rapid phosphorylation of downstream components (Ying et al., 2002). This ability to

rescue BDNF signaling *in vivo* is an exciting avenue for future research in the treatment of neurodevelopmental disorders with neurotrophic signaling deficits.

Overall, results presented in this dissertation shows significant progress in the various roles of ASD/ID-associated gene *ARID1B* in the development of the cerebral cortex. This insight into the underlying pathogenesis of neurodevelopmental disorders paves the way for future studies and brings to light new questions. The field has come a long way in discovering novel therapies for the treatment of neurodevelopment disorders. Pharmacologic techniques to modulate GABAergic activity and neurotrophic signaling is a promising treatment approach given the high incidence of interneuron dysfunction and BDNF signaling deficits. Genetic tools have also become a promising treatment approach. Gene therapy via AAV-mediated delivery has shown success in several animal models and human patients of neurological disorders (Hocquemiller et al., 2016). However, utilizing this strategy as a successful therapy for neurodevelopmental disorders will likely be limited by a critical developmental window for treatment. Additionally, success in genome editing via the CRISPR/Cas system in reprogramming pluripotent stem cells indicates a theoretical possibility of utilizing this strategy in the treatment of neurological diseases (Yang and Huang, 2019). There are still several ethical considerations that need attention before this strategy can be considered a plausible avenue. Gaining a more complete understanding of the mechanisms of ARID1B and other genes involved with neurodevelopment will enhance the individualization of novel therapies for those affected with neurodevelopmental disorders. Furthermore, dissecting individual cell types and specific circuits that regulate pathogenic behaviors will make more targeted therapies with fewer side effects more feasible.

REFERENCES

Antoine, M.W., Langberg, T., Schnepel, P., and Feldman, D.E. (2019). Increased Excitation-Inhibition Ratio Stabilizes Synapse and Circuit Excitability in Four Autism Mouse Models. Neuron *101*, 648-661.e644.

Aoki, Y., Yoncheva, Y.N., Chen, B., Nath, T., Sharp, D., Lazar, M., Velasco, P., Milham, M.P., and Di Martino, A. (2017). Association of White Matter Structure With Autism Spectrum Disorder and Attention-Deficit/Hyperactivity Disorder. JAMA Psychiatry *74*, 1120-1128.

Armstrong, D.D. (2005). Neuropathology of Rett syndrome. Journal of child neurology *20*, 747-753.

Artinian, J., and Lacaille, J.C. (2018). Disinhibition in learning and memory circuits: New vistas for somatostatin interneurons and long-term synaptic plasticity. Brain Res Bull *141*, 20-26.

Ayhan, F., and Konopka, G. (2019). Regulatory genes and pathways disrupted in autism spectrum disorders. Prog Neuropsychopharmacol Biol Psychiatry *89*, 57-64.

Azzarelli, R., Kerloch, T., and Pacary, E. (2014). Regulation of cerebral cortex development by Rho GTPases: insights from in vivo studies. Front Cell Neurosci *8*, 445.

Bachmann, C., Nguyen, H., Rosenbusch, J., Pham, L., Rabe, T., Patwa, M., Sokpor, G., Seong, R.H., Ashery-Padan, R., Mansouri, A.*, et al.* (2016). mSWI/SNF (BAF) Complexes Are Indispensable for the Neurogenesis and Development of Embryonic Olfactory Epithelium. PLoS Genet *12*, e1006274.

Barnes, A.P., and Polleux, F. (2009). Establishment of axon-dendrite polarity in developing neurons. Annu Rev Neurosci *32*, 347-381.

Basu, S.N., Kollu, R., and Banerjee-Basu, S. (2009). AutDB: a gene reference resource for autism research. Nucleic acids research *37*, D832-836.

Belichenko, P.V., Oldfors, A., Hagberg, B., and Dahlstrom, A. (1994). Rett syndrome: 3-D confocal microscopy of cortical pyramidal dendrites and afferents. Neuroreport *5*, 1509-1513.

Belsito, K.M., Law, P.A., Kirk, K.S., Landa, R.J., and Zimmerman, A.W. (2001). Lamotrigine therapy for autistic disorder: a randomized, double-blind, placebo-controlled trial. Journal of autism and developmental disorders *31*, 175-181.

Benson, B.A., and Brooks, W.T. (2008). Aggressive challenging behaviour and intellectual disability. Current opinion in psychiatry *21*, 454-458.

Bortone, D., and Polleux, F. (2009). KCC2 expression promotes the termination of cortical interneuron migration in a voltage-sensitive calcium-dependent manner. Neuron *62*, 53-71.

Bortone, D.S., Olsen, S.R., and Scanziani, M. (2014). Translaminar inhibitory cells recruited by layer 6 corticothalamic neurons suppress visual cortex. Neuron *82*, 474-485.

Bourne, J.N., and Harris, K.M. (2008). Balancing structure and function at hippocampal dendritic spines. Annu Rev Neurosci *31*, 47-67.

Butt, S.J., Stacey, J.A., Teramoto, Y., and Vagnoni, C. (2017). A role for GABAergic interneuron diversity in circuit development and plasticity of the neonatal cerebral cortex. Curr Opin Neurobiol *43*, 149-155.

Calfa, G., Percy, A.K., and Pozzo-Miller, L. (2011). Experimental models of Rett syndrome based on Mecp2 dysfunction. Experimental biology and medicine (Maywood, NJ) *236*, 3-19.

Canetta, S., Bolkan, S., Padilla-Coreano, N., Song, L.J., Sahn, R., Harrison, N.L., Gordon, J.A., Brown, A., and Kellendonk, C. (2016). Maternal immune activation leads to selective functional deficits in offspring parvalbumin interneurons. Molecular psychiatry *21*, 956-968.

Cao, C., Rioult-Pedotti, M.S., Migani, P., Yu, C.J., Tiwari, R., Parang, K., Spaller, M.R., Goebel, D.J., and Marshall, J. (2013). Impairment of TrkB-PSD-95 signaling in Angelman syndrome. PLoS biology *11*, e1001478.

Caputi, A., Melzer, S., Michael, M., and Monyer, H. (2013). The long and short of GABAergic neurons. Curr Opin Neurobiol *23*, 179-186.

Catalano, S.M., and Shatz, C.J. (1998). Activity-dependent cortical target selection by thalamic axons. Science *281*, 559-562.

Celen, C., Chuang, J.C., Luo, X., Nijem, N., Walker, A.K., Chen, F., Zhang, S., Chung, A.S., Nguyen, L.H., Nassour, I.*, et al.* (2017). Arid1b haploinsufficient mice reveal neuropsychiatric phenotypes and reversible causes of growth impairment. Elife *6*.

Chahrour, M., and Zoghbi, H.Y. (2007). The story of Rett syndrome: from clinic to neurobiology. Neuron *56*, 422-437.

Chang, Q., Khare, G., Dani, V., Nelson, S., and Jaenisch, R. (2006). The disease progression of Mecp2 mutant mice is affected by the level of BDNF expression. Neuron *49*, 341-348.

Chapleau, C.A., Larimore, J.L., Theibert, A., and Pozzo-Miller, L. (2009). Modulation of dendritic spine development and plasticity by BDNF and vesicular trafficking: fundamental roles in neurodevelopmental disorders associated with mental retardation and autism. J Neurodev Disord *1*, 185-196.

Chen, R.Z., Akbarian, S., Tudor, M., and Jaenisch, R. (2001). Deficiency of methyl-CpG binding protein-2 in CNS neurons results in a Rett-like phenotype in mice. Nat Genet *27*, 327-331.

Chen, X., Liu, Z., Ma, C., Ma, L., and Liu, X. (2019). Parvalbumin Interneurons Determine Emotional Valence Through Modulating Accumbal Output Pathways. Front Behav Neurosci *13*, 110.

Chen, Y.J., Zhang, M., Yin, D.M., Wen, L., Ting, A., Wang, P., Lu, Y.S., Zhu, X.H., Li, S.J., Wu, C.Y.*, et al.* (2010). ErbB4 in parvalbumin-positive interneurons is critical for neuregulin 1 regulation of long-term potentiation. Proc Natl Acad Sci U S A *107*, 21818-21823.

Choi, K.Y., Yoo, M., and Han, J.H. (2015). Toward understanding the role of the neuron-specific BAF chromatin remodeling complex in memory formation. Experimental & molecular medicine *47*, e155.

Cossart, R. (2011). The maturation of cortical interneuron diversity: how multiple developmental journeys shape the emergence of proper network function. Curr Opin Neurobiol *21*, 160-168.

Cui, Y., Costa, R.M., Murphy, G.G., Elgersma, Y., Zhu, Y., Gutmann, D.H., Parada, L.F., Mody, I., and Silva, A.J. (2008). Neurofibromin regulation of ERK signaling modulates GABA release and learning. Cell *135*, 549-560.

Curia, G., Papouin, T., Seguela, P., and Avoli, M. (2009). Downregulation of tonic GABAergic inhibition in a mouse model of fragile X syndrome. Cereb Cortex *19*, 1515-1520.

Cybulska-Klosowicz, A., Posluszny, A., Nowak, K., Siucinska, E., Kossut, M., and Liguz-Lecznar, M. (2013). Interneurons containing somatostatin are affected by learning-induced cortical plasticity. Neuroscience *254*, 18-25.

Daily, D.K., Ardinger, H.H., and Holmes, G.E. (2000). Identification and evaluation of mental retardation. Am Fam Physician *61*, 1059-1067, 1070.

Daily, J.L., Nash, K., Jinwal, U., Golde, T., Rogers, J., Peters, M.M., Burdine, R.D., Dickey, C., Banko, J.L., and Weeber, E.J. (2011). Adeno-associated virus-mediated rescue of the cognitive defects in a mouse model for Angelman syndrome. PloS one *6*, e27221.

Day, J.J., and Sweatt, J.D. (2011). Epigenetic mechanisms in cognition. Neuron *70*, 813-829.

de Anda, F.C., Rosario, A.L., Durak, O., Tran, T., Graff, J., Meletis, K., Rei, D., Soda, T., Madabhushi, R., Ginty, D.D*., et al.* (2012). Autism spectrum disorder susceptibility gene TAOK2 affects basal dendrite formation in the neocortex. Nat Neurosci *15*, 1022-1031.

DeFilippis, M. (2018). Depression in Children and Adolescents with Autism Spectrum Disorder. Children *5*.

Di Martino, A., and Tuchman, R.F. (2001). Antiepileptic drugs: affective use in autism spectrum disorders. Pediatric neurology *25*, 199-207.

Dutar, P., Vaillend, C., Viollet, C., Billard, J.M., Potier, B., Carlo, A.S., Ungerer, A., and Epelbaum, J. (2002). Spatial learning and synaptic hippocampal plasticity in type 2 somatostatin receptor knock-out mice. Neuroscience *112*, 455-466.

Einstein, E.B., Patterson, C.A., Hon, B.J., Regan, K.A., Reddi, J., Melnikoff, D.E., Mateer, M.J., Schulz, S., Johnson, B.N., and Tallent, M.K. (2010). Somatostatin signaling in neuronal cilia is critical for object recognition memory. J Neurosci *30*, 4306-4314.

Ellison, J.W., Rosenfeld, J.A., and Shaffer, L.G. (2013). Genetic Basis of Intellectual Disability. Annual Review of Medicine *64*, 441-450.

Engin, E., Stellbrink, J., Treit, D., and Dickson, C.T. (2008). Anxiolytic and antidepressant effects of intracerebroventricularly administered somatostatin: behavioral and neurophysiological evidence. Neuroscience *157*, 666-676.

Eppig, J.T., Blake, J.A., Bult, C.J., Kadin, J.A., and Richardson, J.E. (2015). The Mouse Genome Database (MGD): facilitating mouse as a model for human biology and disease. Nucleic acids research *43*, D726-736.

Fakhoury, M. (2015). Autistic spectrum disorders: A review of clinical features, theories and diagnosis. International journal of developmental neuroscience : the official journal of the International Society for Developmental Neuroscience *43*, 70-77.

Fatemi, S.H., Reutiman, T.J., Folsom, T.D., and Thuras, P.D. (2009). GABA(A) receptor downregulation in brains of subjects with autism. Journal of autism and developmental disorders *39*, 223-230.

Fernandez, F., Morishita, W., Zuniga, E., Nguyen, J., Blank, M., Malenka, R.C., and Garner, C.C. (2007). Pharmacotherapy for cognitive impairment in a mouse model of Down syndrome. Nat Neurosci *10*, 411-413.

Fiala, J.C., Spacek, J., and Harris, K.M. (2002). Dendritic Spine Pathology: Cause or Consequence of Neurological Disorders? Brain Research Reviews *39*, 29-54.

Fitzpatrick, S.E., Srivorakiat, L., Wink, L.K., Pedapati, E.V., and Erickson, C.A. (2016). Aggression in autism spectrum disorder: presentation and treatment options. Neuropsychiatric disease and treatment *12*, 1525-1538.

Fuchs, T., Jefferson, S.J., Hooper, A., Yee, P.H., Maguire, J., and Luscher, B. (2017a). Disinhibition of somatostatin-positive GABAergic interneurons results in an anxiolytic and antidepressant-like brain state. Molecular psychiatry *22*, 920-930.

Fuchs, T., Jefferson, S.J., Hooper, A., Yee, P.P., Maguire, J., and Luscher, B. (2017b). Disinhibition of somatostatin-positive interneurons by deletion of postsynaptic GABAA receptors. Molecular psychiatry *22*, 787.

Fukuda, T., Itoh, M., Ichikawa, T., Washiyama, K., and Goto, Y.-i. (2005). Delayed Maturation of Neuronal Architecture and Synaptogenesis in Cerebral Cortex of

Mecp2-Deficient Mice. Journal of Neuropathology & Experimental Neurology *64*, 537-544.

Gatto, C.L., and Broadie, K. (2010). Genetic controls balancing excitatory and inhibitory synaptogenesis in neurodevelopmental disorder models. Front Synaptic Neurosci *2*, 4.

Gibson, J.R., Bartley, A.F., Hays, S.A., and Huber, K.M. (2008). Imbalance of neocortical excitation and inhibition and altered UP states reflect network hyperexcitability in the mouse model of fragile X syndrome. Journal of neurophysiology *100*, 2615-2626.

Gibson, W.T., Hood, R.L., Zhan, S.H., Bulman, D.E., Fejes, A.P., Moore, R., Mungall, A.J., Eydoux, P., Babul-Hirji, R., An, J.*, et al.* (2012). Mutations in EZH2 cause Weaver syndrome. Am J Hum Genet *90*, 110-118.

Gierdalski, M., Jablonska, B., Siucinska, E., Lech, M., Skibinska, A., and Kossut, M. (2001). Rapid regulation of GAD67 mRNA and protein level in cortical neurons after sensory learning. Cereb Cortex *11*, 806-815.

Gilbert, J., and Man, H.Y. (2017). Fundamental Elements in Autism: From Neurogenesis and Neurite Growth to Synaptic Plasticity. Front Cell Neurosci *11*, 359.

Gogolla, N., Leblanc, J.J., Quast, K.B., Sudhof, T.C., Fagiolini, M., and Hensch, T.K. (2009). Common circuit defect of excitatory-inhibitory balance in mouse models of autism. J Neurodev Disord *1*, 172-181.

Gomez, T.M., Robles, E., Poo, M., and Spitzer, N.C. (2001). Filopodial calcium transients promote substrate-dependent growth cone turning. Science *291*, 1983-1987.

Gomez, T.M., and Spitzer, N.C. (1999). In vivo regulation of axon extension and pathfinding by growth-cone calcium transients. Nature *397*, 350-355.

Guy, J., Gan, J., Selfridge, J., Cobb, S., and Bird, A. (2007). Reversal of neurological defects in a mouse model of Rett syndrome. Science *315*, 1143-1147.

Guy, J., Hendrich, B., Holmes, M., Martin, J.E., and Bird, A. (2001). A mouse Mecp2-null mutation causes neurological symptoms that mimic Rett syndrome. Nat Genet *27*, 322-326.

Halgren, C., Kjaergaard, S., Bak, M., Hansen, C., El-Schich, Z., Anderson, C.M., Henriksen, K.F., Hjalgrim, H., Kirchhoff, M., Bijlsma, E.K.*, et al.* (2012). Corpus callosum abnormalities, intellectual disability, speech impairment, and autism in patients with haploinsufficiency of ARID1B. Clin Genet *82*, 248-255.

Han, K., Chen, H., Gennarino, V.A., Richman, R., Lu, H.-C., and Zoghbi, H.Y. (2015). Fragile X-like behaviors and abnormal cortical dendritic spines in cytoplasmic FMR1-interacting protein 2-mutant mice. Hum Mol Genet *24*, 1813-1823.

Han, S., Tai, C., Westenbroek, R.E., Yu, F.H., Cheah, C.S., Potter, G.B., Rubenstein, J.L., Scheuer, T., de la Iglesia, H.O., and Catterall, W.A. (2012). Autistic-like behaviour in Scn1a+/- mice and rescue by enhanced GABA-mediated neurotransmission. Nature *489*, 385-390.

Harris, K.D., Hochgerner, H., Skene, N.G., Magno, L., Katona, L., Bengtsson Gonzales, C., Somogyi, P., Kessaris, N., Linnarsson, S., and Hjerling-Leffler, J. (2018). Classes and continua of hippocampal CA1 inhibitory neurons revealed by single-cell transcriptomics. PLoS biology *16*, e2006387.

Harris, K.M., and Kater, S.B. (1994). Dendritic spines: cellular specializations imparting both stability and flexibility to synaptic function. Annu Rev Neurosci *17*, 341-371.

Harris, S.W., Hessl, D., Goodlin-Jones, B., Ferranti, J., Bacalman, S., Barbato, I., Tassone, F., Hagerman, P.J., Herman, H., and Hagerman, R.J. (2008). Autism profiles of males with fragile X syndrome. American journal of mental retardation : AJMR *113*, 427-438.

Hashemi, E., Ariza, J., Rogers, H., Noctor, S.C., and Martinez-Cerdeno, V. (2017). The Number of Parvalbumin-Expressing Interneurons Is Decreased in the Prefrontal Cortex in Autism. Cereb Cortex *27*, 1931-1943.

He, M., Tucciarone, J., Lee, S., Nigro, M.J., Kim, Y., Levine, J.M., Kelly, S.M., Krugikov, I., Wu, P., Chen, Y.*, et al.* (2016). Strategies and Tools for Combinatorial Targeting of GABAergic Neurons in Mouse Cerebral Cortex. Neuron *91*, 1228-1243.

Heidenreich, M., and Zhang, F. (2016). Applications of CRISPR-Cas systems in neuroscience. Nat Rev Neurosci *17*, 36-44.

Hellal, F., Hurtado, A., Ruschel, J., Flynn, K.C., Laskowski, C.J., Umlauf, M., Kapitein, L.C., Strikis, D., Lemmon, V., Bixby, J.*, et al.* (2011). Microtubule stabilization reduces scarring and causes axon regeneration after spinal cord injury. Science *331*, 928-931.

Hevner, R.F., Daza, R.A., Englund, C., Kohtz, J., and Fink, A. (2004). Postnatal shifts of interneuron position in the neocortex of normal and reeler mice: evidence for inward radial migration. Neuroscience *124*, 605-618.

Hilscher, M.M., Leao, R.N., Edwards, S.J., Leao, K.E., and Kullander, K. (2017). Chrna2-Martinotti Cells Synchronize Layer 5 Type A Pyramidal Cells via Rebound Excitation. PLoS biology *15*, e2001392.

Ho, L., and Crabtree, G.R. (2010). Chromatin remodelling during development. Nature *463*, 474-484.

Ho, L., Ronan, J.L., Wu, J., Staahl, B.T., Chen, L., Kuo, A., Lessard, J., Nesvizhskii, A.I., Ranish, J., and Crabtree, G.R. (2009). An embryonic stem cell chromatin remodeling complex, esBAF, is essential for embryonic stem cell self-renewal and pluripotency. Proc Natl Acad Sci U S A *106*, 5181-5186.

Hocquemiller, M., Giersch, L., Audrain, M., Parker, S., and Cartier, N. (2016). Adeno-Associated Virus-Based Gene Therapy for CNS Diseases. Human gene therapy *27*, 478-496.

Hoyer, J., Ekici, A.B., Endele, S., Popp, B., Zweier, C., Wiesener, A., Wohlleber, E., Dufke, A., Rossier, E., Petsch, C.*, et al.* (2012). Haploinsufficiency of ARID1B, a member of the SWI/SNF-a chromatin-remodeling complex, is a frequent cause of intellectual disability. Am J Hum Genet *90*, 565-572.

Hu, H., Gan, J., and Jonas, P. (2014). Interneurons. Fast-spiking, parvalbumin(+) GABAergic interneurons: from cellular design to microcircuit function. Science *345*, 1255263.

Hur, E.M., and Zhou, F.Q. (2010). GSK3 signalling in neural development. Nat Rev Neurosci *11*, 539-551.

Hutsler, J.J., and Zhang, H. (2010). Increased dendritic spine densities on cortical projection neurons in autism spectrum disorders. Brain research *1309*, 83-94.

Huttenlocher, P.R. (1974). Dendritic development in neocortex of children with mental defect and infantile spasms. Neurology *24*, 203-203.

Irwin, S.A., Idupulapati, M., Gilbert, M.E., Harris, J.B., Chakravarti, A.B., Rogers, E.J., Crisostomo, R.A., Larsen, B.P., Mehta, A., Alcantara, C.J.*, et al.* (2002). Dendritic spine and dendritic field characteristics of layer V pyramidal neurons in the visual cortex of fragile-X knockout mice. American journal of medical genetics *111*, 140-146.

Isrie, M., Hendriks, Y., Gielissen, N., Sistermans, E.A., Willemsen, M.H., Peeters, H., Vermeesch, J.R., Kleefstra, T., and Van Esch, H. (2012). Haploinsufficiency of ANKRD11 causes mild cognitive impairment, short stature and minor dysmorphisms. European journal of human genetics : EJHG *20*, 131-133.

Ito-Ishida, A., Ure, K., Chen, H., Swann, J.W., and Zoghbi, H.Y. (2015). Loss of MeCP2 in Parvalbumin-and Somatostatin-Expressing Neurons in Mice Leads to Distinct Rett Syndrome-like Phenotypes. Neuron *88*, 651-658.

Jamain, S., Radyushkin, K., Hammerschmidt, K., Granon, S., Boretius, S., Varoqueaux, F., Ramanantsoa, N., Gallego, J., Ronnenberg, A., Winter, D*., et al.* (2008). Reduced social interaction and ultrasonic communication in a mouse model of monogenic heritable autism. Proc Natl Acad Sci U S A *105*, 1710-1715.

Jentarra, G.M., Olfers, S.L., Rice, S.G., Srivastava, N., Homanics, G.E., Blue, M., Naidu, S., and Narayanan, V. (2010). Abnormalities of cell packing density and dendritic complexity in the MeCP2 A140V mouse model of Rett syndrome/X-linked mental retardation. BMC neuroscience *11*, 19.

Jiang, H., Guo, W., Liang, X., and Rao, Y. (2005). Both the establishment and the maintenance of neuronal polarity require active mechanisms: critical roles of GSK-3beta and its upstream regulators. Cell *120*, 123-135.

Jiang, M., Ash, R.T., Baker, S.A., Suter, B., Ferguson, A., Park, J., Rudy, J., Torsky, S.P., Chao, H.T., Zoghbi, H.Y*., et al.* (2013). Dendritic arborization and spine dynamics are abnormal in the mouse model of MECP2 duplication syndrome. J Neurosci *33*, 19518-19533.

Jung, E.-M., Moffat, J.J., Liu, J., Dravid, S.M., Gurumurthy, C.B., and Kim, W.-Y. (2017). Arid1b haploinsufficiency disrupts cortical interneuron development and mouse behavior. Nature Neuroscience *20*, 1694-1707.

Jung, E.M., Ka, M., and Kim, W.Y. (2016). Loss of GSK-3 Causes Abnormal Astrogenesis and Behavior in Mice. Molecular neurobiology *53*, 3954-3966.

Jung, E.M., Moffat, J.J., and Kim, W.Y. (2015). Regenerative potential of targeting glycogen synthase kinase-3 signaling in neural tissues. Neural Regen Res *10*, 1912-1913.

Ka, M., Chopra, D.A., Dravid, S.M., and Kim, W.Y. (2016a). Essential Roles for ARID1B in Dendritic Arborization and Spine Morphology of Developing Pyramidal Neurons. J Neurosci *36*, 2723-2742.

Ka, M., Condorelli, G., Woodgett, J.R., and Kim, W.Y. (2014a). mTOR regulates brain morphogenesis by mediating GSK3 signaling. Development *141*, 4076-4086.

Ka, M., Jung, E.M., Mueller, U., and Kim, W.Y. (2014b). MACF1 regulates the migration of pyramidal neurons via microtubule dynamics and GSK-3 signaling. Dev Biol *395*, 4-18.

Ka, M., and Kim, W.Y. (2016). Microtubule-Actin Crosslinking Factor 1 Is Required for Dendritic Arborization and Axon Outgrowth in the Developing Brain. Mol Neurobiol *53*, 6018-6032.

Ka, M., and Kim, W.Y. (2018). ANKRD11 associated with intellectual disability and autism regulates dendrite differentiation via the BDNF/TrkB signaling pathway. Neurobiol Dis *111*, 138-152.

Ka, M., Kook, Y.H., Liao, K., Buch, S., and Kim, W.Y. (2016b). Transactivation of TrkB by Sigma-1 receptor mediates cocaine-induced changes in dendritic spine density and morphology in hippocampal and cortical neurons. Cell death & disease *7*, e2414.

Ka, M., Moffat, J.J., and Kim, W.Y. (2017). MACF1 Controls Migration and Positioning of Cortical GABAergic Interneurons in Mice. Cereb Cortex *27*, 5525-5538.

Karayannis, T., Au, E., Patel, J.C., Kruglikov, I., Markx, S., Delorme, R., Heron, D., Salomon, D., Glessner, J., Restituito, S*., et al.* (2014). Cntnap4 differentially contributes to GABAergic and dopaminergic synaptic transmission. Nature *511*, 236-240.

Kast, R.J., and Levitt, P. (2019). Precision in the development of neocortical architecture: From progenitors to cortical networks. Prog Neurobiol *175*, 77-95.
Kaufmann, W.E., and Moser, H.W. (2000). Dendritic Anomalies in Disorders Associated with Mental Retardation. Cerebral Cortex *10*, 981-991.
Kepecs, A., and Fishell, G. (2014). Interneuron cell types are fit to function. Nature *505*, 318-326.
Kim, D., Jeong, H., Lee, J., Ghim, J.W., Her, E.S., Lee, S.H., and Jung, M.W. (2016). Distinct Roles of Parvalbumin- and Somatostatin-Expressing Interneurons in Working Memory. Neuron *92*, 902-915.
Kim, W.-Y., Zhou, F.-Q., Zhou, J., Yokota, Y., Wang, Y.-M., Yoshimura, T., Kaibuchi, K., Woodgett, J.R., Anton, E., and Snider, W.D. (2006). Essential roles for GSK-3s and GSK-3 primed substrates in neurotrophin-induced and hippocampal axon growth. Neuron *52*, 981-996.
Kim, W.Y., Wang, X., Wu, Y., Doble, B.W., Patel, S., Woodgett, J.R., and Snider, W.D. (2009). GSK-3 is a master regulator of neural progenitor homeostasis. Nat Neurosci *12*, 1390-1397.
Klausberger, T., and Somogyi, P. (2008). Neuronal diversity and temporal dynamics: the unity of hippocampal circuit operations. Science *321*, 53-57.
Kogan, M.D., Blumberg, S.J., Schieve, L.A., Boyle, C.A., Perrin, J.M., Ghandour, R.M., Singh, G.K., Strickland, B.B., Trevathan, E., and van Dyck, P.C. (2009). Prevalence of parent-reported diagnosis of autism spectrum disorder among children in the US, 2007. Pediatrics *124*, 1395-1403.
Kornberg, R.D. (1974). Chromatin structure: a repeating unit of histones and DNA. Science *184*, 868-871.
Krumm, N., O'Roak, B.J., Shendure, J., and Eichler, E.E. (2014). A de novo convergence of autism genetics and molecular neuroscience. Trends Neurosci *37*, 95-105.
Kucharsky Hiess, R., Alter, R., Sojoudi, S., Ardekani, B.A., Kuzniecky, R., and Pardoe, H.R. (2015). Corpus callosum area and brain volume in autism spectrum disorder: quantitative analysis of structural MRI from the ABIDE database. Journal of autism and developmental disorders *45*, 3107-3114.
Kuki, T., Fujihara, K., Miwa, H., Tamamaki, N., Yanagawa, Y., and Mushiake, H. (2015). Contribution of parvalbumin and somatostatin-expressing GABAergic neurons to slow oscillations and the balance in beta-gamma oscillations across cortical layers. Front Neural Circuits *9*, 6.
Lalli, G. (2014). Regulation of neuronal polarity. Exp Cell Res *328*, 267-275.
Lauterborn, J.C., Rex, C.S., Kramar, E., Chen, L.Y., Pandyarajan, V., Lynch, G., and Gall, C.M. (2007). Brain-derived neurotrophic factor rescues synaptic plasticity in a mouse model of fragile X syndrome. J Neurosci *27*, 10685-10694.
Le Magueresse, C., and Monyer, H. (2013). GABAergic interneurons shape the functional maturation of the cortex. Neuron *77*, 388-405.
Lee, E., Lee, J., and Kim, E. (2017). Excitation/Inhibition Imbalance in Animal Models of Autism Spectrum Disorders. Biol Psychiatry *81*, 838-847.
Lee, S., Hjerling-Leffler, J., Zagha, E., Fishell, G., and Rudy, B. (2010). The largest group of superficial neocortical GABAergic interneurons expresses ionotropic serotonin receptors. J Neurosci *30*, 16796-16808.
Lee, S.H., Kwan, A.C., and Dan, Y. (2014). Interneuron subtypes and orientation tuning. Nature *508*, E1-2.
Lessard, J., Wu, J.I., Ranish, J.A., Wan, M., Winslow, M.M., Staahl, B.T., Wu, H., Aebersold, R., Graef, I.A., and Crabtree, G.R. (2007). An essential switch in

subunit composition of a chromatin remodeling complex during neural development. Neuron *55*, 201-215.
Lewis, T.L., Jr., Courchet, J., and Polleux, F. (2013). Cell biology in neuroscience: Cellular and molecular mechanisms underlying axon formation, growth, and branching. J Cell Biol *202*, 837-848.
Li, X.S., Trojer, P., Matsumura, T., Treisman, J.E., and Tanese, N. (2010). Mammalian SWI/SNF--a subunit BAF250/ARID1 is an E3 ubiquitin ligase that targets histone H2B. Molecular and cellular biology *30*, 1673-1688.
Lim, L., Mi, D., Llorca, A., and Marin, O. (2018). Development and Functional Diversification of Cortical Interneurons. Neuron *100*, 294-313.
Lin, L.C., and Sibille, E. (2015). Somatostatin, neuronal vulnerability and behavioral emotionality. Molecular psychiatry *20*, 377-387.
Lo-Castro, A., Brancati, F., Digilio, M.C., Garaci, F.G., Bollero, P., Alfieri, P., and Curatolo, P. (2013). Neurobehavioral phenotype observed in KBG syndrome caused by ANKRD11 mutations. American journal of medical genetics Part B, Neuropsychiatric genetics : the official publication of the International Society of Psychiatric Genetics *162b*, 17-23.
Lodato, S., Rouaux, C., Quast, K.B., Jantrachotechatchawan, C., Studer, M., Hensch, T.K., and Arlotta, P. (2011). Excitatory projection neuron subtypes control the distribution of local inhibitory interneurons in the cerebral cortex. Neuron *69*, 763-779.
Lopez, A.J., and Wood, M.A. (2015). Role of nucleosome remodeling in neurodevelopmental and intellectual disability disorders. Front Behav Neurosci *9*, 100.
Luo, L., and O'Leary, D.D. (2005). Axon retraction and degeneration in development and disease. Annu Rev Neurosci *28*, 127-156.
Machado-Salas, J.P. (1984). Abnormal dendritic patterns and aberrant spine development in Bourneville's disease--a Golgi survey. Clinical neuropathology *3*, 52-58.
Mao, W., Watanabe, T., Cho, S., Frost, J.L., Truong, T., Zhao, X., and Futai, K. (2015). Shank1 regulates excitatory synaptic transmission in mouse hippocampal parvalbumin-expressing inhibitory interneurons. The European journal of neuroscience *41*, 1025-1035.
Marin-Padilla, M. (1976). Pyramidal cell abnormalities in the motor cortex of a child with Down's syndrome. A Golgi study. The Journal of comparative neurology *167*, 63-81.
Marin, O. (2012). Interneuron dysfunction in psychiatric disorders. Nat Rev Neurosci *13*, 107-120.
Martens, J.A., and Winston, F. (2003). Recent advances in understanding chromatin remodeling by Swi/Snf complexes. Current Opinion in Genetics & Development *13*, 136-142.
Martínez-Cerdeño, V. (2017). Dendrite and spine modifications in autism and related neurodevelopmental disorders in patients and animal models. Developmental neurobiology *77*, 393-404.
Martinez de Lagran, M., Benavides-Piccione, R., Ballesteros-Yanez, I., Calvo, M., Morales, M., Fillat, C., Defelipe, J., Ramakers, G.J., and Dierssen, M. (2012). Dyrk1A influences neuronal morphogenesis through regulation of cytoskeletal dynamics in mammalian cortical neurons. Cereb Cortex *22*, 2867-2877.
Matson, J.L., and Nebel-Schwalm, M.S. (2007). Comorbid psychopathology with autism spectrum disorder in children: an overview. Research in developmental disabilities *28*, 341-352.

Mayer, C., Hafemeister, C., Bandler, R.C., Machold, R., Batista Brito, R., Jaglin, X., Allaway, K., Butler, A., Fishell, G., and Satija, R. (2018). Developmental diversification of cortical inhibitory interneurons. Nature *555*, 457-462.

McKinney, B.C., Grossman, A.W., Elisseou, N.M., and Greenough, W.T. (2005). Dendritic spine abnormalities in the occipital cortex of C57BL/6 Fmr1 knockout mice. American journal of medical genetics Part B, Neuropsychiatric genetics : the official publication of the International Society of Psychiatric Genetics *136b*, 98-102.

McNaughton, C.H., Moon, J., Strawderman, M.S., Maclean, K.N., Evans, J., and Strupp, B.J. (2008). Evidence for social anxiety and impaired social cognition in a mouse model of fragile X syndrome. Behavioral neuroscience *122*, 293-300.

Mehler, M.F. (2008). Epigenetics and the nervous system. Annals of neurology *64*, 602-617.

Mei, Y., Monteiro, P., Zhou, Y., Kim, J.A., Gao, X., Fu, Z., and Feng, G. (2016). Adult restoration of Shank3 expression rescues selective autistic-like phenotypes. Nature *530*, 481-484.

Miyoshi, G., and Fishell, G. (2011). GABAergic interneuron lineages selectively sort into specific cortical layers during early postnatal development. Cereb Cortex *21*, 845-852.

Moffat, J.J., Ka, M., Jung, E.M., Smith, A.L., and Kim, W.Y. (2017). The role of MACF1 in nervous system development and maintenance. Semin Cell Dev Biol *69*, 9-17.

Morita, T., and Sobue, K. (2009). Specification of neuronal polarity regulated by local translation of CRMP2 and Tau via the mTOR-p70S6K pathway. J Biol Chem *284*, 27734-27745.

Nagaoka, A., Takehara, H., Hayashi-Takagi, A., Noguchi, J., Ishii, K., Shirai, F., Yagishita, S., Akagi, T., Ichiki, T., and Kasai, H. (2016). Abnormal intrinsic dynamics of dendritic spines in a fragile X syndrome mouse model in vivo. Sci Rep *6*, 26651-26651.

Namba, T., Funahashi, Y., Nakamuta, S., Xu, C., Takano, T., and Kaibuchi, K. (2015). Extracellular and Intracellular Signaling for Neuronal Polarity. Physiol Rev *95*, 995-1024.

Narayanan, R., Pirouz, M., Kerimoglu, C., Pham, L., Wagener, R.J., Kiszka, K.A., Rosenbusch, J., Seong, R.H., Kessel, M., Fischer, A.*, et al.* (2015). Loss of BAF (mSWI/SNF) Complexes Causes Global Transcriptional and Chromatin State Changes in Forebrain Development. Cell reports *13*, 1842-1854.

Neale, B.M., Kou, Y., Liu, L., Ma'ayan, A., Samocha, K.E., Sabo, A., Lin, C.F., Stevens, C., Wang, L.S., Makarov, V.*, et al.* (2012). Patterns and rates of exonic de novo mutations in autism spectrum disorders. Nature *485*, 242-245.

Nectoux, J., Florian, C., Delepine, C., Bahi-Buisson, N., Khelfaoui, M., Reibel, S., Chelly, J., and Bienvenu, T. (2012). Altered microtubule dynamics in Mecp2-deficient astrocytes. Journal of neuroscience research *90*, 990-998.

Nelson, S.B., and Valakh, V. (2015). Excitatory/Inhibitory Balance and Circuit Homeostasis in Autism Spectrum Disorders. Neuron *87*, 684-698.

Newson, J.J., and Thiagarajan, T.C. (2018). EEG Frequency Bands in Psychiatric Disorders: A Review of Resting State Studies. Front Hum Neurosci *12*, 521.

Nigro, M.J., Hashikawa-Yamasaki, Y., and Rudy, B. (2018). Diversity and Connectivity of Layer 5 Somatostatin-Expressing Interneurons in the Mouse Barrel Cortex. J Neurosci *38*, 1622-1633.

O'Roak, B.J., Vives, L., Fu, W., Egertson, J.D., Stanaway, I.B., Phelps, I.G., Carvill, G., Kumar, A., Lee, C., Ankenman, K.*, et al.* (2012a). Multiplex targeted sequencing

identifies recurrently mutated genes in autism spectrum disorders. Science *338*, 1619-1622.

O'Roak, B.J., Vives, L., Girirajan, S., Karakoc, E., Krumm, N., Coe, B.P., Levy, R., Ko, A., Lee, C., Smith, J.D.*, et al.* (2012b). Sporadic autism exomes reveal a highly interconnected protein network of de novo mutations. Nature *485*, 246-250.

Oblak, A.L., Gibbs, T.T., and Blatt, G.J. (2011). Reduced GABAA receptors and benzodiazepine binding sites in the posterior cingulate cortex and fusiform gyrus in autism. Brain research *1380*, 218-228.

Park, K.K., Liu, K., Hu, Y., Smith, P.D., Wang, C., Cai, B., Xu, B., Connolly, L., Kramvis, I., Sahin, M.*, et al.* (2008). Promoting axon regeneration in the adult CNS by modulation of the PTEN/mTOR pathway. Science *322*, 963-966.

Paul, A., Crow, M., Raudales, R., He, M., Gillis, J., and Huang, Z.J. (2017). Transcriptional Architecture of Synaptic Communication Delineates GABAergic Neuron Identity. Cell *171*, 522-539.e520.

Peca, J., Feliciano, C., Ting, J.T., Wang, W., Wells, M.F., Venkatraman, T.N., Lascola, C.D., Fu, Z., and Feng, G. (2011). Shank3 mutant mice display autistic-like behaviours and striatal dysfunction. Nature *472*, 437-442.

Penagarikano, O., Abrahams, B.S., Herman, E.I., Winden, K.D., Gdalyahu, A., Dong, H., Sonnenblick, L.I., Gruver, R., Almajano, J., Bragin, A.*, et al.* (2011). Absence of CNTNAP2 leads to epilepsy, neuronal migration abnormalities, and core autism-related deficits. Cell *147*, 235-246.

Pennacchio, L.A. (2003). Insights from human/mouse genome comparisons. Mammalian genome : official journal of the International Mammalian Genome Society *14*, 429-436.

Penzes, P., Cahill, M.E., Jones, K.A., VanLeeuwen, J.E., and Woolfrey, K.M. (2011). Dendritic spine pathology in neuropsychiatric disorders. Nat Neurosci *14*, 285-293.

Peterson, C.L., and Workman, J.L. (2000). Promoter targeting and chromatin remodeling by the SWI/SNF complex. Current Opinion in Genetics & Development *10*, 187-192.

Pi, H.J., Hangya, B., Kvitsiani, D., Sanders, J.I., Huang, Z.J., and Kepecs, A. (2013). Cortical interneurons that specialize in disinhibitory control. Nature *503*, 521-524.

Piton, A., Jouan, L., Rochefort, D., Dobrzeniecka, S., Lachapelle, K., Dion, P.A., Gauthier, J., and Rouleau, G.A. (2013). Analysis of the effects of rare variants on splicing identifies alterations in GABAA receptor genes in autism spectrum disorder individuals. European journal of human genetics : EJHG *21*, 749-756.

Pla, R., Borrell, V., Flames, N., and Marin, O. (2006). Layer acquisition by cortical GABAergic interneurons is independent of Reelin signaling. J Neurosci *26*, 6924-6934.

Pronneke, A., Scheuer, B., Wagener, R.J., Mock, M., Witte, M., and Staiger, J.F. (2015). Characterizing VIP Neurons in the Barrel Cortex of VIPcre/tdTomato Mice Reveals Layer-Specific Differences. Cereb Cortex *25*, 4854-4868.

Qu, G.J., Ma, J., Yu, Y.C., and Fu, Y. (2016). Postnatal development of GABAergic interneurons in the neocortical subplate of mice. Neuroscience *322*, 78-93.

Ramamoorthi, K., and Lin, Y. (2011). The contribution of GABAergic dysfunction to neurodevelopmental disorders. Trends in molecular medicine *17*, 452-462.

Reid, K.A., Smiley, E., and Cooper, S.A. (2011). Prevalence and associations of anxiety disorders in adults with intellectual disabilities. J Intellect Disabil Res *55*, 172-181.

Roberts, D.A., Balderson, D., Pickering-Brown, S.M., Deakin, J.F., and Owen, F. (1996). The relative abundance of dopamine D4 receptor mRNA in post mortem brains of schizophrenics and controls. Schizophrenia research *20*, 171-174.

Robertson, C.E., Ratai, E.M., and Kanwisher, N. (2016). Reduced GABAergic Action in the Autistic Brain. Curr Biol *26*, 80-85.

Ronan, J.L., Wu, W., and Crabtree, G.R. (2013). From neural development to cognition: unexpected roles for chromatin. Nature Reviews Genetics *14*, 347.

Ropers, H.H., and Wienker, T. (2015). Penetrance of pathogenic mutations in haploinsufficient genes for intellectual disability and related disorders. Eur J Med Genet *58*, 715-718.

Rubenstein, J.L., and Merzenich, M.M. (2003). Model of autism: increased ratio of excitation/inhibition in key neural systems. Genes, brain, and behavior *2*, 255-267.

Rudy, B., Fishell, G., Lee, S., and Hjerling-Leffler, J. (2011). Three groups of interneurons account for nearly 100% of neocortical GABAergic neurons. Dev Neurobiol *71*, 45-61.

Santen, G.W., Aten, E., Sun, Y., Almomani, R., Gilissen, C., Nielsen, M., Kant, S.G., Snoeck, I.N., Peeters, E.A., Hilhorst-Hofstee, Y.*, et al.* (2012a). Mutations in SWI/SNF chromatin remodeling complex gene ARID1B cause Coffin-Siris syndrome. Nat Genet *44*, 379-380.

Santen, G.W., Kriek, M., and van Attikum, H. (2012b). SWI/SNF complex in disorder: SWItching from malignancies to intellectual disability. Epigenetics *7*, 1219-1224.

Saunders, J.A., Tatard-Leitman, V.M., Suh, J., Billingslea, E.N., Roberts, T.P., and Siegel, S.J. (2013). Knockout of NMDA receptors in parvalbumin interneurons recreates autism-like phenotypes. Autism Res *6*, 69-77.

Selby, L., Zhang, C., and Sun, Q.-Q. (2007). Major defects in neocortical GABAergic inhibitory circuits in mice lacking the fragile X mental retardation protein. Neuroscience Letters *412*, 227-232.

Seney, M.L., Tripp, A., McCune, S., Lewis, D.A., and Sibille, E. (2015). Laminar and cellular analyses of reduced somatostatin gene expression in the subgenual anterior cingulate cortex in major depression. Neurobiol Dis *73*, 213-219.

Sengottuvel, V., Leibinger, M., Pfreimer, M., Andreadaki, A., and Fischer, D. (2011). Taxol facilitates axon regeneration in the mature CNS. J Neurosci *31*, 2688-2699.

Shi, S.H., Jan, L.Y., and Jan, Y.N. (2003). Hippocampal neuronal polarity specified by spatially localized mPar3/mPar6 and PI 3-kinase activity. Cell *112*, 63-75.

Shibutani, M., Horii, T., Shoji, H., Morita, S., Kimura, M., Terawaki, N., Miyakawa, T., and Hatada, I. (2017). Arid1b Haploinsufficiency Causes Abnormal Brain Gene Expression and Autism-Related Behaviors in Mice. Int J Mol Sci *18*.

Silberberg, G., and Markram, H. (2007). Disynaptic inhibition between neocortical pyramidal cells mediated by Martinotti cells. Neuron *53*, 735-746.

Sim, J.C., White, S.M., and Lockhart, P.J. (2015). ARID1B-mediated disorders: Mutations and possible mechanisms. Intractable Rare Dis Res *4*, 17-23.

Sirmaci, A., Spiliopoulos, M., Brancati, F., Powell, E., Duman, D., Abrams, A., Bademci, G., Agolini, E., Guo, S., Konuk, B.*, et al.* (2011). Mutations in ANKRD11 cause KBG syndrome, characterized by intellectual disability, skeletal malformations, and macrodontia. Am J Hum Genet *89*, 289-294.

Siucinska, E., and Kossut, M. (2006). Short-term sensory learning does not alter parvalbumin neurons in the barrel cortex of adult mice: a double-labeling study. Neuroscience *138*, 715-724.

Skene, J.H. (1989). Axonal growth-associated proteins. Annu Rev Neurosci *12*, 127-156.

Somogyi, P., Freund, T.F., and Cowey, A. (1982). The axo-axonic interneuron in the cerebral cortex of the rat, cat and monkey. Neuroscience *7*, 2577-2607.

Son, E.Y., and Crabtree, G.R. (2014). The role of BAF (mSWI/SNF) complexes in mammalian neural development. American journal of medical genetics Part C, Seminars in medical genetics *166c*, 333-349.

Srivastava, A.K., and Schwartz, C.E. (2014). Intellectual disability and autism spectrum disorders: causal genes and molecular mechanisms. Neuroscience and biobehavioral reviews *46 Pt 2*, 161-174.

Steffenburg, S., Gillberg, C.L., Steffenburg, U., and Kyllerman, M. (1996). Autism in Angelman syndrome: a population-based study. Pediatric neurology *14*, 131-136.

Tabuchi, K., Blundell, J., Etherton, M.R., Hammer, R.E., Liu, X., Powell, C.M., and Sudhof, T.C. (2007). A neuroligin-3 mutation implicated in autism increases inhibitory synaptic transmission in mice. Science *318*, 71-76.

Takahashi, T., Yamanishi, T., Nobukawa, S., Kasakawa, S., Yoshimura, Y., Hiraishi, H., Hasegawa, C., Ikeda, T., Hirosawa, T., Munesue, T.*, et al.* (2017). Band-specific atypical functional connectivity pattern in childhood autism spectrum disorder. Clinical neurophysiology : official journal of the International Federation of Clinical Neurophysiology *128*, 1457-1465.

Tang, L., Nogales, E., and Ciferri, C. (2010). Structure and function of SWI/SNF chromatin remodeling complexes and mechanistic implications for transcription. Progress in Biophysics and Molecular Biology *102*, 122-128.

Taniguchi, H., Lu, J., and Huang, Z.J. (2013). The spatial and temporal origin of chandelier cells in mouse neocortex. Science *339*, 70-74.

Tasic, B., Menon, V., Nguyen, T.N., Kim, T.K., Jarsky, T., Yao, Z., Levi, B., Gray, L.T., Sorensen, S.A., Dolbeare, T.*, et al.* (2016). Adult mouse cortical cell taxonomy revealed by single cell transcriptomics. Nat Neurosci *19*, 335-346.

Tremblay, R., Lee, S., and Rudy, B. (2016). GABAergic Interneurons in the Neocortex: From Cellular Properties to Circuits. Neuron *91*, 260-292.

Trillingsgaard, A., and JR, O.S. (2004). Autism in Angelman syndrome: an exploration of comorbidity. Autism : the international journal of research and practice *8*, 163-174.

Tripp, A., Kota, R.S., Lewis, D.A., and Sibille, E. (2011). Reduced somatostatin in subgenual anterior cingulate cortex in major depression. Neurobiol Dis *42*, 116-124.

Tsaneva-Atanasova, K., Burgo, A., Galli, T., and Holcman, D. (2009). Quantifying Neurite Growth Mediated by Interactions among Secretory Vesicles, Microtubules, and Actin Networks. Biophysical Journal *96*, 840-857.

Tsurusaki, Y., Okamoto, N., Ohashi, H., Kosho, T., Imai, Y., Hibi-Ko, Y., Kaname, T., Naritomi, K., Kawame, H., Wakui, K.*, et al.* (2012). Mutations affecting components of the SWI/SNF complex cause Coffin-Siris syndrome. Nat Genet *44*, 376-378.

Tuoc, T.C., Boretius, S., Sansom, S.N., Pitulescu, M.E., Frahm, J., Livesey, F.J., and Stoykova, A. (2013). Chromatin regulation by BAF170 controls cerebral cortical size and thickness. Dev Cell *25*, 256-269.

Van Houdt, J.K., Nowakowska, B.A., Sousa, S.B., van Schaik, B.D., Seuntjens, E., Avonce, N., Sifrim, A., Abdul-Rahman, O.A., van den Boogaard, M.J., Bottani, A.*, et al.* (2012). Heterozygous missense mutations in SMARCA2 cause Nicolaides-Baraitser syndrome. Nat Genet *44*, 445-449, s441.

van Steensel, F.J., Deutschman, A.A., and Bogels, S.M. (2013). Examining the Screen for Child Anxiety-Related Emotional Disorder-71 as an assessment tool for

anxiety in children with high-functioning autism spectrum disorders. Autism : the international journal of research and practice *17*, 681-692.

Vasileiou, G., Ekici, A.B., Uebe, S., Zweier, C., Hoyer, J., Engels, H., Behrens, J., Reis, A., and Hadjihannas, M.V. (2015). Chromatin-Remodeling-Factor ARID1B Represses Wnt/beta-Catenin Signaling. Am J Hum Genet *97*, 445-456.

Vogel-Ciernia, A., Matheos, D.P., Barrett, R.M., Kramar, E.A., Azzawi, S., Chen, Y., Magnan, C.N., Zeller, M., Sylvain, A., Haettig, J.*, et al.* (2013). The neuron-specific chromatin regulatory subunit BAF53b is necessary for synaptic plasticity and memory. Nat Neurosci *16*, 552-561.

Vogt, D., Cho, K.K.A., Lee, A.T., Sohal, V.S., and Rubenstein, J.L.R. (2015). The parvalbumin/somatostatin ratio is increased in Pten mutant mice and by human PTEN ASD alleles. Cell reports *11*, 944-956.

Wallace, M.L., Burette, A.C., Weinberg, R.J., and Philpot, B.D. (2012). Maternal loss of Ube3a produces an excitatory/inhibitory imbalance through neuron type-specific synaptic defects. Neuron *74*, 793-800.

Walsh, P., Elsabbagh, M., Bolton, P., and Singh, I. (2011). In search of biomarkers for autism: scientific, social and ethical challenges. Nat Rev Neurosci *12*, 603-612.

Wang, W., Xue, Y., Zhou, S., Kuo, A., Cairns, B.R., and Crabtree, G.R. (1996). Diversity and specialization of mammalian SWI/SNF complexes. Genes & development *10*, 2117-2130.

Wang, X., Nagl, N.G., Wilsker, D., Van Scoy, M., Pacchione, S., Yaciuk, P., Dallas, P.B., and Moran, E. (2004). Two related ARID family proteins are alternative subunits of human SWI/SNF complexes. The Biochemical journal *383*, 319-325.

Weinberg, P., Flames, N., Sawa, H., Garriga, G., and Hobert, O. (2013). The SWI/SNF chromatin remodeling complex selectively affects multiple aspects of serotonergic neuron differentiation. Genetics *194*, 189-198.

Wen, L., Lu, Y.S., Zhu, X.H., Li, X.M., Woo, R.S., Chen, Y.J., Yin, D.M., Lai, C., Terry, A.V., Jr., Vazdarjanova, A.*, et al.* (2010). Neuregulin 1 regulates pyramidal neuron activity via ErbB4 in parvalbumin-positive interneurons. Proc Natl Acad Sci U S A *107*, 1211-1216.

White, S.W., Oswald, D., Ollendick, T., and Scahill, L. (2009). Anxiety in children and adolescents with autism spectrum disorders. Clinical psychology review *29*, 216-229.

Williams, S.R., Aldred, M.A., Der Kaloustian, V.M., Halal, F., Gowans, G., McLeod, D.R., Zondag, S., Toriello, H.V., Magenis, R.E., and Elsea, S.H. (2010). Haploinsufficiency of HDAC4 causes brachydactyly mental retardation syndrome, with brachydactyly type E, developmental delays, and behavioral problems. Am J Hum Genet *87*, 219-228.

Wilson, B.G., and Roberts, C.W. (2011). SWI/SNF nucleosome remodellers and cancer. Nature reviews Cancer *11*, 481-492.

Witte, H., and Bradke, F. (2008). The role of the cytoskeleton during neuronal polarization. Curr Opin Neurobiol *18*, 479-487.

Wohr, M., Orduz, D., Gregory, P., Moreno, H., Khan, U., Vorckel, K.J., Wolfer, D.P., Welzl, H., Gall, D., Schiffmann, S.N.*, et al.* (2015). Lack of parvalbumin in mice leads to behavioral deficits relevant to all human autism core symptoms and related neural morphofunctional abnormalities. Transl Psychiatry *5*, e525.

Wonders, C.P., and Anderson, S.A. (2006). The origin and specification of cortical interneurons. Nat Rev Neurosci *7*, 687-696.

Wu, J.I., Lessard, J., Olave, I.A., Qiu, Z., Ghosh, A., Graef, I.A., and Crabtree, G.R. (2007). Regulation of dendritic development by neuron-specific chromatin remodeling complexes. Neuron *56*, 94-108.

Xu, Q., Cobos, I., De La Cruz, E., Rubenstein, J.L., and Anderson, S.A. (2004). Origins of cortical interneuron subtypes. J Neurosci *24*, 2612-2622.

Yabe, I., Soma, H., Takei, A., Fujik, N., and Sasaki, H. (2004). No association between FMR1 premutations and multiple system atrophy. Journal of neurology *251*, 1411-1412.

Yan, Z., Wang, Z., Sharova, L., Sharov, A.A., Ling, C., Piao, Y., Aiba, K., Matoba, R., Wang, W., and Ko, M.S.H. (2008). BAF250B-Associated SWI/SNF Chromatin-Remodeling Complex Is Required to Maintain Undifferentiated Mouse Embryonic Stem Cells. STEM CELLS *26*, 1155-1165.

Yang, G., and Huang, X. (2019). Methods and applications of CRISPR/Cas system for genome editing in stem cells. Cell regeneration (London, England) *8*, 33-41.

Ying, S.W., Futter, M., Rosenblum, K., Webber, M.J., Hunt, S.P., Bliss, T.V., and Bramham, C.R. (2002). Brain-derived neurotrophic factor induces long-term potentiation in intact adult hippocampus: requirement for ERK activation coupled to CREB and upregulation of Arc synthesis. J Neurosci *22*, 1532-1540.

Yoshimura, T., Kawano, Y., Arimura, N., Kawabata, S., Kikuchi, A., and Kaibuchi, K. (2005). GSK-3beta regulates phosphorylation of CRMP-2 and neuronal polarity. Cell *120*, 137-149.

Zhang, C., Milunsky, J.M., Newton, S., Ko, J., Zhao, G., Maher, T.A., Tager-Flusberg, H., Bolliger, M.F., Carter, A.S., Boucard, A.A.*, et al.* (2009). A neuroligin-4 missense mutation associated with autism impairs neuroligin-4 folding and endoplasmic reticulum export. J Neurosci *29*, 10843-10854.

Zheng, N., and Shabek, N. (2017). Ubiquitin Ligases: Structure, Function, and Regulation. Annual review of biochemistry *86*, 129-157.

Zhou, F.Q., Zhou, J., Dedhar, S., Wu, Y.H., and Snider, W.D. (2004). NGF-induced axon growth is mediated by localized inactivation of GSK-3beta and functions of the microtubule plus end binding protein APC. Neuron *42*, 897-912.

Zikopoulos, B., and Barbas, H. (2013). Altered neural connectivity in excitatory and inhibitory cortical circuits in autism. Front Hum Neurosci *7*, 609.

Zou, D., Chen, L., Deng, D., Jiang, D., Dong, F., McSweeney, C., Zhou, Y., Liu, L., Chen, G., Wu, Y.*, et al.* (2016). DREADD in parvalbumin interneurons of the dentate gyrus modulates anxiety, social interaction and memory extinction. Current molecular medicine *16*, 91-102.